Preface

It must be the planets. This was clear to me in 1994 writing my review article about turbulence in natural fluids like the ocean, atmosphere and galaxy. Galaxies of stars must be turbulent or there would be more of them, according to one of the books I was reviewing. This was my introduction to cosmology. If you don't know what is going on, just make something up and move on. Oceanographers do this too. Why don't galaxies fly apart if they are rotating so fast? Dark matter. Why is the ocean mixed when we never see any mixing? Dark mixing. In both cases you need to know about fluid mechanics and turbulence and fossil turbulence to get right answers. Turbulence theory is even worse. Because of a poem, everyone thinks they know turbulence cascades from large scales to small, but it is perfectly obvious by observing the growth of a turbulent wake or a jet or a turbulent anything that turbulence always grows from small scales to large.

Why planets? Planet-mass gravitational fragments appear when matter produced by the big bang gets cool enough to turn from plasma to gas. It's easy. You know the viscosity and density of the gas and you know the rate the universe is expanding. Chug and plug. It took twenty minutes. Earth-mass gas planets now frozen solid are widely separated to match the density and are in clumps of a trillion to match the Jeans acoustic mass of a million stars. Another twenty minutes. I can teach this to freshmen. Every star is formed from mergers of planets, and has thirty million more of its own that it keeps eating till it gets overweight and explodes.

The timing was perfect. The Hubble Space Telescope team and C. R. O'Dell had just produced the Helix Planetary Nebula image showing thousands of evaporating planets and Rudy Schild had just published his quasar microlensing paper with the same conclusion: the dark matter of galaxies is not stars but planets in clumps.

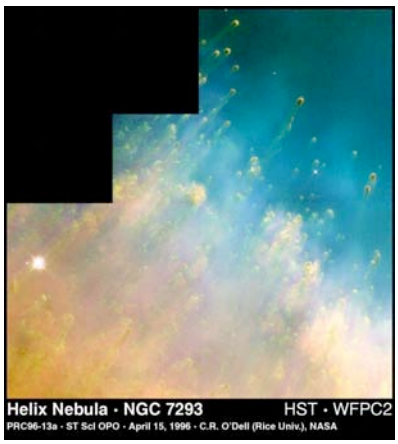

So why are oceanographers not thrilled to know the turbulence in the ocean is mostly fossil turbulence and the mixing is done by fossil turbulence waves in beamed zombie turbulence maser action mixing chimneys? Why are turbulence experts not happy to realize turbulence is an eddy-like state of fluid motion where the inertial vortex forces of turbulent eddies are larger than any other forces that tend to damp the eddies out, so that the cascade of turbulence must be from small scales to large? Why are cosmologists not thrilled to know the standard model of cosmology they use is wrong, but can be easily fixed with a little fluid mechanics?

It's all about money and marketing. Most oceanographers are on soft money and so are most astrophysicists. They dare not stray from standard models or their contracts will not be renewed and their papers not published. This works for a lifetime career in oceanography, but it cannot work much longer in cosmology. The flood of excellent new data will not permit it. Both peer review systems are broken and corrupt but cosmology cannot resist the facts much longer. The attached preprints show why. I am not the only one. An army of rebels are now ready to push the tottering house of cards of the standard ΛCDMHC model over the cliff.

So now it's time for a commercial break:

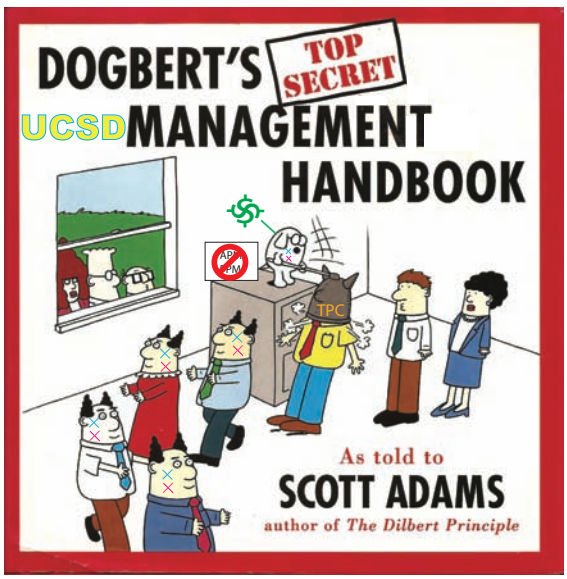

This book is dedicated to the University of California at San Diego system that in its present mode of operation has provided numerous furlough days with no pay to its faculty. It is hoped any proceeds from this book will enhance cookie funds for UCSD freshmen and senior seminars. Funding for these have been sacrificed in the same spirit motivating UC to reduce faculty salaries and increase student fees to solve UC budget problems. The cartoon above is derived from the cover of Scott Adam's book Dogbert's Top Secret Management Handbook and the double-cross symbol of the Chaplin film "The Great Dictator" by me trying to get a raise. It complains that APM and PPM (policy and procedure) manuals of the University of California are not properly followed in the interests of saving time and money by corporate management behaviors and zombie managers, threatening UC policies of shared governance and causing the need for faculty to move toward unionization.

Similar complaints about UC management styles are reflected in the following, emailed recently by Mike Davis and titled "Solidarity".

Mike Davis
1331 33rd St
San Diego CA 92102
mdavis@ucr.edu

Many years ago in the faded Art Nouveaux splendor of a Gorbals (Glasgow) pub, I met a man who told me an extraordinary story about his grandfather, a coalminer who had been killed in a pit disaster before the First World War. A methane explosion, followed by a roof collapse, had trapped his grandfather and his mates deep in the mine, where they were eventually asphyxiated. When rescuers reached their tomb days later, they found a final, defiant message chiseled into the coalface: 'God save our union.'

The spirit of these doomed Scots miners isn't easily replicated in rational choice models of social action. Nor can simple economic calculation explain the fervor with which Lancashire cotton workers, whose wages depended upon Southern cotton and the British domination of India, supported Lincoln and later Gandhi. Likewise, from the 1934 San Francisco General Strike to Justice for Janitors in
the 1980s and 1990s, California working people have repeatedly translated their passion for justice and dignity into the slogan 'an injury to one, is an injury to all.'

The labor and civil rights movements, to be sure, aren't fairy tales, and the heroic moments are often counterbalanced by the petrification of militancy into leaden bureaucracy and the selfish calibration of seniority. Solidarity is too often an orphan. In our case, there are disheartening examples of the tenured strata ignoring the recent picket-lines of catering workers, secretaries, lecturers, and students.

UC faculty, indeed, are much like the residents of Jonathan Swift's city of Laputa: distracted by their departmental micropolitics and the distribution of FTEs while they float on a cloud above the existential distress of K-12 and community education. The Senate faculty also must share responsibility with the Regents for the system's transformation into a vast machine for the transformation of public research into corporate profit. Most UC campuses now more resemble gated communities than public temples of learning.

A lot of us have complained about this situation for years, but our discomfort has seldom moved us to action. But the challenge is now epic-historic: equity and justice are endangered at every level of the Master plan for Education. Obscene wealth still sprawls across the coastal hills, but flat-land inner cities and blue-collar interior valleys face the death of the California dream. Their children - let's not beat around the bush - are being pushed out of higher education. Their future is being cut off at its knees.

The September 24 strike movement, in my opinion, is most important because it defends non-tenured employees and demands public disclosure of the Regents' secret diplomacy. It is an elementary reflex of a progressive, humane consciousness: an antidote to the staggering selfishness and elitism of Andrew Scull and his Gang of 23.

A strike, by matching actions to words, is also the highest form of teach-in. This seed of resistance, of course, will only grow to maturity through cultivation by unionized employees and students. They are the real constant gardeners, and hopefully branches of a unified fight-back will quickly intertwine with the parallel struggles of CSU, community college, K-12 and adult-education workers.

The strike also provides a bully pulpit to counter the still widespread belief that the UC system has a unique dispensation and can once again negotiate its own special deal in Sacramento. Many of our colleagues are simply in denial. This time around, the first-class passengers are in the same frigid water with the kindergarten teachers and community college janitors.

The 24th is the beginning of learning how to shout in unison. And whatever the outcome, it at allows us write our beliefs on the coalface.

* UPTE/CWA has voted to strike UC on September 24

September 24, 2009, is the opening day of Fall Quarter at UCSD.

LA JOLLA

Hundreds at UCSD rally against cuts

Teach-ins, walkouts protest furloughs, student fee hikes

By Eleanor Yang Su
STAFF WRITER

University of California San Diego students returned to class yesterday amid an animated backdrop of walkouts, teach-ins and an employee strike designed to draw attention to severe state budget cuts.

About 200 students and faculty members gathered at an afternoon teach-in to decry the impact of $82 million in state cuts, which have prompted student fee increases, layoffs and unpaid furloughs.

Professors assembled on the steps of the Pepper Canyon Hall courtyard and lamented how the cuts have led to crowded classes and skyrocketing student fees that could shut out poor and minority students.

"Where the hell is the California dream?" asked philosophy professor Gerald Doppelt, rapping as the crowd clapped in unison. "Come to school for a better day. It comes down hard as pay-pay-pay."

Down the road, an additional 200 students, faculty and staff members rallied in an event billed as a walkout, marching with research and technical employees who held a one-day strike over furloughs and labor negotiations.

Demonstrators carried signs that read, "The University of California: Formerly a Great Public Institution."

It's unclear how many of UCSD's 28,500 students walked out of classes yesterday,

SEE UCSD, B4

Faculty members, students and staffers listened to speeches in the courtyard of Pepper Canyon Hall at the University of California San Diego yesterday. *Howard Lipin / Union-Tribune*

UCSD protests against faculty salary cuts and increased student fees to offset California budget shortfalls, San Diego Union, September 24, 2009.

▶ UCSD
CONTINUED FROM B1

State funding has not kept up with enrollment

but the university's second-in-command, Paul Drake, said he believes the majority of classes went smoothly.

More than 1,000 professors were expected to walk out of classes at UC campuses across the state yesterday.

Several UCSD professors said they held class, but spent some time explaining the importance and effects of the cuts to students.

"Today is just a preliminary step toward reclaiming the UC system for the people of California," literature professor Jorge Mariscal said. "In the last 25 years, the system has become increasingly privatized as public support has been cut."

UC will receive $2.6 billion in state funding this year, roughly 14 percent of the 10-campus system's overall budget. While state funding has grown over the past two decades, it has not kept pace with student enrollment, so per-student funding has decreased.

Several students at the teach-in said they did not regret missing class to attend the event.

"I think it was a real good idea," said Kimberly Cooper, whose communications class was canceled for the teach-in. "We got to come to this and learn more. Plus it's just the first day, so we didn't miss out on much."

Communications professor Barry Brown canceled a class of 300 after receiving five student requests.

"They said they wanted to have class canceled to make a statement about this being a day of action," he said.

Brown, who said he showed up at his class to make sure students had received his e-mail, added that not a single student complained.

In addition to concerns about student fee increases and bulging class sizes, many on the faculty are upset about furloughs that began this month.

The furloughs will result in a 6 percent to 8 percent salary cut for most professors, Drake said. Unlike California State University professors, UC faculty members cannot take furloughs on instruction days. If they do, it will be recorded in their personnel review file.

"Our highest priority is our students," Drake said. "They are taking a fee increase, and we should not deny them the education they paid for."

Not all faculty members agree with that mind-set, said Bill Hodgkiss, chairman of UCSD's Academic Senate.

"Some people feel it's an appropriate public statement to not teach, because a cut to university does hurt and does matter," Hodgkiss said.

Eleanor Yang Su: (619) 542-4564; eleanor.su@uniontrib.com

New Cosmology II

cosmology modified by modern fluid mechanics

Carl H. Gibson
Professor of Engineering Physics and Oceanography,
Departments of Mechanical and Aerospace Engineering
and Scripps Institution of Oceanography,
Center for Astrophysics and Space Sciences,
Editor-in-Chief for the Journal of Cosmology and Cosmology,
University of California San Diego, La Jolla CA 92093-0411, USA
cgibson@ucsd.edu, http://sdcc3.ucsd.edu/~ir118

ABSTRACT

This book is intended to introduce anyone interested in cosmology, astrophysics and astronomy to new versions that include modern fluid mechanical methods. It consists of papers in progress by myself with Rudy Schild and Theo Nieuwenhuizen that compare predictions of new cosmology with those of old cosmology in light of the flood of information from rapidly improving telescopes in space and on earth. Preprints for the Journal of Cosmology describe the formation and evolution of protogalaxyclusters at the beginning of the plasma epoch and the formation of protogalaxies at the end. The Nieuwenhuizen preprint[1] summarizes CMB evidence of weak turbulence in the plasma epoch by K. Sreenivasan and A. Bershadskii driven by protosuperclustervoid viscous-gravitational fragmentation beginning at 30,000 years. Stretching of protogalaxies by the expanding universe along a fossilized turbulent vortex line viewed end-on explains Stephan's Quintet and the mysterious redshifts in this compact group discovered by Margaret and Geoff Burbidge.

Introduction

Standard cosmology is fatally flawed, like a Sudoku puzzle with a bad guess. The bad guess occurred because information about modern fluid mechanics and even not-so-modern fluid mechanics was ignored in favor of traditional but bad guesses handed down through many generations of graduate students and their professional progeny for over a hundred years since James Jeans proposed his theory of gravitational instability in 1902. Jeans worked without the benefit of the Hubble Space Telescope at a time when the existence of galaxies was debatable and the mass and collision cross section of the

[1] This paper was written in honor of K. Sreenivasan. arXiv 0809.2330 has been withdrawn because it is superseded by arXiv:0906.5087

neutrino was not in the imagination of anyone. Thus it was not at all unreasonable in 1902 for him to model the gravitational instability of a gas by assuming an inviscid fluid in ideal flow with gravity using linear acoustic equations, leading to the Jeans length scale formed from the speed of sound, the density and Newton's gravitational constant. Unfortunately, when cosmologists realized gravitational structures like globular star clusters are nearly as old as the big bang they had a problem. The Jeans scale during the plasma epoch was larger than the scale of causal connection *ct*, where *c* is the speed of light and *t* is the time since the big bang. Information travels with the speed of light, so objects separated by more that *ct* have no way of reacting gravitationally. The bad guess was made knowing most of the universe is invisible and prevents spinning galaxies from flying apart. This dark matter is 3% ordinary baryonic matter composed of protons and neutrons and 97% something else with lots of mass and the collisionless properties of neutrinos. Since the speed of sound of baryonic matter increases with temperature to 60% of the speed of light in the plasma epoch it was assumed that the non-baryonic dark matter must be cold to reduce its Jeans scale to the point that it could be less than *ct* in the plasma and thus condense. Cold-dark-matter seeds could then form and cluster in the early universe forming massive CDM halos into which the baryonic material could fall by gravity to form stars, galaxies and galaxy clusters in this order rather than the reverse as observed and predicted by new cosmology. Wrong. Problems with this standard old cosmology ΛCDMHC model are discussed in the following preprints.

Pictures from the recently repaired Hubble space telescope have just appeared. Stephan's Quintet of galaxies was beautifully imaged, but is discussed incorrectly as a merger of galaxies rather than a thin chain galaxy cluster stretching along a fossil turbulence vortex line existing at the end of the plasma epoch when protogalaxies were formed within protosuperclusters. See the final preprint for the evidence.

Evolution of proto-galaxy-clusters to their present form: theory and observations

Carl H. Gibson [1,2]

[1] University of California San Diego, La Jolla, CA 92093-0411, USA
[2] cgibson@ucsd.edu, http://sdcc3.ucsd.edu/~ir118

and

Rudolph E. Schild[3,4]

[3] Center for Astrophysics, 60 Garden Street, Cambridge, MA 02138, USA
[4] rschild@cfa.harvard.edu

ABSTRACT

From hydro-gravitational-dynamics theory HGD, gravitational structure formation begins 30,000 years after the turbulent big bang by fragmentation into super-cluster-voids and super-clusters. Proto-galaxies in linear and spiral clusters are the smallest fragments to emerge from the plasma epoch at decoupling at 10^{13} s with a turbulent morphology determined by the plasma turbulence and the Nomura scale 10^{20} m, which is determined by gravity, the fossilized density and rate-of-strain of the 10^{12} s time of first structure and the large photon viscosity of the plasma. After decoupling, the gas proto-galaxies fragment into 10^{36} kg proto-globular-star-cluster PGC clumps of earth-mass 10^{25} kg hot gas clouds that eventually freeze to form primordial-fog-particle PFP dark matter planets. This is the galaxy dark matter BDM. The non-baryonic-dark-matter NBDM is so weakly collisional that it fragments only after decoupling to form galaxy cluster halos. It does not guide galaxy formation according to the cold-dark-matter hierarchical clustering CDMHC theory, which is fluid mechanically untenable and obsolete. NBDM has 97% of the mass of the universe and serves to bind together rotating clusters of galaxies by gravitational forces. The rotation of galaxies reflects density gradients of big bang turbulent mixing and the sonic expansion of proto-super-cluster-voids. The spin axis appears for low wavenumber spherical harmonic components of CMB temperature anomalies, the Milky Way and galaxies of the local group, and extends to 4.5×10^{25} m (1.5 Gpc) in quasar polarization vectors, supporting a big bang turbulence origin. Gas proto-galaxies

stick together by frictional processes of the frozen gas planets, just as PGCs have been meta-stable for the 13.7 Gyr age of the universe. Evidence of PGC-friction is inferred from the local group Hubble diagram and from redshift anomalies of Hickson compact galaxy groups such as the Stephan Quintet compared to Sloan Digital Sky Survey SDSS galaxy observations.

INTRODUCTION

The standard model of cosmology is in the process of rapid decomposition as a relentless flood of new data confronts old ideas [1,2]. New space telescopes cover an ever-widening band of frequencies. Ground based telescopes are linked and controlled by ever more powerful computers that track events as they happen and freely distribute all information nearly real time on the internet. The standard model of cosmology is cold-dark-matter hierarchical-clustering CDMHC based on an acoustic length scale proposed in 1902 by Jeans [1] as the single (fluid mechanically untenable) criterion for gravitational structure formation (see Table 1). In 1902 only the Milky Way nebula of stars was recognized as a galaxy. As pointed out by Hoyle, Burbidge and Narlikar 2000 [3] spiral nebula (galaxy) Messier 51 had been detected in 1855 by Lord Rosse, and it was only speculated that such objects were Milk-Way-like galaxies, a view strongly dismissed by Agnes Clerke in her 1905 well-known popular book *The System of Stars* based on her perception of the results and conclusions of professional astronomers of the day:

> *The question whether nebulae are external galaxies hardly any longer needs discussion. It has been answered by the progress of research. No competent thinker, with the whole of the available evidence before him, can now, it is safe to say, maintain any single nebula to be a star system of co-ordinate rank with the Milky Way. A practical certainty has been attained that the entire contents, stellar and nebula, of the sphere belong to one mighty aggregation, and stand in ordered mutual relations within the limits of one all embracing scheme [4].*

As Hoyle et al. note in their preface, pressures of big science funding have badly corrupted the peer review system of astrophysics and cosmology. Papers that deviate from the standard model in any way are likely to be dismissed out of hand by referees and scientific editors that depend on big science funds for survival. It was pointed out in 1996 [10] that the Jeans 1902 fluid mechanical analysis of standard cosmology is fatally flawed and obsolete from the neglect of various basic principles of fluid mechanics termed hydro-gravitational-dynamics HGD [7-23], but publication of this information has so far not been allowed in any "reputable" astrophysical journal. Contrary to the linear instability criterion of Jeans 1902, gravitational instability is highly non-linear, fluid mechanically limited and absolute [13]. It is easy to show that viscous and turbulent forces

are critically important and that diffusivity of the nearly collision-less non-baryonic-dark-matter NBDM prevents Jeans condensation and hierarchical clustering of CDM halos during the plasma epoch before decoupling. Artificial "Plummer forces" etc. introduced to fit data from observations by numerical simulations (see Table 1 and Dehnen 2001) compensate for the physical impossibility of CDM halo formation and clustering [5,6]. The "Plummer force length scales" required to permit numerical simulations to match super-void observations [31] match the Nomura scale $L_N = 10^{20}$ m, reflecting proto-globular-star-cluster PGC friction from planets-in-clumps as the dominant form of galaxy dark matter, as inferred from quasar microlensing observations by Schild in 1996 [24].

Proto-galaxy-clusters form at the last stage of the plasma epoch guided by weak turbulence along vortex lines produced by expanding proto-supercluster-voids encountering fossil density gradients of big bang turbulence [16,17] producing baroclinic torques and turbulence on the expanding void boundaries. In this paper we focus on the evolution of proto-galaxy-clusters during the present gas epoch. Examples of gas proto-galaxy-clusters are shown in Figure 1, from the Hubble Space Telescope Advanced Camera for Surveys HST/ACS observing the Tadpole galaxy merger UGC 10214. We see that these dimmest objects (magnitude 24-28) with $z > 0.5$ clearly reflect their formation along turbulent vortex lines of the plasma epoch, and clearly reflect the gentle nature of the early universe as these gas proto-galaxy-clusters expand ballistically and with the expansion of the universe against frictional forces of the baryonic dark matter. The mechanism of momentum transfer between gas proto-galaxies is much better described by the 1889 meteoroid collision mechanism of G. H. Darwin [2] than by the 1902 collisionless-gas mechanism of J. H. Jeans [1].

From HGD, the chains of star clumps shown in Fig. 1 have been incorrectly identified as "chain galaxies" rather than chains of proto-galaxies since their discovery in the Hawaiian Deep Field by Cowlie et al. 1995 at magnitude 25-26. The rows of clumps are not edge-on spirals and the tadpoles are not end-on chain galaxies as suggested by Elmegreen et al. 2004 [39]; they are remnants of gravitationally produced plasma fragments along turbulent vortex lines of the primordial plasma produced at the Nomura scale of plasma proto-galaxies. In the following we show end-on proto-galaxy-clusters can best be explained as the "fingers of God" structures observed in the Sloan Digital Sky Survey II and by the Hickson 1993 Compact Group HCG class of galaxy clusters [29] exemplified by Stephan's Quintet [22], Figure 2. A complex system of star wakes, gobular star cluster wakes and dust trails leaves no room to doubt that the dark matter halo is dominated by PGCs of planets from which the stars and GCs form on agitation, and that the SQ galaxies have separated from a primordial plasma chain-proto-galaxy-cluster.

The linear gas-proto-galaxy clusters of Fig. 1 show the universe soon after decoupling must have been quite gentle for them to survive. This contrasts with the standard model

of galaxy formation where the first galaxies are CDM haloes that have grown by hierarchical clustering to about 10^{36} kg (a globular cluster mass) and collected a super-star amount of gas in their gravitational potential wells, about 10^{32} kg (100 solar mass). As soon as the gas cools sufficiently so that its Jeans scale permits condensation it does so to produce one super-star and one extremely bright supernova.

The combined effect of these mini-galaxy supernovae is so powerful that the entire universe of gas is re-ionized according to CDMHC. The problem with this scenario is that it never happened. It rules out the formation of old globular star clusters that require very gentle gas motions. The extreme brightness of the first light is not observed. Re-ionization is not necessary to explain why neutral gas is not observed in quasar spectra once it is understood that the dark matter of galaxies is frozen PFP primordial planets in PGC clumps.

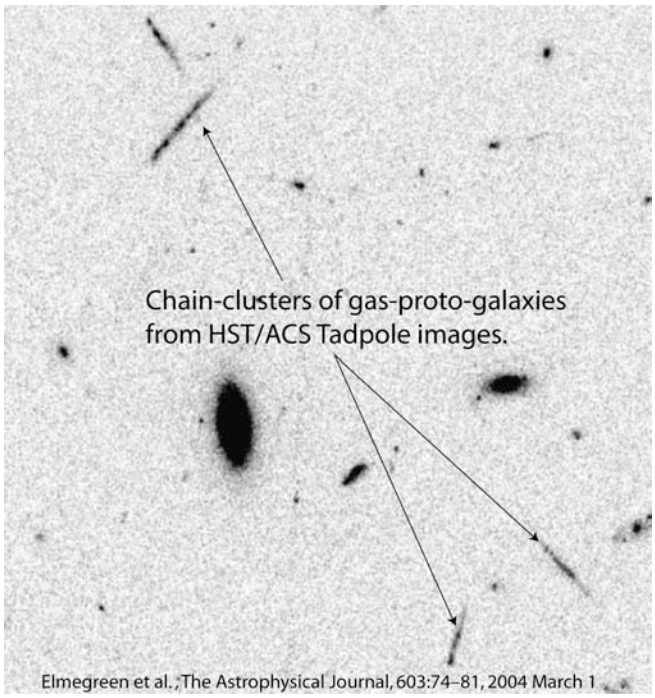

Figure 1. Chain-clusters of gas-proto-galaxies GPGs reflect their origin by gravitational fragmentation along turbulent vortex lines of the plasma epoch at decoupling time t ~ 10^{13} s (300,000 years) after the big bang. Only ~0.1% of the baryonic dark matter BDM (planets in clumps) has formed old-globular-star-cluster OGC small stars in these proto-galaxies. More than 80% of the dimmest proto-galaxies (magnitudes 24-28) are in linear proto-galaxy-clusters termed chains, doubles and tadpoles. The tadpole tails and the luminosity between all GPGs are stars formed from frictional BDM planets that form gas when agitated and accrete to form stars.

The chain-clusters of GPGs in Fig. 1 confirm the prediction of HGD that the early universe was quite gentle compared to that required by CDM and that the proto-galaxies start their evolution in the gas epoch at very small scales compared to galaxy sizes observed today. From HGD, each GPG in the linear clusters has about 10^{42} kg of BDM dark matter PGCs. The foreground elliptical and spiral galaxies shown in Fig. 1 have not acquired mass by merging according to CDMHC. The BDM gradually diffuses out of the 10^{20} m proto-galaxy core to form the 10^{22} m BDM halo against PGC frictional forces. The PGC frictional forces inhibit the ballistic growth of the linear GPGs as well as growth due to the expansion of the universe and trigger the formation of halo star trails.

From HGD, gas-proto-galaxies soon after formation are quite sticky from PGC friction. Even though plasma-proto-galaxies are stretching apart along turbulent vortex lines with the maximum rate of strain of the turbulence the central GPGs formed may not be able to separate. An example is shown in Figure 2, the spectacular Stephan's Quintet SQ. Three galaxies in a narrow range of angles have precisely the same redshift $z = 0.022$, one has $z = 0.019$ but one has a highly anomalous $z = 0.0027$. SQ is one of many highly compact galaxy clusters termed Hickson Compact Groups HCG. Nearly half of the HCG galaxy clusters have at least one highly anomalous redshift member.

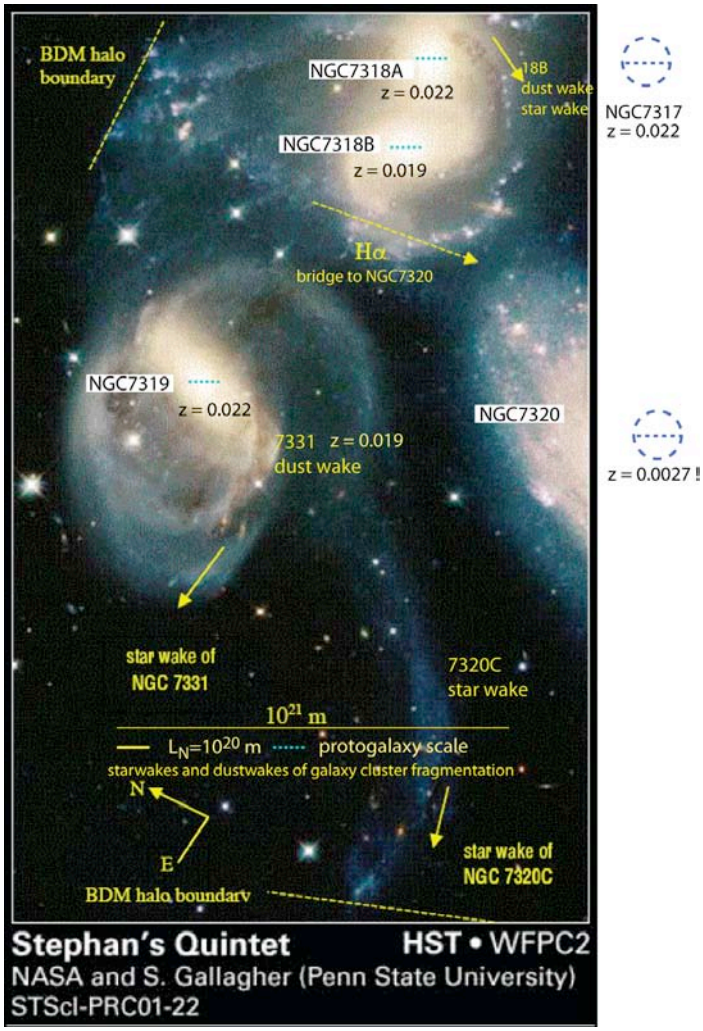

Figure 2. Stephan's Quintet (SQ, HCG 92, Arp 319, VV 288) very compact and mysterious galaxy cluster (Stephan 1877). The Trio NGC7319, NGC7318A, NGC7317 have redshift 0.022, NGC 7318B with redshift 0.019 that matches that of NGC7331, but nearby NGC7320 at redshift 0.0027 ! All are connected by star trails, star cluster trails and dust trails suggesting an end-on chain-cluster of proto-galaxies formed along a turbulent vortex line [22].

Burbidge and Burbidge 1961 measure and report the highly anomalous nature of the SQ galaxy redshifts. For virial equilibrium the closely aligned NGC 7313AB galaxies would require an M/L ratio of 300 from dynamical models, but NGC 7320 requires M/L of 10,000, much too large to be credible. A connecting gas bridge to NGC 7320 proves it is not a chance intruder but a separated companion [22]. One possibility is that galaxies

may somehow be ejected by an AGN mother galaxy with intrinsic redshifts [3,33,34,35], which accounts for the observational fact that giant AGN elliptical galaxies are observed with many more nearby quasars than chance will allow. A more likely possibility from HGD is that Hickson Compact Groups and SQ are simply end-on views of chain-galaxy-clusters and that sometimes quasars are included in such end-on linear clusters (see Fig. 8). The Trio is still stuck together by PGC friction and 7313B and 7320 have separated ballistically and from the expansion of the universe. Their close angular proximity is an optical illusion due to their nearness to earth and perspective.

From known properties of the hot big bang universe the Schwarz viscous and turbulent scales of Table 1 show fragmentation will occur early at massive proto-super-cluster scales by formation of expanding super-cluster-voids independent of the NBDM.

Table 1. Length scales of gravitational instability

Length Scale Name	Definition	Physical Significance
Jeans Acoustic	$L_J = V_S/(\rho G)^{1/2}$	Acoustic time matches free fall time
Schwarz Viscous	$L_{SV} = (\gamma\nu/\rho G)^{1/2}$	Viscous forces match gravitational forces
Schwarz Turbulent	$L_{ST} = (\varepsilon/[\rho G]^{3/2})^{1/2}$	Turbulent forces match gravitational forces
Schwarz Diffusive	$L_{SD} = (D^2/\rho G)^{1/4}$	Diffusive speed matches free fall speed
Horizon, causal connection	$L_H = ct$	Range of possible gravitational interaction
Plummer force scale	L_{CDM}	Artificial numerical CDM halo sticking length

V_S is sound speed, ρ is density, G is Newton's constant, γ is the rate of strain, ν is the kinematic viscosity, ε is the viscous dissipation rate, D is the diffusivity, *c* is light speed, *t* is time.

The plan of the present paper is to first review the very different predictions of HGD and CDMHC theories with respect to galaxy formation and evolution. Then Observations are discussed, followed by a Conclusion.

THEORY

Figure 3 shows the sequence of gravitational structure formation events according to hydro-gravitational-dynamics HGD cosmology leading to primordial gas-proto-galaxies and galaxies of the present time. A hot big bang is assumed at 13.7 Gyr before the present time, followed by an inflation event where big bang turbulent temperature microstructure is fossilized by stretching of space beyond the scale of causal connection $L_H = ct$, where *c* is the speed of light and *t* is the time. Gravitational instability produces the first structure

in the plasma epoch by fragmentation, as proto-supercluster-voids begin to grow at 10^{12} seconds (30,000 years) leaving proto-superclusters in between. The proto-super-clusters do not collapse by gravity but expand with the expansion of space working against the photon viscosity. Viscous dissipation rates can be estimated from $\varepsilon \sim \nu\gamma^2$, giving $\varepsilon \sim 400$ m^2 s^{-1}. Photon-electron collision lengths were $\sim 10^{18}$ m, less than the horizon scale $L_H = 3x10^{20}$ m as required by continuum mechanics. Viscous dissipation rates in the gas epoch after decoupling decreased with ν and γ to $\varepsilon \sim 10^{-13}$ m^2 s^{-1} values small enough to permit formation of dark matter planets in clumps and the small stars of old globular star clusters.

The criterion for fragmentation is that the Schwarz viscous scale L_{SV} matches L_H (see Table 1). The NBDM decouples from the plasma because it is weakly collisional. The voids grow as rarefaction waves that approach the sound speed $c/3^{1/2}$. Turbulence is produced at expanding void boundaries by baroclinic torques. Observations confirm that the Reynolds number of the turbulence is rather weak. Fragmentations and void formations occur at smaller and smaller scales until the plasma to gas transition (decoupling) at 10^{13} seconds (300,000 years). The weak turbulence produces plasma-proto-galaxies by fragmentation, with NBDM filled voids formed along stretching and spinning turbulent vortex lines.

In Fig. 3, a. Cosmic Microwave Background temperature anisotropies reflect structures formed in the plasma epoch. b. From HGD the photon viscosity of the plasma epoch prevents turbulence until the viscous Schwarz scale L_{SV} becomes less than the Hubble scale (horizon scale, scale of causal connection) $L_H = ct$, where c is the speed of light and t is the time. The first plasma structures were proto-super-cluster voids and proto-superclusters at 10^{12} seconds (30,000 years). c. Looking back in space is looking back in time. Proto-galaxies were the last fragmentations of the plasma (orange circles with green halos) at 10^{13} seconds. d. The scale of the gravitational structure epoch is only $3x10^{21}$ m compared to present supercluster sizes of 10^{24} m and the largest observed super-void scales of 10^{25} m. e. Turbulence in the plasma epoch is generated by baroclinic torques on the boundaries of the expanding super-voids.

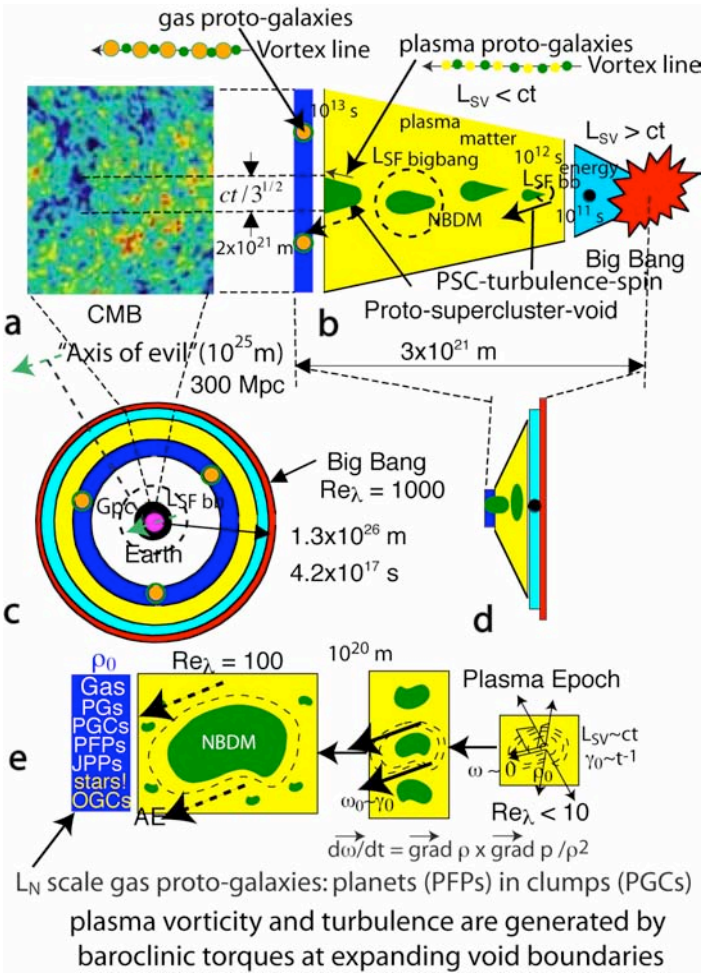

Figure 3. Protogalaxy formation at the end of the plasma epoch by hydro-gravitational-dynamics HGD theory.

Gas chains of proto-galaxies are formed at decoupling, as shown by the cartoon at the top of Fig. 3a. Because photons suddenly decouple from electrons the viscosity of the fluid suddenly decreases by a factor ~ 10^{13}, greatly decreasing the viscous Schwarz scale and the fragmentation mass. Two fragmentation scales work simultaneously with the same gravitational free fall time to produce Jeans mass clumps PGCs of earth mass gas planets PFPs, which today is the baryonic dark matter of galaxies.

Figure 4 illustrates super-void and galaxy formation following the standard cosmological model (ΛCDMHC) advocated in the Peebles 1993 book *Principles of Physical Cosmology*. According to the Peebles 1993 timetable (Table 25.1, p 611) [25] super-clusters, walls and voids form at redshift $z \sim 1$; that is, at least 5 Gyr after the big bang versus

0.0003 Gyr from Gibson 1996 [14] and HGD. But completely empty super-voids have been detected by radio telescopes with sizes at least 300 Mpc or 10^{25} m, 10% of the horizon scale $L_H = 10^{26}$ m [30]. Peebles 2007 [26] recognizes that observations of empty voids on locally observed scales of 10^{24} m is a possibly insuperable problem for CDMHC models.

Fig. 4 contrasts the predictions of ΛCDMHC theory of galaxy and void formation with observations and the predictions of HGD theory. Failures are indicated by red Xs. HGD cosmology is driven by turbulent combustion at Planck scales from Planck-Kerr instability, with Taylor microscale Reynolds number $Re_\lambda \sim 1000$. Gluon viscosity terminates the event after cooling from 10^{32} K Planck temperatures to 10^{28} K strong force freeze-out temperatures where quarks and gluons can appear. Turbulent temperature patterns are frozen as turbulence fossils by exponential inflation of space driven by negative stresses of both turbulence and gluon viscosity pulling 10^{90} kg of mass-energy out of the vacuum against the Planck tension c^4/G. The mass-energy of our present horizon is only $\sim 10^{53}$ kg, so we can see only $\sim 10^{-40}$ fraction of the universe produced by the big bang. A black dot in the blue inflation triangle of Fig. 3 symbolizes the ~ 20% temperature fluctuations expected from big bang turbulence, contrasting with tiny quantum-mechanical fluctuations expected in the standard model in Fig. 4.

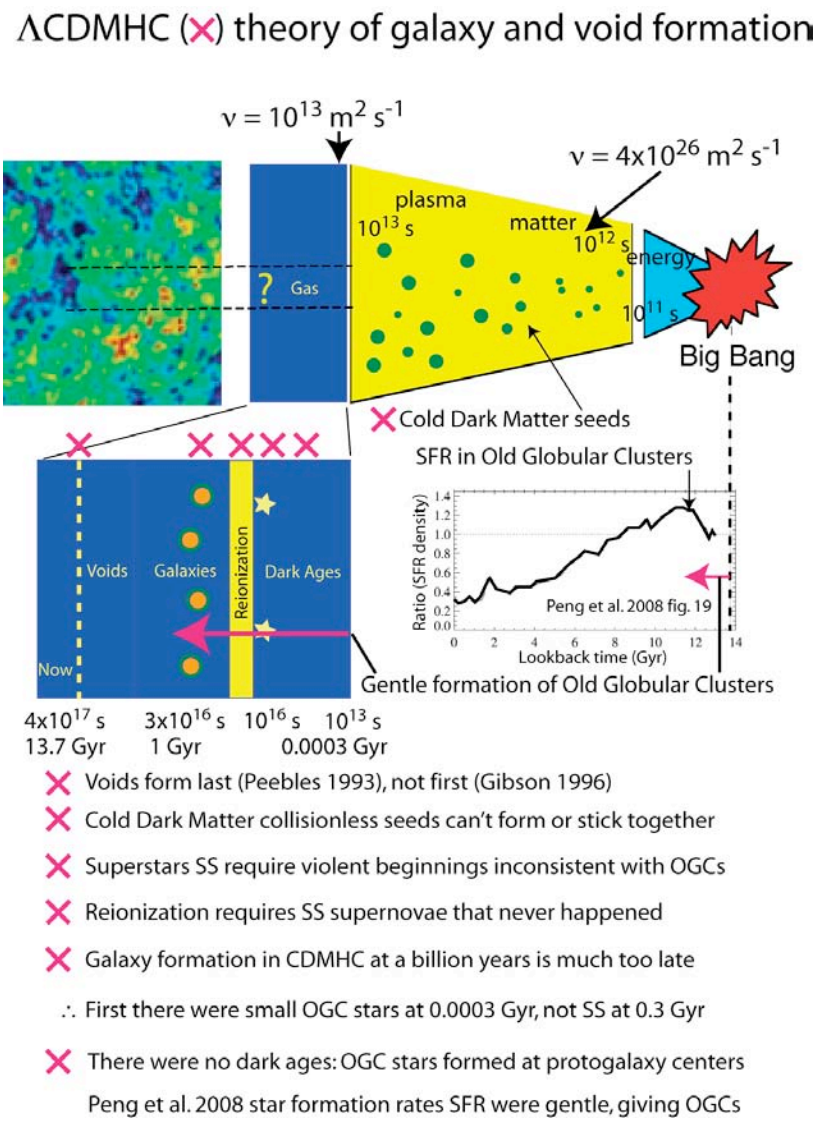

Figure 4. Void and galaxy formation by the standard ΛCDM theory are impossible to reconcile with observations and fluid mechanical HGD theory (see text). Several failed aspects of ΛCDMHC theory are indicated by red Xs. It is fatally flawed and must be abandoned.

In CDMHC models voids form last rather than first, so this difference is most easily tested by observations. The time of first void formation from HGD is 10^{12} s, compared to ~ 10^{17} s for CDMHC. Star formation rates of Peng et al. 2008 favor small old globular-cluster stars. These could not possibly be formed under the violent conditions of galaxy formation and mergers intrinsic to CDMHC.

We now examine available observations for comparison with theories of galaxy formation and evolution.

OBSERVATIONS

Evidence of the large primordial super-voids of HGD theory (Fig. 1) is shown in Figure 5, from Rudick et al. 2008. Focusing on the direction of the anomalous "cold spot" of the CMB it was found that a 10^{25} m (300 Mpc) completely empty region could explain the ~ $7x10^{-5}$ ^{o}K CMB cold spot by the integrated Sachs-Wolfe method. The empty region is estimated to be at redshifts $z \sim 1$, and is therefore completely impossible to explain by CDMHC models where super-voids are formed last rather than first (Fig. 4). The probability of such a void forming from concordance CDM models is estimated [30] to be < 10^{-10}.

Tinker and Conroy 2008 [31] explain the void phenomenon by numerical simulations and produce a relatively empty super-void of scale 10^{24} m using numerical simulations and numerically convenient but entirely imaginary "Plummer forces" [6]. As mentioned previously, Plummer forces are physically untenable for weakly collisional NBDM materials such as CDM.

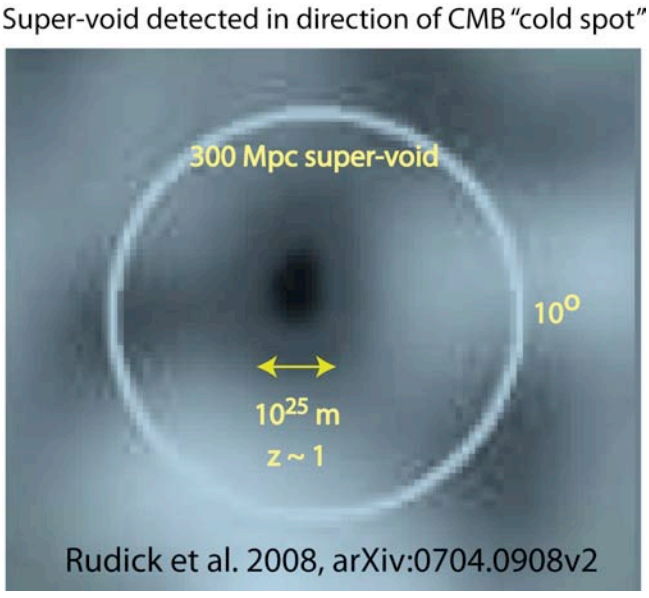

Figure 5. Super-void detection by the radio telescope very large aperture (NVSS) survey in the direction of the anomalous cold spot of the CMB. Such large voids are expected from HGD but are impossible to explain using CDM models [30].

Figure 6 summarizes observational evidence that the dimming of supernova Ia events is not evidence for dark energy and a cosmological constant Λ, but is merely a systematic error due to the presence in the near vicinity of shrinking white dwarf stars approaching the Chandrasekhar instability limit of BDM frozen planets partially evaporated by strong spin radiation (1.44 M_{Sun}). Dimness of the SNe Ia events increases with their magnitudes, and cannot be explained by uniform grey dust as shown by the top curve using estimates of Reiss et al. 2004 [36].

In Fig. 6, open circles emphasize SNe Ia events unobscured by evaporated BDM planet atmospheres (no dark energy) for the Reiss et al. dimness models. Solid red ovals emphasize events partially obscured by planet atmospheres (non-linear grey dust). Thousands of BDM planets (right insert) in the Helix planetary nebula are evaporated by spin radiation from the central white dwarf. From HGD the Helix PNe is not ejected from a massive precursor; instead, the BDM planets are evaporated in place. The observed dimness is caused by fossil turbulence electron density fluctuations in gas with density $\rho \sim 10^{-12}$ kg m^{-3} sufficient to permit turbulence. The large 20-30% dimness at $z \sim 0.5$ cannot be explained by reasonable quantities of dust or gases alone in the observed 10^{13} m planet atmospheres shown in the Helix PNe BDM planets insert: it requires fossil electron-density turbulence forward scattering.

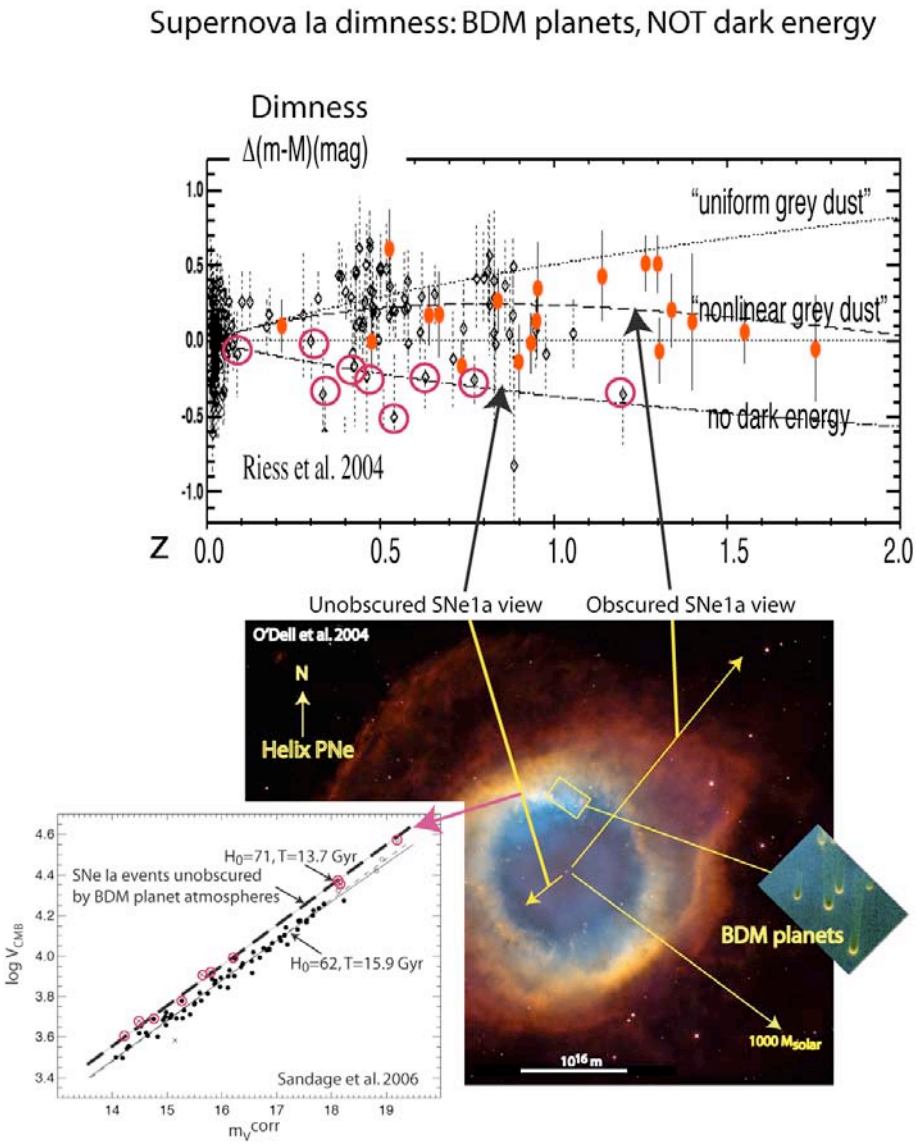

Figure 6. Observations that show the anomalous dimness of supernova Ia events of Reiss et al. 2004 and the anomalously low Hubble constants of Sandage et al. 2006 [37] can be attributed to BDM planet atmospheres, not dark energy [20]. The nearby Helix planetary nebula PNe at $6x10^{18}$ m has a central white dwarf with polar jet that evaporates the ambient BDM planets of its PGC. A close-up view is shown in the insert on the right.

From HGD, all stars are formed from BDM planets in PGCs. All PGCs have the primordial density $\rho_0 \sim 4x10^{-17}$ kg m^{-3}, which matches the density of globular star clusters. The

size of the planets, their atmospheres, and separations observed are consistent with this primordial density [20].

The Fig. 6 insert at lower left shows the Sandage et al. 2006 SNe Ia study of the Hubble Constant H_0, carefully corrected for Cepheid variable distances and locations. The age of the universe is 15.9 Gyr from this study, which is unacceptably large. However, open red circles show SNe Ia event lines of sight unobscured by BDM planet atmospheres from HGD. These agree very well with the CMB age of the universe of 13.7 Gyr. Gamma ray burst dimmnesses clinch this interpretation [38].

Figure 7 shows velocities V_{LG} in km s-1 of the local group of galaxies as a function of their distances in Mpc so the slope of a line from the origin is a measure of the Hubble Constant.

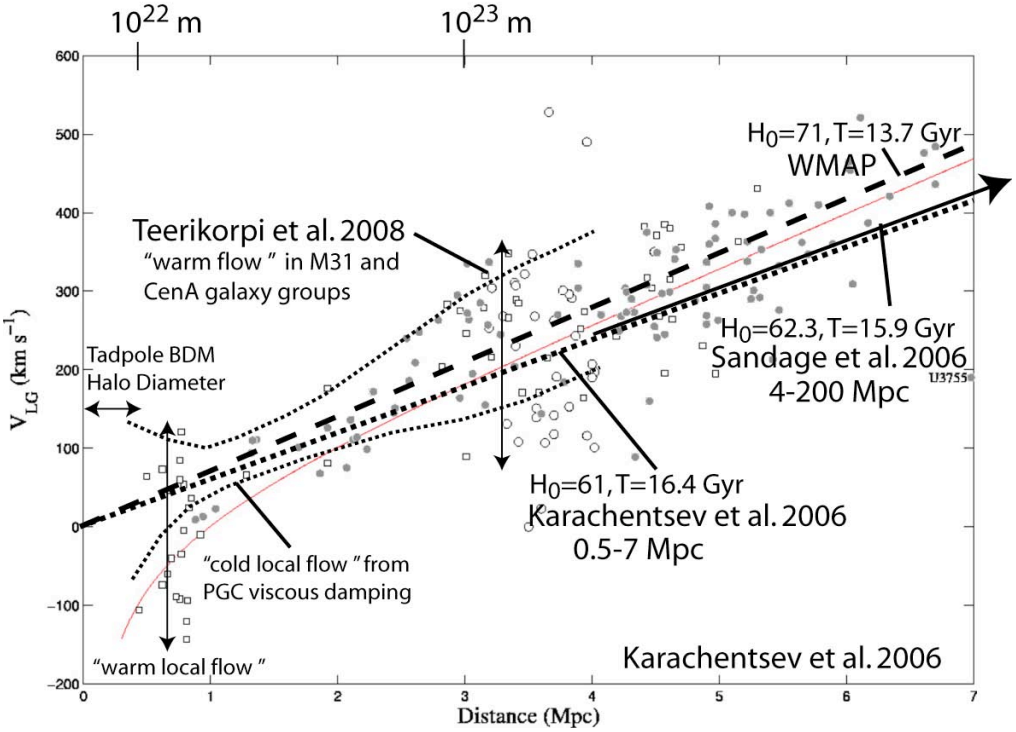

Figure 7. Estimates of the Hubble Constant for galaxies in the local group show wide scatter out to distances of a Mpc due to frictional interactions of BDM halos. The Tadpole BDM halo size is shown by the horizontal double arrow [23]. Beyond this distance the galaxies begin to separate due to Hubble flow. Warm flows in M31 and CenA galaxy groups have H_0 dispersions similar to that of galaxies near the Milky

Way, as shown by vertical double arrows. The dotted line is an extrapolation to the Sandage et al. 2006 Hubble constants shown in Fig. 6, at 4 to 200 Mpc.

Figure 8 shows a Sloan Digital Sky Survey map of local galaxies compared to the HGD interpretation of Stephan's Quintet as an end-on chain of gas proto-galaxies. In the top panel, note that galaxies with old stars, indicated by red dots, are often aligned in thin pencils termed "fingers of god". Blue dots denote younger galaxies with more blue stars. The reason for this is that the galaxies are relatively near to earth, with redshift $z \sim 0.1$ or less, so perspective causes a decrease in angular separation for distant galaxies that are already nearly aligned. An arrow shows 10^{25} m, about 10% of the present horizon L_H. The red pencil-like features are interpreted from HGD as chain clusters of old galaxies aligned by vortex lines in the plasma epoch that have continued moving along these directions ballistically and from the homogeneous straining of the universe during the gas epoch. Dashed circles indicate 10^{24} m. PGC frictional stickiness has inhibited separation of the galaxies along their axes and in transverse direction, as shown for Stephan's Quintet.

Fig. 8a summarizes the history of SQ formation starting from the time of first fragmentation to plasma to gas transition. Fig. 8b shows SQ at present, with the Trio about $4x10^{24}$ m distant and NGC 7320 with redshift 0.0027 at about 10^{23} m. A cartoon of the SQ galaxies is shown near the origin of the SDSS II Galaxy Map.

It seems clear from Fig. 8 that the Trio of SQ galaxies are not clustered by chance or by merging but were formed simultaneously in a linear cluster of proto-galaxies along a turbulent vortex line of the plasma epoch. For 13.7 Gyr they have resisted separation by the expansion of the universe due to PGC friction from frictional interactions of galaxy BDM dark matter planets in galaxy dark matter halos [22].

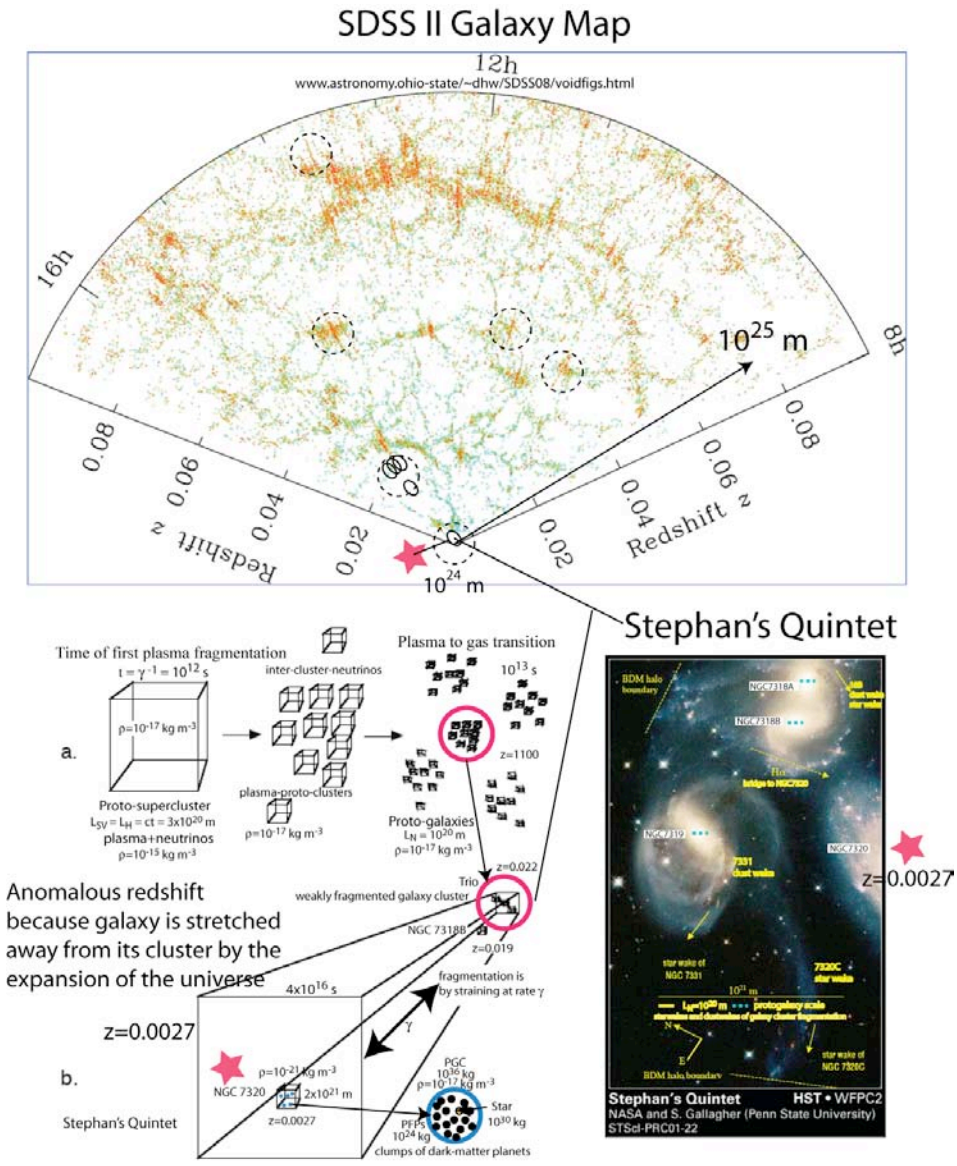

Figure 8. Stephan's Quintet provides evidence that linear galaxy clusters were formed by fragmentation in the plasma epoch along turbulent vortex lines [22]. Red stars indicate the most anomalous galaxy NGC 7320 with redshift $z = 0.0027$ in three views.

The HGD interpretation of Fig. 8 is that PGC friction inhibits the separation of galaxies in the gas epoch by collisional and tidal interactions of BDM planet halos. The Arp 1973 suggestion that NGC 7331 has ejected the other galaxies with intrinsic redshifts is unnecessary, and would require introduction of an unknown class of new physical laws.

CONCLUSION

Observations exclude the ΛCDMHC standard model for galaxy and void formation as the last steps of gravitational structure formation rather than the first from HGD where the Jeans 1902 theory that provides the basis of CDM is obsolete and fluid mechanically untenable. HGD explains the formation of galaxies as the last stage of gravitational fragmentation starting early in the plasma epoch with proto-super-clusters and proto-super-voids, and finishing with plasma-proto-galaxy morphology determined by weak turbulence from gravitational void expansions and fossil turbulence density gradients from the epoch of strong big bang turbulence. The evolution of gas proto-galaxies from HGD is extremely gentle compared to an unnecessarily violent epoch of super-star formation, supernovae and re-ionization required by ΛCDMHC. These CDM events never happened.

Dimming of SNe Ia events by evaporated BDM planet atmospheres provides an HGD alternative to the new physical laws required by the dark energy hypothesis, Λ, and the Sandage et al. 2006 evidence that the universe age is 15.9 Gyr. The alternative is that there is no dark energy, there is no Λ, and corrections for dimming give a universe age of 13.7 Gyr.

Stephan's Quintet confirms predictions of HGD about the evolution of chain gas-proto-galaxy clusters and the importance of PGC friction to stick proto-galaxies together and resist ballistic forces and universe-space-expansion that try to move them apart. The interpretation of SQ and chain-galaxy-clusters by HGD theory provides an alternative to suggestions [3,33,34,35] that central galaxies in chain clusters can emit galaxies and quasars with intrinsic redshifts. Globular cluster wakes, star wakes and dust wakes clearly show the galaxies of SQ were formed in a linear chain and have all separated, never merged, as the galaxy cluster has evolved against the PGC friction of the galaxy-dark-matter-halos consisting of frozen planets in GC-mass clumps.

Further evidence of proto-globular-star-cluster friction from dark-matter-planet interactions is provided by the Hubble diagrams of Fig. 7 for the local group and Fig. 6 from Sandage et al. 2006 at larger distances up to 200 Mpc from SN Ia. PGC-friction explains the random scatter of galaxy velocities in clusters for ~ Mpc lengths scales small enough for BDM halos to interact. At larger scales the expansion of the universe becomes the dominant mechanism to separate galaxies.

REFERENCES

1. Jeans, J. H. 1902. The stability of spherical nebula, Phil. Trans., 199A, 0-49.
2. Darwin, G. H. 1889. On the mechanical conditions of a swarm of meteorites, and on theories of cosmogony, Phil. Trans., 180, 1-69.

3. Hoyle, F., Burbidge, G. and Narlikar, J. V. 2000. A Different Approach to Cosmology, From a static universe through the big bang towards reality, Cambridge Univ. Press, Cambridge UK.
4. Clerke, Agnes M. 1905. The System of the Stars, Adam & Charles Black, London UK.
5. Plummer, H. C. 1911. Mon. Not. Roy. Astron. Soc., 71, 460.
6. Dehnen, W. 2001. Toward optimum softening in 3D N-body codes: Minimizing the force error, Mon. Not. Roy. Astron. Soc., 324, 273-291.
7. Gibson, C.H. (1991). Kolmogorov similarity hypotheses for scalar fields: sampling intermittent turbulent mixing in the ocean and galaxy, Proc. Roy. Soc. Lond. A, 434, 149-164.
8. Gibson, C. H. (2006). Turbulence, update of article in Encyclopedia of Physics, R. G. Lerner and G. L. Trigg, Eds., Addison-Wesley Publishing Co., Inc., pp.1310-1314.
9. Gibson, C. H. (1981). Buoyancy effects in turbulent mixing: Sampling turbulence in the stratified ocean, AIAA J., 19, 1394.
10. Gibson, C. H. (1968a). Fine structure of scalar fields mixed by turbulence: I. Zero-gradient points and minimal gradient surfaces, Phys. Fluids, 11: 11, 2305-2315.
11. Gibson, C. H. (1968b). Fine structure of scalar fields mixed by turbulence: II. Spectral theory, Phys. Fluids, 11: 11, 2316-2327.
12. Gibson, C. H. (1986). Internal waves, fossil turbulence, and composite ocean microstructure spectra," J. Fluid Mech. 168, 89-117.
13. Gibson, C. H. (1999). Fossil turbulence revisited, J. of Mar. Syst., 21(1-4), 147-167, astro-ph/9904237
14. Gibson, C.H. (1996). Turbulence in the ocean, atmosphere, galaxy and universe, Appl. Mech. Rev., 49, no. 5, 299–315.
15. Gibson, C.H. (2000). Turbulent mixing, diffusion and gravity in the formation of cosmological structures: The fluid mechanics of dark matter, J. Fluids Eng., 122, 830–835.
16. Gibson, C.H. (2004). The first turbulence and the first fossil turbulence, Flow, Turbulence and Combustion, 72, 161–179.
17. Gibson, C.H. (2005). The first turbulent combustion, Combust. Sci. and Tech., 177: 1049–1071, arXiv:astro-ph/0501416.
18. Gibson, C.H. (2006). The fluid mechanics of gravitational structure formation, astro-ph/0610628.
19. Gibson, C.H. (2008). Cold dark matter cosmology conflicts with fluid mechanics and observations, J. Applied Fluid Mech., Vol. 1, No. 2, pp 1-8, 2008, arXiv:astro-ph/0606073.
20. Gibson, C.H. & Schild, R.E. (2007). Interpretation of the Helix Planetary Nebula using Hydro-Gravitational-Dynamics: Planets and Dark Energy, arXiv:astro-ph/0701474.

21. Schild, R.E & Gibson, C.H. (2008). Lessons from the Axis of Evil, axXiv:astro-ph/0802.3229v2.
22. Gibson, C.H. & Schild, R.E. (2007). Interpretation of the Stephan Quintet Galaxy Cluster using Hydro-Gravitational-Dynamics: Viscosity and Fragmentation, arXiv[astro-ph]:0710.5449.
23. Gibson, C.H. & Schild, R.E. (2002). Interpretation of the Tadpole VV29 Merging Galaxy System using Hydro-Gravitational Theory, arXiv:astro-ph/0210583.
24. Schild, R. 1996. Microlensing variability of the gravitationally lensed quasar Q0957+561 A,B, ApJ, 464, 125.
25. Peebles, P. J. E. 1993. Principles of Physical Cosmology, Princeton University Press, Princeton, NJ.
26. Peebles, P. J. E. 2007. Galaxies as a cosmological test, arXiv: 0712.2757v1.
27. Peng, E. W. et al. 2008, The ACS Virgo Cluster Survey. XV. The Formation Efficiencies of Globular Clusters in Early-Type Galaxies: The Effects of Mass and Environment, ApJ, 681, 197-224.
28. Dunkley, J. et al. (2008). Five-year Wilkinson Microwave Anisotropy Probe (WMAP) Observations: Likelihoods and Parameters from the WMAP data, subm. ApJS; arXiv:0803.0586v1.
29. Hickson, P. 1993. Atlas of Compact Groups of Galaxies, Gordon & Breach, New York, New York.
30. Rudnick, L., Brown, S. and Williams, L. R. 2008. Extragalactic radio sources and the WMAP Cold Spot, arXiv:0704.0908v2.
31. Tinker, J. L. and Conroy, C. 2008. The Void Phenomenon Explained, arXiv:0804.2475v2.
32. Burbidge, E. M., and Burbidge, G. R. 1961. A Further Investigation of Stephan's Quintet, ApJ, 134, 244.
33. Burbidge, G. R. 2003. NGC 6212, 3C 345, and other quasi-stellar objects associated with them, ApJ, 586, L119.
34. Arp, H. 1973. Stephan's quintet of interacting galaxies, ApJ, 183, 411.
35. Arp, H. 1998. The origin of companion galaxies, ApJ, 496, 661.
36. Reiss et al. 2004. Type Ia supernova discoveries at z > 1 from the Hubble Space Telescope: Evidence for past deceleration and constraints on dark energy evolution, ApJ, 607, 665-687.
37. Sandage et al. 2006. The Hubble constant: A summary of the HST Program for the luminosity calibration of Type Ia supernovae by means of Cepheids, ApJ, 653, 843.
38. Gibson, C. H. and Schild, R. E. 2009. Hydro-Gravitational-Dynamics of planets and dark energy, J. Appl. Fluid Mech., 2(1), 1, arXiv:0808.3228v1.
39. Elmegreen, D. M., Elmegreen, B. G. and Sheets, C. M. 2004. Chain galaxies in the Tadpole Advanced Camera for Surveys field, ApJ, 603, 74-81.

Turbulent formation of protogalaxies at the end of the plasma epoch: theory and observations

Rudolph E. Schild[1,2]

[1] Center for Astrophysics, 60 Garden Street, Cambridge, MA 02138, USA
[2] rschild@cfa.harvard.edu

and

Carl H. Gibson [3,4]

[3] University of California San Diego, La Jolla, CA 92093-0411, USA
[4] cgibson@ucsd.edu, http://sdcc3.ucsd.edu/~ir118

ABSTRACT

The standard model of gravitational structure formation is based on the Jeans 1902 acoustic theory, neglecting nonlinear instabilities controlled by viscosity, turbulence and diffusion. A linear instability length scale equal to the sound speed times the gravitational freefall time emerges. Because the Jeans scale L_J for the hot primordial plasma is always slightly larger than the scale of causal connection *ct*, where *c* is the speed of light and *t* is the time after the big bang, it has been assumed that no plasma structures could form without guidance from a cold (so $L_{J\ CDM}$ is small) collisionless cold-dark-matter CDM fluid to give condensations that gravitationally collect the plasma. Galaxies by this CDM model are therefore produced by gradual hierarchical-clustering of CDM halos to galaxy mass over billions of years, contrary to observations showing that well formed galaxies existed much earlier. No observations exist of CDM halos. However, Gravitational instability is non-linear and absolute, controlled by viscous and turbulent forces or by diffusivity at Schwarz length scales smaller than *ct*. Because the universe during the plasma epoch is rapidly expanding, the first structures formed were at density minima by fragmentation when the viscous-gravitional scale L_{SV} first matched *ct* at 30,000 years to produce protosupercluster voids and protosuperclusters. Weak turbulence produced at expanding void boundaries guide the morphology of smaller fragments down to protogalaxy size just before transition to gas at 300,000 years. The size of the protogalaxies reflect the plasma Kolmogorov scale with a linear and spiral morphology predicted by the Nomura direct numerical simulations and confirmed by deep field space

telescope observations. On transition to gas the kinematic viscosity decreases by ten trillion so the protogalaxies fragment at Jeans scale clouds, each with a trillion earth-mass planets, as predicted by Gibson 1996 and observed by Schild 1996. The planets promptly form stars near the cores of the protogalaxies, but as the universe cools the planets gradually freeze to form the galaxy dark matter. Space telescope observations of the most distant galaxies confirm the Kolmogorov scale size and Nomura geometry of the protogalaxies. High resolution images of planetary nebula and supernova remnants reveal thousands of frozen hydrogen-helium dark matter planets with large atmospheres evaporated by such events. Galaxy mergers show frictional trails of young globular clusters formed in place, proving that dark matter halos of galaxies consist of dark matter planets in metastable clumps. Galaxy evolution is guided by friction from this galaxy dark matter.

INTRODUCTION

The standard model of gravitational structure formation and the formation of galaxies is based on a linear acoustic instability theory proposed by James Hopwood Jeans in 1902 in a lengthy monograph titled "The stability of a spherical nebula" transmitted to the Philosophical Transactions of the Royal Society of London Series A (Vol. 1999, pp. 1-53) through G. H. Darwin, son of Charles Darwin. The purpose of the work was to understand how the solar system might have formed from a gas cloud. Galaxies and the expansion of the universe were not known at that time. The alternative theory due to G. H. Darwin in his 1889 paper (Vol. 180, pp. 1-69) was titled "On the mechanical conditions of a swarm of meteorites, and on theories of cosmogony". Neither of the theories are correct as a description of how either the solar system or galaxies were formed. Darwin's theory focusing on meteorites [1] is a better guide than Jeans' in both cases since accretion within clumps of primordial planets and effective viscosity from planet collisions are crucial and the collapse of gas clouds following Jeans 1902 [2] is irrelevant. The Jeans acoustic scale has only one known application, which is to set the mass of globular star clusters at the plasma to gas transition (decoupling), but it is for different reasons than described by Jeans. Modern fluid mechanical concepts [3-19] applied to cosmology are termed hydro-gravitational-dynamics HGD. Relevant length scales are summarized in Table 1.

The fluid mechanics of Jeans 1902 is that of the 19th century. Jeans started with the Euler equations that neglect viscous forces, used linear perturbations stability analysis that neglects turbulence forces, and took no account of diffusivity effects arising from weakly collisional non-baryonic dark matter that probably constitutes about 97% of the rest mass of the universe where the universe is flat with density approximately equal to the present critical density of $\rho_{Crit} = 10^{-26}$ kg m^{-3} with no dark energy or cosmological constant Λ. Jeans' assumptions lead to linear acoustic momentum conservation equations for the gas,

so the Jeans 1902 acoustic instability scale is $L_J = V_S / (\rho G)^{1/2}$, where V_S is the speed of sound, $\tau_g = (\rho G)^{-1/2}$ is the gravitational free fall time, ρ is the density and G is Newton's constant of gravitation.

The Jeans criterion for gravitational structure formation is that a large cloud of gas with density ρ is unstable to gravitational structure formation only on scales larger than J_H. By this criterion it is impossible to make any structures at all in the plasma epoch of the universe because the sound speed $V_{S-plasma} = c / 3^{1/2}$ is so large that $L_J > L_H$, where $L_H = ct$ is the horizon scale or scale of causal connection at time *t* after the big bang and *c* is the speed of light. Even after the plasma turns to gas at $t \approx 10^{13}$ seconds (300,000 years) the Jeans mass is an enormous million solar masses so the first stars cannot form until much later and planets can never form from gas at average temperatures because the density of the expanding universe decreases more rapidly than the sound speed with time. The problem with the Jeans criterion is that it is simply wrong [10]. Gravitational instability is absolute not linear [11], meaning that in a fluid with density fluctuations, structure will immediately begin to form at all scales of available density fluctuations unless prevented by the molecular diffusivity of the nearly collisionless non-baryonic dark matter or by viscous or turbulence forces. Mass moves toward density maxima and away from density minima at all scales unless prevented by forces or diffusivity.

When the plasma turns to gas it becomes a fog of planets [10] that become galaxy dark matter, as observed [20]. The only known form of non-baryonic dark matter NBDM is neutrinos, but there may be other massive neutrino-like particles formed in the early universe at temperatures unavailable in laboratories or there may be more ordinary neutrinos than known from present estimates. The evidence indicates the existence of something non-baryonic and quite massive that prevents the disintegration of galaxy clusters by gravitational forces, just as baryonic dark matter is needed to inhibit the disintegration of individual galaxies by centrifugal forces, but at this time no one knows what it is.

Density perturbations exist in the plasma because the big bang was triggered by a form of turbulent combustion at Planck temperature 10^{35} K termed the Planck-Kerr instability [12,13]. Planck particles and anti-particles appear by quantum tunneling and form the Planck scale equivalent of positronium. Positronium is produced by supernova temperatures of 10^{10} K sufficient to cause electron positron pair production, where the antiparticle pairs form a relatively stable combinations in orbit. Prograde captures give 42% release of the Planck particle rest mass energy which can only go into producing more Planck particles to fuel similar interactions. This gives a turbulent big bang with Reynolds number of about a million, terminated when cooling permits formation of quarks and gluons and a strong increase of viscosity and viscous stress that can cause an exponential in-

crease in space to approximately a meter size in 10^{-33} seconds from 10^{-27} meters (10^{8} Planck lengths). The speed is about 10^{25} c. This inflation epoch produces the first fossil turbulence because all the turbulent temperature fluctuations of big bang turbulence are stretched beyond the scale of causal connection $L_H = ct$.

These fossils of big bang turbulence then trigger the formation of density fluctuations in the hydrogen and helium formed in the first three minutes by nucleosynthesis. The density fluctuations then seed the first gravitational structure formation [14]. The mechanism is not by the Jeans criterion but under the control of viscosity, turbulence or particle diffusivity, depending on which of three Schwarz scales is largest for the fluid in question. Because the collision length for non-baryonic dark matter is larger than $L_H = ct$ for the plasma epoch, only viscous forces or turbulence forces can prevent structure formation. Fragmentation of the non-baryonic dark matter occurs after the end of the plasma epoch, so this material is nearly irrelevant to the first structure formation, which begins when the horizon scale matches the Schwarz viscous scale at about 10^{12} seconds after the big bang (30,000 years) and the mass scale is that of superclusters. The plasma epoch is dominated by viscous forces with only weak turbulence because the photon viscosity is very large. Photons scatter from the free electrons of the plasma and transmit momentum because the electrons strongly couple to the ions to maintain electrical neutrality. Reynolds numbers are close to critical values so the Schwarz viscous and turbulent scales are nearly identical. The first structures to form are voids because the universe is expanding. Condensations occur only after decoupling. The voids expand at the sonic speed of the plasma epoch which is $c / 3^{1/2}$, so we have significantly larger supervoids than superclusters as discussed in the following sections [15].

Because observations showed early structure must have occurred, cosmologists resorted to a *deus ex machina* solution (magic): they invented cold dark matter in order to create the present standard cosmological model. Following Jeans, it was assumed that a cold non-baryonic material must exist with sound speed sufficiently small that gravitational condensations in the plasma epoch could occur; that is, with $L_{J_{CDM}} < L_H$. Seeds of CDM were assumed to condense to provide gravitational potential wells into which the baryonic plasma would fall. The seeds would magically merge and stick over time, collecting more and more of the baryonic material until stars could form, and the clumps could cluster to larger and larger scales to produce galaxies and galaxy clusters and last superclusters of galaxies. This is hierarchical clustering, so the standard model is often called CDMHC. No CDM halo has ever been observed. In the following we suggest they do not exist and that CDM does not exist. Neither does the latest addition to the standard cosmological model; that is, dark energy and the cosmological constant Λ [16–19].

Instead, the plasma fragmentation beginning at 10^{12} s continues to smaller and smaller scales. Galaxies represent the smallest mass gravitational structures formed in the plasma before decoupling at 10^{13} s (300,000 years). Galaxy morphology reflects the turbulence existing in the plasma when they were formed. Protogalaxies fragmented along turbulent vortex lines at the Kolmogorov scale of the plasma and with a chain and spiral morphology demonstrated by the direct numerical simulations of Nomura. This morphology and a consistent protogalaxy length scale termed the Nomura scale is observed in a variety of Hubble Space Telescope observations discussed in the rest of this chapter [15].

At decoupling the kinematic viscosity ν decreased from photon viscosity values of $\sim 10^{26}$ m^2 s^{-1} to hot gas values of 10^{13} m^2 s^{-1}, a factor of ten trillion. This decreased the mass scale of fragmentation from that of protogalaxies to that of planets. Simultaneously the gas protogalaxies fragmented at the Jeans mass of globular star clusters, giving hot gas clouds of planet mass in million solar mass clumps. As the universe expands it cools. The gas clouds of hydrogen and helium eventually begin to freeze to form the galaxy dark matter, which is proto-globular-star-cluster PGC clumps of primordial-fog-particle PFP planets [10] as observed [20]. All stars form in PGCs from the trillion planets contained by a binary accretion process that gives larger and larger Jovian planets. The first stars to form were therefore small and long-lived, as observed in ancient globular star clusters. Structure formation from fluid mechanics naturally explains globular star clusters, which have always been a mystery. In standard ΛCDMHC cosmology, the first stars to form are superstars that re-ionize the universe to explain why so much hydrogen is missing in high red-shift quasar spectra. In our hydro-gravitational-dynamics HGD cosmology the missing hydrogen is tied up in frozen planets, the superstars (Population III) never happened, and Reionization of the Universe never happened [15].

Table 1. Length scales of gravitational instability

Length Scale Name	Definition	Physical Significance
Jeans Acoustic	$L_J = V_S/(\rho G)^{1/2}$	Acoustic time matches free fall time
Schwarz Viscous	$L_{SV} = (\gamma\nu/\rho G)^{1/2}$	Viscous forces match gravitational forces
Schwarz Turbulent	$L_{ST} = (\varepsilon/[\rho G]^{3/2})^{1/2}$	Turbulent forces match gravitational forces
Schwarz Diffusive	$L_{SD} = (D^2/\rho G)^{1/4}$	Diffusive speed matches free fall speed
Horizon, causal connection	$L_H = ct$	Range of possible gravitational interaction
Nomura, smallest plasma piece	$L_N = 10^{20}$ m	Proto-galaxy-fragmentation on vortex lines

V_S is sound speed, ρ is density, G is Newton's constant, γ is the rate of strain, ν is the kinematic viscosity, ε is the viscous dissipation rate, D is the diffusivity, *c* is light speed, *t* is time.

THEORY

Figure 1 shows the sequence of gravitational structure formation events leading to the present time according to hydro-gravitational-dynamics HGD cosmology.

The big bang mechanism is one of turbulent combustion limited by gluon viscosity, where the maximum Taylor microscale Reynolds number $Re_\lambda = 1000$ occurred at $t = 10^{-33}$ seconds at 10^8 L_P, where $L_P = 10^{-35}$ is the Planck scale of quantum-gravitational instability [12,13]. The only particles possible during this epoch of high temperatures were Planck particles and Planck anti-particles that interact in the manner of electron-positron pair production to efficiently produce more Planck particles until the event cools enough for quarks and gluons to appear. Large negative Reynolds stresses expand space according to Einstein's theory of general relativity. During the big bang turbulence epoch, indicated in Fig. 1a by the red star, the kinematic viscosity ν is the mean free path for particle collisions L_P times the speed of the particle. Even though the particle speeds were light speeds *c* at $t = 0$, the collision distances were small, giving a small initial kinematic viscosity $\nu_0 = 3x10^{-27}$ m^2 s^{-1}. The Planck scale Reynolds number is near critical so L_P matches the Kolmogorov and Batchelor scales [3] of big bang turbulence and turbulent mixing.

The end of the big bang turbulence epoch occurred when the temperatures and particle speeds decreased as the Reynolds numbers increased till quarks and gluons could appear. This phase change is termed the strong force freeze out, with length scale $L_{SF} = 10^8$ L_P, or 10^{-27} m. Gluons are particles that carry momentum for the quarks, similar to photons carrying forces from momentum differences between the electrons and protons of the plasma epoch. It is assumed that the gluon viscosity is dramatically larger than the Planck viscosity, just as the photon viscosity is dramatically larger than the proton-proton collision viscosity of the plasma epoch, so that large negative gluon viscous stresses will accelerate the expansion of space exponentially during the inflation epoch indicated by the blue triangle. Other mechanisms such as the Guth false vacuum may be important for driving inflation. Whichever mechanism is dominant, many observations support an inflationary event.

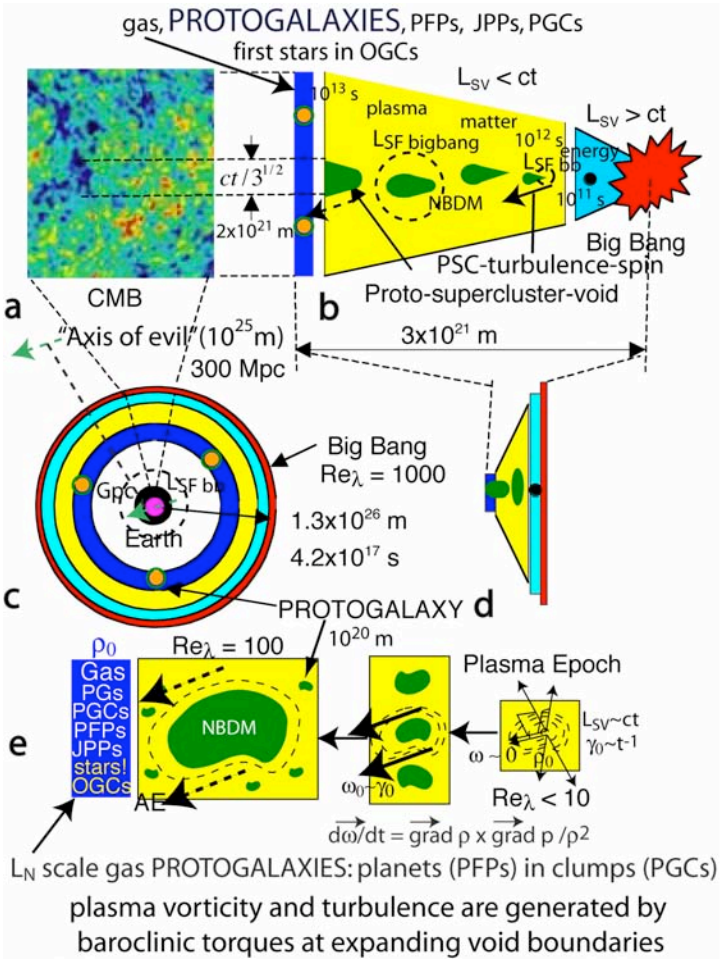

Figure 1. Protogalaxy formation at the end of the plasma epoch by hydro-gravitational-dynamics HGD theory. a. Cosmic Microwave Background temperature anisotropies reflect structures formed in the plasma epoch. b. From HGD the photon viscosity of the plasma epoch prevents turbulence until the viscous Schwarz scale L_{SV} becomes less than the Hubble scale (horizon scale, scale of causal connection) $L_H = ct$, where c is the speed of light and t is the time. The first plasma structures were proto-super-cluster voids and proto-super-clusters at 10^{12} seconds (30,000 years). c. Looking back in space is looking back in time. Protogalaxies were the last fragmentations of the plasma (orange circles with green halos) at 10^{13} seconds. d. The scale of the gravitational structure epoch is only $3x10^{21}$ m compared to present supercluster sizes of 10^{24} m and the largest observed supervoid scales of 10^{25} m. e. Turbulence in the plasma epoch is generated by baroclinic torques on the boundaries of the expanding super-voids.

During inflation, turbulent temperature fluctuations are fossilized by stretching beyond the scale of causal connection L_H. The mass-energy and entropy vastly increase, presumably by the rapid stretching of superstrings with Planck tension $c^4/G = 1.2x10^{44}$ kg m s^{-2} [21]. The black dot in the inflation epoch symbolizes fossilized turbulent temperature fluctuations that can guide nucleosynthesis and preserve big bang turbulence information for testing using CMB temperature anisotropy patterns. In a period of 10^{-27} seconds the size of the big bang universe increases from 10^{-27} m to a few meters with density exceeding 10^{80} kg m^{-3}. The mass-energy of the universe within our present horizon scale $L_H = 10^{26}$ m is about 10^{52} kg, about 10^{-40} of the mass-energy created by the big bang. The mass-energy of the universe before inflation was less than 10^{16} kg so the increase was by a factor of 10^{74}. Guth describes this as the ultimate free lunch [21].

The transition between energy domination and mass domination occurred at about 10^{11} s, the beginning of the plasma epoch shown in Fig. 1b. The plasma is absolutely unstable and will fragment once the Schwarz viscous scale L_{SV} matches the horizon scale L_H. This occurs at time $t = 10^{12}$ s when the density of a flat universe is 10^{-15} kg m^{-3}. Most of this density, about 97%, is non-baryonic dark matter, NBDM, presumably some combination of neutrinos. The rest is plasma. None of it is dark energy. This gives a primordial density ρ_0 of $4x10^{-17}$ kg m^{-3}, which matches the density of old globular star clusters OGC. Because the universe continues to expand, fragmentation of the plasma at density minima is favored over condensation at density maxima. Voids appear in the plasma at 10^{12} seconds and proceed to expand as rarefaction waves at speeds limited by the speed of sound $c/3^{1/2}$ for 10^{13} seconds until decoupling. The material between the protosupercluster voids is protosuperclusters with mass 10^{46} kg, that of a thousand galaxies. The proto-super-clusters never collapse gravitationally but continue to expand with the universe. This is a key point; instead of a messy chaotic formation scenario of mergers the expansion was tranquil and preserved primordial alignments and densities. The present scale of superclusters is observed to be 10^{24} m.

Smaller scale fragmentations occur in the plasma epoch at density minima up to the time of plasma to gas transition (decoupling). The last fragmentation is to produce protogalaxies at 10^{13} seconds, as shown in Fig. 1b. The morphology of the protogalaxies is determined by weak turbulence generated by baroclinic torques on the surfaces of the supervoids as they expand. The direction of the spins is determined by the fossil strong force freeze-out density gradient at length scale L_{SF}. This spin direction determines the small wavenumber spherical harmonic directions for the CMB, the spins of galaxies in the local group, and even the spin of the Milky Way. All are directed toward the “axis of evil” [17], which has length scales in quasar polarizations to a Gpc, or $3x10^{25}$ m, as shown in Fig. 1c.

Figure 2 illustrates erroneous concepts of cold dark matter hierarchical clustering (CDMHC) theory, which is at present the standard cosmological model along with the equally erroneous concept of dark energy and a cosmological constant Λ (ΛCDMHC). The standard model has no turbulence in the big bang but predicts Gaussian scale independent fluctuations and white noise spectrum of CMB fluctuations from the big bang and inflation epochs. All structure formation in the plasma epoch is attributed to the non-baryonic dark matter NBDM.

According to CDMHC seeds or halos of CDM form because their Jeans scale L_J is less than L_H. This is physically impossible because the diffusivity of any form of NBDM will cause the diffusive Schwarz scale L_{SD} of the material to exceed L_H. Even if a seed could form it could not stick to another seed because sticking requires collisions of the CDM particles, no matter how cold they might be. In Fig. 2 each erroneous CDM concept is indicated by a red X.

It is claimed by CDMHC that the baryonic matter plasma is inviscid and falls into the CDM halos where it oscillates without viscous damping to give the acoustic peaks observed in the CMB temperature anisotropy spectrum. However, the plasma is far from inviscid, with a photon viscosity of $\nu = 4x10^{26}$ m^2 s^{-1} [11]. Even if CDM halos existed, the plasma is far too viscous to enter the halo and oscillate acoustically.

Other erroneous concepts of CDMHC are listed in Fig. 2. The CDM halos gradually cluster and collect gas for 300 My of dark ages (10^{16} s) in mini-galaxies which form the first superstars, one per mini-galaxy, in an enormous set of supernovae that re-ionizes all the gas formed at decoupling. The re-ionization concept is unnecessary to explain the lack of UV-absorbing gas as observed in quasar spectra because the gas is sequestered as dark matter planets in PGC clumps.

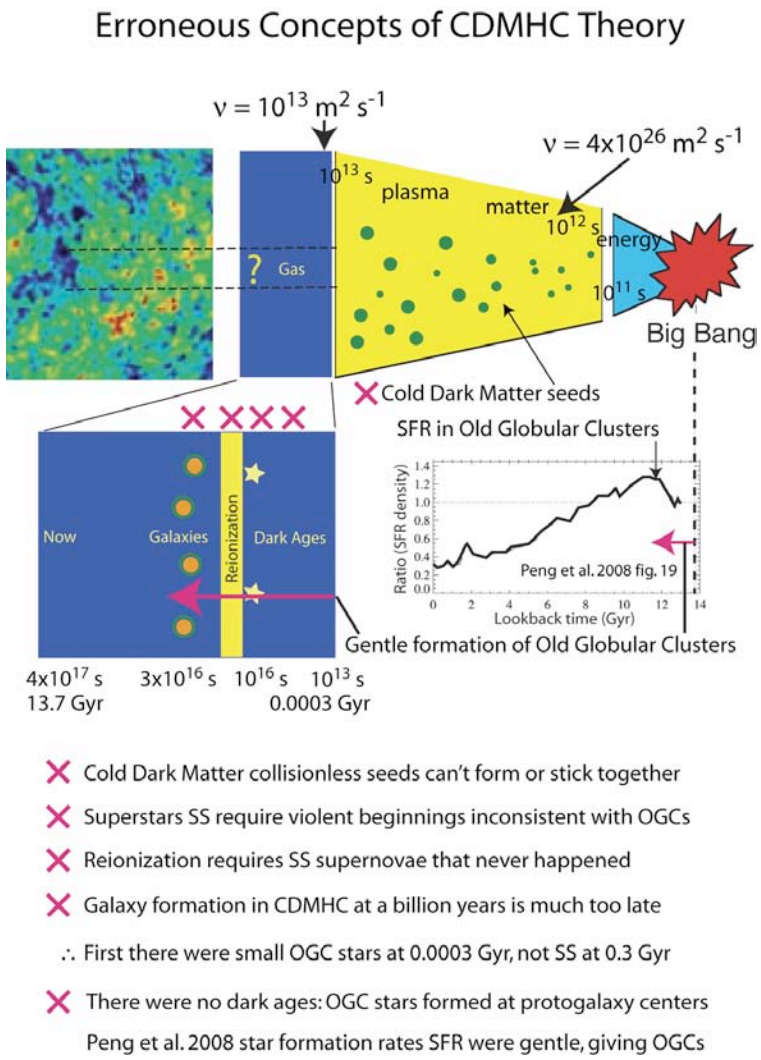

Figure 2. Galaxy formation by the standard ΛCDM model is impossible to reconcile with observations and fluid mechanical theory (see text). Failed aspects of the model are indicated by red Xs.

The first CDMHC galaxies to form occur much too late to be consistent with observations, at about a billion years after the big bang ($3x10^{16}$ s). The star formation rate SFR in Peng et al. 2008 Fig. 19 [23] cannot be superstars because superstars can only occur supported by violent turbulence stresses that would prevent formation of the very small stars observed to exist in old globular star clusters OGC.

From HGD and the mass of small stars it is easy to show from the Schwarz length scale criteria of Table 1 that the maximum viscous dissipation rate ε to permit the formation of

a small OGC star is 10^{-12} m^2 s^{-3}. However, strong turbulence is required with ε values of $5x10^{-4}$ m^2 s^{-3} to permit formation of superstars and the re-ionization of the universe. If such large ε values existed before the first star formed, no old-globular-clusters OGCs could have formed because their small stars would be inhibited by turbulence produced as NBDM CDM halos filled with baryonic gas. Since OGCs are observed in all galaxies, the superstars and re-ionization concepts of CDMHC must be ruled out.

OBSERVATIONS

The fifth year WMAP observations of the CMB have been released, as shown in Figure 3. Fig. 3a shows the Dunkley et al. 2008 5th year WMAP spherical harmonic temperature anisotropy data, with un-binned samples as light dots in the background [24].

The range of the un-binned samples in Fig. 3a is a measure of the intermittency (non-Gaussianity) of the turbulence associated with the samples. The range indicated by circles and arrows is smaller at the sonic peak than at higher wavenumbers. This is attributed to the weak turbulence produced in the plasma at the boundaries of the expanding supervoids. The wider scatter at high wavenumbers k is attributed to the greater intermittency of big bang turbulence, which has a higher Reynolds number. An Obukhov-Corrsin turbulent mixing spectrum $\beta\chi\varepsilon^{-1/3}k^{-5/3}$ is fitted to the lowest wavenumber CMB spectrum, where β is a universal constant, χ is the dissipation rate of temperature variance and ε is the dissipation rate of velocity variance. It is assumed that the measured spherical harmonic CMB spectrum multiplied by l(1+l) is not much different than a turbulent dissipation spectrum $k^2\phi$.

The red solid curve labeled CDM+ν=0 in Fig. 3a is a CDM model without viscosity forced by ad hoc (GIGO) numerical assumptions to fit the data. Photon viscosity will not permit the baryonic plasma to enter the CDM potential wells even if they were physically possible, and will not permit any sonic oscillations because of viscous damping. Therefore the green dashed curve from big bang turbulence theory labeled CDM+ν should apply.

Evidence of turbulence from the expansion of super-voids producing baroclinic torques and vorticity at void boundaries is shown by a series of turbulence statistical parameters computed by Bershadskii and Sreenivasan from the low wavenumber CMB spectrum in Fig. 3b, 3c, and 3d and compared to the same parameters computed for atmospheric, laboratory and numerical simulations of turbulence over a wide range of Reynolds numbers.

Figure 3b compares Weiner-filtered CMB data with extended self similarity turbulence data for various order structure functions. The agreement clearly demonstrates the CMB

temperature anisotropies in the indicated angular size range 0.5 to 4 degrees studied were produced by turbulence. From HGD the turbulence reflects baroclinic torques at gravitationally driven expanding void boundaries.

Figure 3c compares the same CMB and turbulence data using a statistical parameter to test for Gaussianity. Again, the agreement with turbulence is remarkable. Both sets of CMB and turbulence data deviate from Gaussianity in the same way in the angular size range studied.

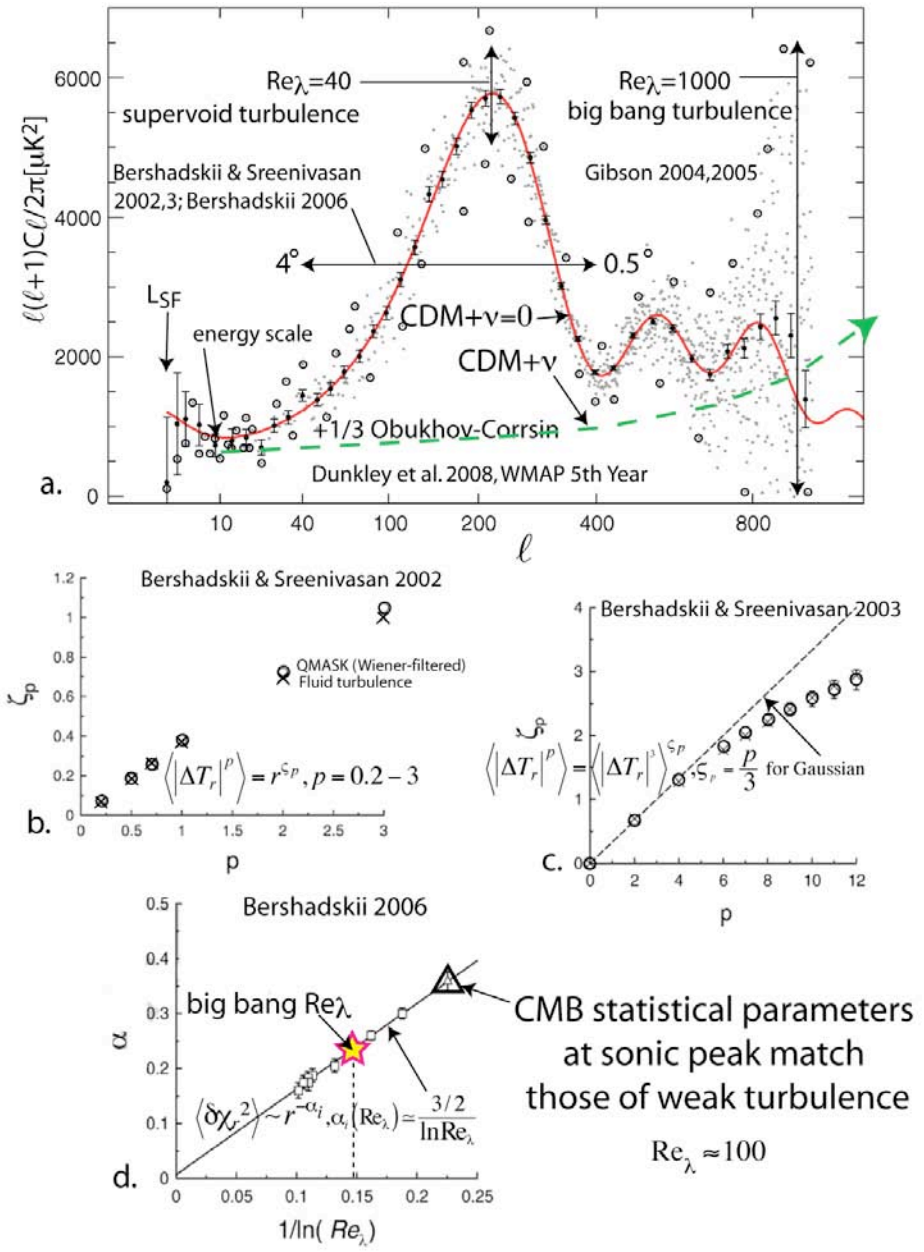

Figure 3. a. Spherical harmonic spectrum of CMB temperature anisotropies from the fifth year WMAP observations, Dunkley et al. 2008 [24]. The large sonic peak at wavenumbers near 200 reflects weak turbulence produced by gravitationally driven protosupervoid expansion according to Fig. 1, not inviscid CDM (solid red). The dashed green line represents a viscous CDM model; that is, with no sonic signal and should match the +1/3 Obukhov-Corrsin turbulent mixing dissipation spectrum of big

bang turbulence. Turbulence parameters are compared to CMB statistics in b. [25], c. [26] and d. [27] as described in the text.

Figure 3d shows an estimate of the sonic peak Reynolds number estimated by Bershadskii 2006 to be about $Re_\lambda \sim 100$. A more precise estimate is $Re_\lambda = 40$ as shown near the peak, using the expression derived for the temperature anisotropy variance as a function of separation distance r between sampling points. The power law exponent is a function of Re_λ. The value of Re_λ for the CMB is extracted using a series expansion of $\alpha(Re_\lambda)$ for high Reynolds number as a function of $1/\ln Re_\lambda$. It turns out for turbulence that only the first term is important, as shown, so that the CMB data near the sonic peak gives $Re_\lambda = 40$ as indicated by the bold triangle. For comparison, the big bang turbulence Re_λ value of 1000 is shown by a bold star. There can be little doubt from the combination of evidence shown in Fig. 3 abcd that the plasma epoch was weakly turbulent in the range of scales including the sonic peak. As noted by Alexander Bershadskii (2001 personal communication to CHG) "the fingerprints of Kolmogorov are all over the sky".

As shown in Fig. 1e, the last stage of plasma fragmentations guided by weak turbulence is the formation of proto-galaxy-mass objects with a linear morphology reflecting vortex tubes of the turbulence where the rates-of-strain that enhance fragmentation of the plasma to form voids is maximum.

Figure 4 (bottom) is an image from the Hubble Space Telescope Advanced Camera for Surveys (HST-ACS) showing two proto-galaxy-chain clusters in the dim background of the Tadpole galaxy merger. Virtually all (94%) very dim galaxies from HST-ACS; that is, with magnitudes greater than 24, have such a linear morphology as expected from HGD [15]. The objects consist of bright nuclei separated by a dimmer glow that we interpret as proto-galaxies with a concentration of first-stars near the cores, with star-forming galaxy dark matter (planets in clumps) in between.

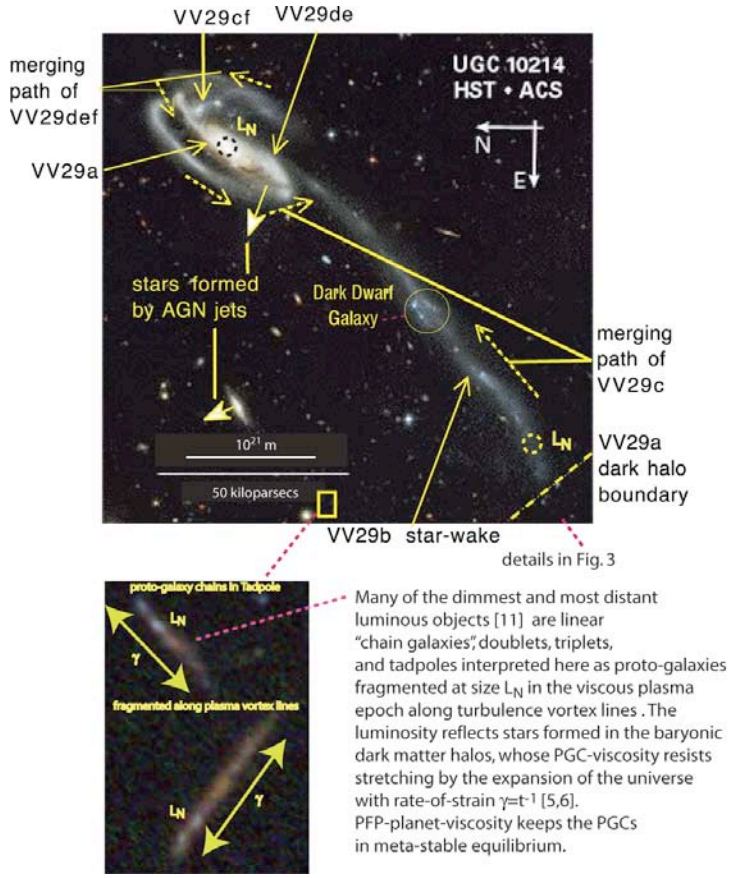

Figure 4. Tadpole galaxy merger (top), with background chains of protogalaxies shown in enlargement of small area at bottom center (bottom).

The star-clumps have a uniform size set by the turbulence and fluid mechanics to be the Nomura scale 10^{20} m (Table 1) with the Nomura morphology of weak turbulence [15].

Fig. 4 (top) shows the formation of star trails and dust trails in the baryonic dark matter halo of the Tadpole central galaxy VV29a as galactic objects VV29cdef merge in frictional spirals on the VV29a disk plane [19]. A sharp VV29a dark halo boundary is clear in the high-resolution HST-ACS images. The eponymous VV29b spiral filament shows numerous young globular star clusters [28] aligned in a direction pointing precisely at the point of frictional merger as the objects move through the dark matter halo triggering star formation by tidal forces in a L_N scale diameter star wake. The size of VV29a dark matter halo diffused from the L_N scale central core of old small stars is $8x10^{21}$ m, or 0.9 Mpc. From this evidence, the concept of frictionless tidal tails in galaxy mergers appears to be obsolete [29].

CONCLUSION

A fluid mechanical analysis of gravitational structure formation termed hydro-gravitational-dynamics HGD shows that the CDMHC model is inconsistent with theory and observations and must be abandoned. From HGD, gravitational structure formation is driven entirely by the baryonic matter of the plasma epoch. The first structures are proto-super-cluster-voids and proto-super-clusters, followed by proto-galaxies at decoupling. The proto-galaxies are formed in very weakly turbulent plasma, but possess the morphology of weak turbulence in that the protogalaxies are stretched along the vortex lines of the plasma turbulence with a diameter reflecting their viscous-inertial-vortex-gravitational origin at the Nomura scale 10^{20} m. Although our description of HGD seems to emphasize turbulence processes, the universe described is in fact more tranquil than previously envisioned, and can preserve primordial alignments seen in many cosmological structures, in particular proto-galaxies.

REFERENCES

1. Darwin, G. H. 1889. On the mechanical conditions of a swarm of meteorites, and on theories of cosmogony, Phil. Trans., 180, 1-69.
2. Jeans, J. H. 1902. The stability of spherical nebula, Phil. Trans., 199A, 0-49.
3. Gibson, C.H. (1991). Kolmogorov similarity hypotheses for scalar fields: sampling intermittent turbulent mixing in the ocean and galaxy, Proc. Roy. Soc. Lond. A, 434, 149-164.
4. Gibson, C. H. (2006). Turbulence, update of article in Encyclopedia of Physics, R. G. Lerner and G. L. Trigg, Eds., Addison-Wesley Publishing Co., Inc., pp.1310-1314.
5. Gibson, C. H. (1981). Buoyancy effects in turbulent mixing: Sampling turbulence in the stratified ocean, AIAA J., 19, 1394.
6. Gibson, C. H. (1968a). Fine structure of scalar fields mixed by turbulence: I. Zero-gradient points and minimal gradient surfaces, Phys. Fluids, 11: 11, 2305-2315.
7. Gibson, C. H. (1968b). Fine structure of scalar fields mixed by turbulence: II. Spectral theory, Phys. Fluids, 11: 11, 2316-2327.
8. Gibson, C. H. (1986). Internal waves, fossil turbulence, and composite ocean microstructure spectra," J. Fluid Mech. 168, 89-117.
9. Gibson, C. H. (1999). Fossil turbulence revisited, J. of Mar. Syst., 21(1-4), 147-167, astro-ph/9904237
10. Gibson, C.H. (1996). Turbulence in the ocean, atmosphere, galaxy and universe, Appl. Mech. Rev., 49, no. 5, 299–315.
11. Gibson, C.H. (2000). Turbulent mixing, diffusion and gravity in the formation of cosmological structures: The fluid mechanics of dark matter, J. Fluids Eng., 122, 830–835.

12. Gibson, C.H. (2004). The first turbulence and the first fossil turbulence, Flow, Turbulence and Combustion, 72, 161–179.
13. Gibson, C.H. (2005). The first turbulent combustion, Combust. Sci. and Tech., 177: 1049–1071, arXiv:astro-ph/0501416.
14. Gibson, C.H. (2006). The fluid mechanics of gravitational structure formation, astro-ph/0610628.
15. Gibson, C.H. (2008). Cold dark matter cosmology conflicts with fluid mechanics and observations, J. Applied Fluid Mech., Vol. 1, No. 2, pp 1-8, 2008, arXiv:astro-ph/0606073.
16. Gibson, C.H. & Schild, R.E. (2007). Interpretation of the Helix Planetary Nebula using Hydro-Gravitational-Dynamics: Planets and Dark Energy, arXiv:astro-ph/0701474.
17. Schild, R.E & Gibson, C.H. (2008). Lessons from the Axis of Evil, axXiv[astro-ph]:0802.3229v2.
18. Gibson, C.H. & Schild, R.E. (2007). Interpretation of the Stephan Quintet Galaxy Cluster using Hydro-Gravitational-Dynamics: Viscosity and Fragmentation, arXiv[astro-ph]:0710.5449.
19. Gibson, C.H. & Schild, R.E. (2002). Interpretation of the Tadpole VV29 Merging Galaxy System using Hydro-Gravitational Theory, arXiv:astro-ph/0210583.
20. Schild, R. 1996. Microlensing variability of the gravitationally lensed quasar Q0957+561 A,B, ApJ, 464, 125.
21. Greene, B. 1999. The Elegant Universe, Superstrings, Hidden Dimensions, and the Quest for the Ultimate Theory, W. W. Norton & Compant, New York.
22. Guth, A. H. 1997. The Inflationary Universe, The Quest for a New Theory of Cosmic Origins, Helix Books, Addison-Wesley Pub. Co., Inc., New York.
23. Peng, E. W. et al. 2008, The ACS Virgo Cluster Survey. XV. The Formation Efficiencies of Globular Clusters in Early-Type Galaxies: The Effects of Mass and Environment, ApJ, 681, 197-224.
24. Dunkley, J. et al. (2008). Five-year Wilkinson Microwave Anisotropy Probe (WMAP) Observations: Likelihoods and Parameters from the WMAP data, subm. ApJS; arXiv:0803.0586v1.
25. Bershadskii, A., and Sreenivasan, K.R. 2002. Multiscaling of cosmic microwave background radiation, Phys. Lett. A, 299, 149-152.
26. Bershadskii, A., and Sreenivasan, K.R. 2003. Extended self-similarity of the small-scale cosmic microwave background anisotropy Phys. Lett. A, 319, 21-23.
27. Bershadskii, A. 2006. Isotherms clustering in cosmic microwave background, Physics Letters A, 360, 210-216.
28. Tran, H. D., Sirianni, M., & 32 others 2003. Advanced Camera for Surveys Observations of Young Star Clusters in the Interacting Galaxy UGC 10214, ApJ, 585, 750.
29. Toomre, A., & Toomre, J. 1972. Galactic Bridges and Tails, ApJ, 178, 623.

SPIE Newsroom Dec. 1, 2007, re CORS Vol. 6680 26-27 Aug. 2007 Proceedings of SPIE

Vertical stratified turbulent transport mechanism indicated by remote sensing

Carl H. Gibson, R. Norris Keeler, Valery G. Bondur

Satellite and shipboard data reveal the intermittent vertical information transport mechanism of turbulence and internal waves that mixes the ocean, atmosphere, planets and stars.

Astronauts noticed they could see deep bottom features and internal waves within the ocean from space platforms (Figure 1), but were not believed because no known physical mechanism permits remote sensing through kilometers of opaque water. The information transport mechanism is generic to all large stratified intermittently turbulent bodies of natural fluid[1–8]. Vertical (radial) heat, mass, momentum and energy transport are affected. The mechanism involves turbulence[1], fossil turbulence[2] and nonlinear internal waves[3]. A three year series of oceanographic experiments were organized to test Russian claims they could detect submerged turbulence, internal waves, bottom depth and topography from space satellites.

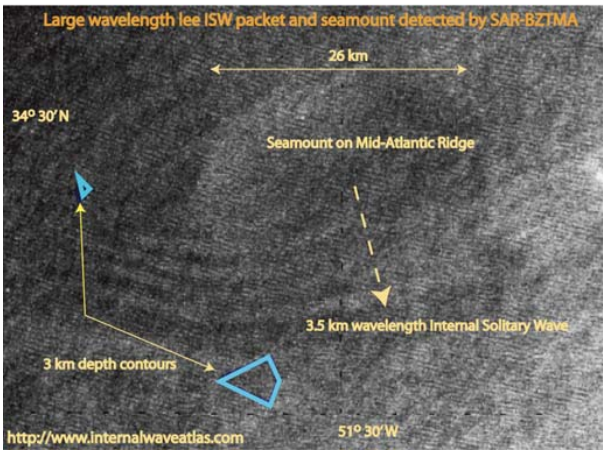

Figure 1. Seamount and internal tidal waves from space. How is this information transmitted?

The Remote Anthropogenic Sensing Program (RASP 2002, 2003, 2004) used the turbulent Honolulu wastewater outfall at Sand Island with full sea truth during space satellite observations. Buoyancy traps wastewater at depth 50 meters to prevent contamination of surface waters and beaches. Remarkably, outfall fossil and zombie turbulence[4] patches can dominate mixing in Mamala Bay at distances exceeding 20 km in areas exceeding 200 km^2.

The mechanism

[1] Turbulence is defined as an eddy-like state of fluid motion where the inertial-vortex forces $\vec{v} \times \vec{\omega}$ of the eddies are larger than any other forces that tend to damp the eddies out, where $\vec{v}$ is the velocity and $\vec{\omega}$ is the vorticity. Thus, turbulence always cascades from small scales to large.

[2] Fossil turbulence is defined as a perturbation in any hydrophysical field produced by turbulence that persists after the fluid ceases to be turbulent at the scale of the perturbation.

[3] When active turbulence cascades to the (Ozmidov scale) maximum vertical size permitted by buoyancy $L_R = \left(\varepsilon / N^3\right)^{1/2}$ it fossilizes, and the turbulent kinetic energy is radiated near vertically as fossil and zombie turbulence waves.

[4] Zombie turbulence is produced when density gradients of fossil turbulence patches are tilted by internal waves to create vorticity at rates $(\nabla\rho \times \nabla p) / \rho^2$.

SPIE Newsroom Dec. 1, 2007, re CORS Vol. 6680 26-27 Aug. 2007 Proceedings of SPIE

Figure 2 shows RASP data and how it was obtained and analyzed. Brightness anomaly wavelengths suggest Ozmidov scales at fossilization from strong turbulence events radiate narrow spatial-frequency packets of fossil turbulence waves near-vertically. Detected wavelengths (40-160 meters) are confirmed by thermistor-chain internal-wave measurements and surface-wave detectors. Horizontally towed and vertically dropped microstructure profilers contoured viscous and temperature dissipation rates and tested for hydrodynamic states of the patches. Intermittent mixing chimneys were detected.

The mechanism for vertical transport is termed "Beamed Zombie Turbulence Maser Action" (BZTMA), and occurs in intermittent mixing chimneys. The outfall fossil turbulence patches drift away from their source with ambient currents, and absorb energy from bottom generated fossil turbulence waves to form zombie turbulence and zombie turbulence waves in an efficient maser action that moves length-scale-information for the bottom waves to the sea surface where the zombie-turbulence-waves (ZTWS) break and permit its detection. Vertical ZTW chimneys follow paths of previous ZTWs, just as lightning flashes follow ionized paths of previous lightning flashes. The BZTMA mechanism is an extension of Kolmogorovian universal similarity theory with extensions to scalar mixing [2]. Consequently it is generic to natural fluids such as the ocean, atmosphere, planets and stars.

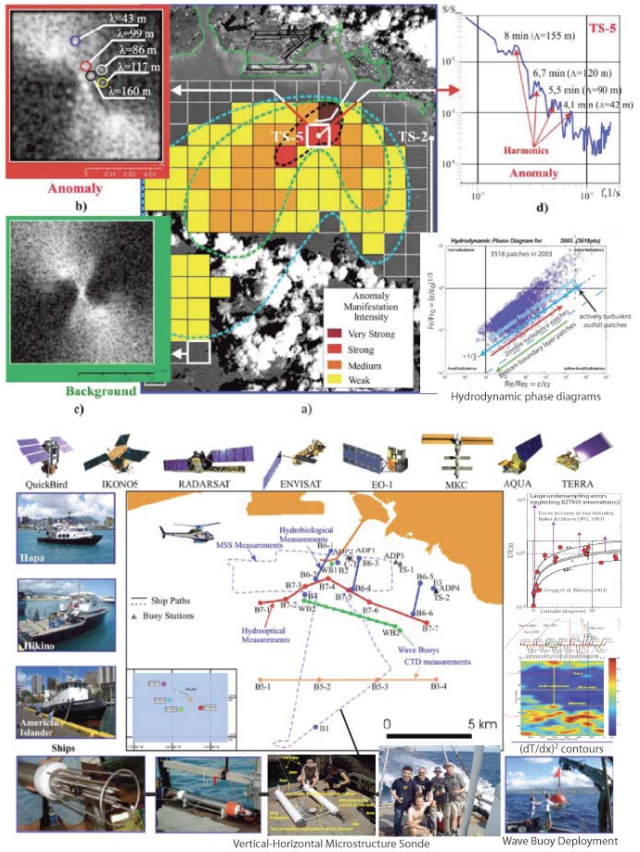

Figure 2. Sea surface brightness anomalies are detected [7] (top) by comparing 2D-spectra near the outfall (red) with background regions (green). Corresponding internal wavelengths (right) suggest fossil turbulence waves radiated from the bottom. Key RASP microstructure results are shown (bottom), with ships, satellites, microstructure detectors, platforms, and section paths.

Astrophysical implications

Application of modern fluid mechanics to astrophysics [8] reveals the dark matter of galaxies as thirty million Primordial-Fog-Particle earth-mass frozen-gas planets (PFPs) per star in Proto-Globular-star-Cluster-mass clumps (PGCs), but requires the use of BZTMA to explain why stars form and die in different ways and why it is not necessary to believe in dark energy. Figure 3 shows 12 decades of Kolmogorov-Corrsin-Obukhov electron density spectra from earth scales to PGC scales that require planetary atmospheres evaporated by nearby supernovae (II) and their resulting pulsars. This requires strong BZTMA mixing by planet accretion. Otherwise the carbon cores of stars will not be mixed away, giving supernovae Ia.

Conclusions

Stratified turbulent mixing in natural fluids is dominated by the most powerful turbulent events of a vertical column, which fossilize and radiate nonlinear internal waves near-vertically. These mix to form fossil turbulence patches, secondary zombie turbulence events, mixing chimneys and information transport to the surface by the BZTMA mechanism. This explains why deeply submerged seamounts and internal waves (Fig. 1) can be seen and why vast undersampling errors are typical in physical oceanography when fossil turbulence and fossil turbulence waves are neglected.

SPIE Newsroom Dec. 1, 2007, re CORS Vol. 6680 26-27 Aug. 2007 Proceedings of SPIE

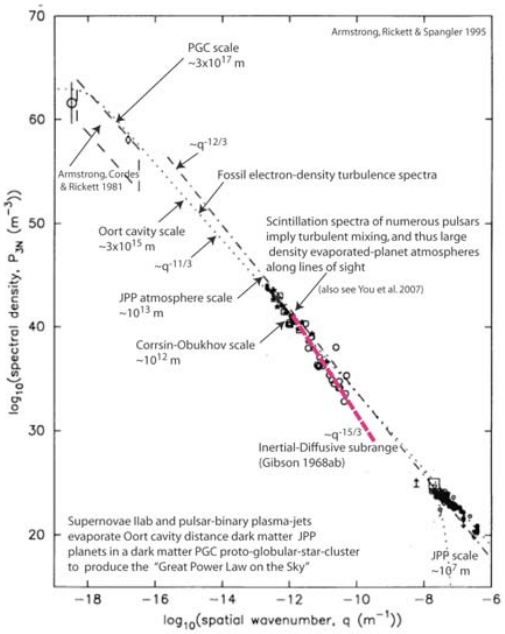

Figure 3. Application of BZTMA mixing theory to understand pulsar electron density fluctuation spectra and star formation from planets. Jovian PFP (primordial–fog-particle) Planets (JPPs) comprise the baryonic dark matter of all galaxies and develop turbulent atmospheres when evaporated by radiation from rapidly spinning white dwarf and neutron stars.

Author information

Prof. Carl H. Gibson is a faculty member of MAE and SIO Departments of UCSD and a member of the Center for Astrophysics and Space Sciences. He specializes in turbulence, fossil turbulence, turbulent mixing, and turbulent transport processes in the ocean, atmosphere, planets, stars, and cosmology. With Norris Keeler and Valery Bondur, he proposed tests, using the Honolulu municipal outfall, of Russian claims that submerged turbulence can be detected remotely from space satellites. The successful RASP 2002, 2003 and 2004 expeditions are reported in the SPIE 2007 CORS 6680 conference. Scripps Institution of Oceanog. Dept.,University of Cal. San Diego, La Jolla CA 92093-0411
USA, 858 534-3184. cgibson@ucsd.edu, sdcc3.ucsd.edu/~ir118

Dr. R. Norris Keeler headed the Physics Department of Lawrence Livermore National Laboratory, was President of the International High Pressure Society, Director of Materiel for the US Navy, and is now a Director of Directed Technologies, Inc. He initiated tests of Russian claims they could detect submerged turbulence by remote sensing, resulting in the RASP 2002, 2003 and 2004 expeditions and many scientific papers.
norris_keeler@directedtechnologies.com

Prof. Valery G. Bondur directs a large group of Russian specialists in remote sensing of geophysical parameters. He is a member of the Russian Academy of Sciences and President of the International Eurasian Academy of Sciences. He helped design and carry out the international Remote Anthropogenic Sensing Program (RASP) 2002, 2003 and 2004 expeditions reported in SPIE Coastal Ocean Remote Sensing Proceedings 6680, Aug. 2007. Aerocosmos Scientific Ctr. of Aerospace Monitoring, Moscow, Russia, vgbondur@online.ru

We wish to acknowledge Robert Arnone's invitation (to RNK) to contribute [1] to CORS 6680.

References

1. Gibson, C.H., Bondur, V.G., Keeler, R.N., Leung, P.T., Prandke, H., & Vithanage, D. 2007. Submerged turbulence detection with optical satellites, Proc. of SPIE, Coastal Remote Sensing, Aug. 26-27, edited by R. J. Frouin, Z. Lee, Vol. 6680, 6680X1-8. doi: 10.1117/12.732257

2. Gibson, C. H. 1991. Kolmogorov similarity hypotheses for scalar fields: sampling intermittent turbulent mixing in the ocean and Galaxy, Proc. Roy. Soc. Lond. 434, 149-164 (astro-ph/9904269)

3. Gibson, C.H. 1986. Internal waves, fossil turbulence, and composite ocean microstructure spectra, J. Fluid Mech., 168, 89-117.

4. Keeler, R. N., Bondur, V. G., and Gibson, C. H. 2005. Optical satellite imagery detection of internal wave effects from a submerged turbulent outfall in the stratified ocean, Geophys. Res. Lett., 32, L12610, doi:10.1029/2005GL022390.

5. Gibson, C.H., Bondur, V.G., Keeler, R.N. & Leung, P.T. 2006. Remote sensing of submerged oceanic turbulence and fossil turbulence, Int. J. Dyn. Fluids,, Vol. 2, No. 2, pp. 111-135.

6. Gibson, C.H., Bondur, V.G., Keeler, R.N. & Leung, P.T. 2008. Energetics of the beamed zombie turbulence maser action mechanism for remote detection of submerged oceanic turbulence, J. Appl. Fluid Mech., Vol. 1, No. 1, pp. 11-42.

7. Bondur V.G., Complex satellite monitoring of coastal water areas 2005. 31st International Symposium on Remote Sensing of Environment. ISRSE June 20-24, St. Petersburg, Russian Federation.

8. Gibson, C. H. & Schild, R. E. 2007. Interpretation of the Helix planetary nebula using hydro-gravitational-dynamics: planets and dark energy, astro-ph/0701474.

Wed. 2/22/06 16:30h OS36A-25 (46B-25) Ocean Sciences 2006 Feb. 20-24

Optical and Radar Satellite Detections of Submerged Turbulence

Carl H. Gibson (UCSD MAE and SIO Departments, La Jolla, CA, USA. cgibson@ucsd.edu)
Valery G. Bondur (Aerocosmos Scientific Center of Aerospace Monitoring, Moscow, Russia)
R. Norris Keeler (Directed Technologies, Arlington, VA, USA)
Pak Tao Leung (Department of Oceanography, Texas A&M University, TX, USA)

Results from the Remote Anthropogenic Sensor Program (RASP 2002-2004) are presented. Surface manifestations of stratified turbulence from the Honolulu Sand Island Municipal Outfall observed by Ikonos and Quickbird optical satellites are compared to horizontal and vertical microstructure sampling. Narrow spatial frequency band 30-250 m wavelength sea surface brightness anomalies were detected in the optical images at distances up to 20 km from the 70 m deep diffuser in SE and SW directions offshore matching GPS tracks of parachute drifters set at the diffuser near the 50 m trapping depths indicated by microstructure profiles of turbidity, salinity, temperature and density. Outfall fossil turbulence patches beam internal waves in an efficient maser action that transmits most of the stratified turbulent kinetic energy near-vertically. Fossil turbulence waves break to smooth the sea surface over the diffuser with increased near surface viscous and temperature dissipation rates. Advected outfall fossil turbulence patches extract energy from 30-250 m wavelength internal solitary waves in patterns transmitted to the sea surface in chimneys by zombie turbulence internal wave maser action. The detected solitary waves apparently originate as fossil turbulence waves from bottom boundary layer turbulence events at length scales reflecting Ozmidov scales at fossilization. Strong mixing by the beamed zombie turbulence maser action (BZTMA) mixing chimney mechanism was observed following a rain event that advected outfall fossil turbulence patches far offshore. Mixing detected by SAR images extended to distances of 45 km and by optical images to 20 km. Outfall fossil turbulence patch lifetimes were thousands of stratification periods. Thorpe overturn scales and hydrodynamic phase diagram classifications were computed for nearly 20K microstructure patches. Because the BZTMA mixing mechanism is oriented vertically it affects many problems of oceanic mixing and remote sensing of submerged turbulence. The deep dark mixing paradox is resolved since vertical sampling methods will probably under sample such an intermittent nonlinear process driven by rare bottom turbulence events. Visibility of the bottom and large tidal solitons in deep water by SAR and astronauts can be understood as surface manifestations of turbulence produced by these features directly coupled to the surface by BZTMA. Internal tides become the effect of strong turbulent mixing over topography rather than its cause. The cascade of tidal energy is directly from barotropic tides to bottom turbulence, which causes a complex cascade of internal waves and more turbulence on a wide range of scales.

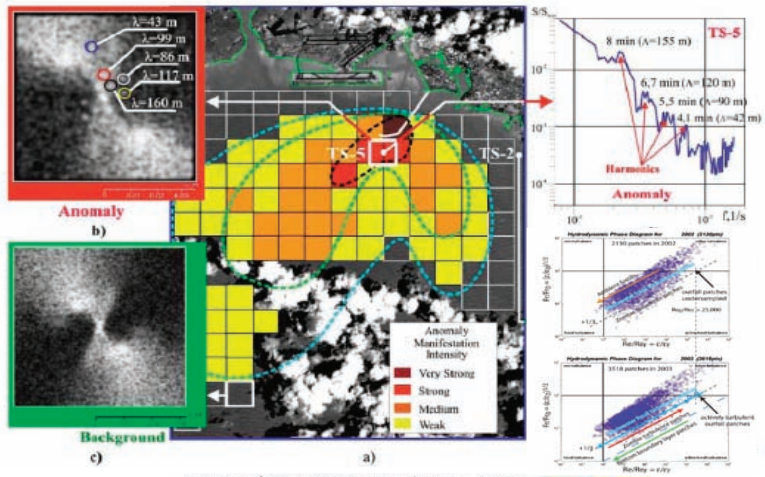

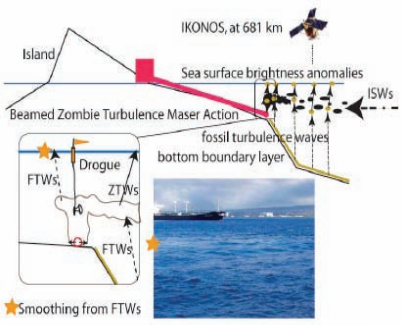

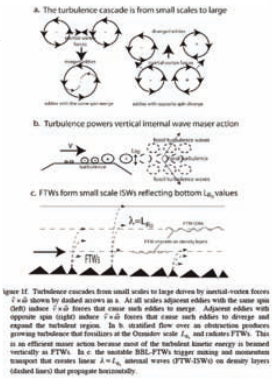

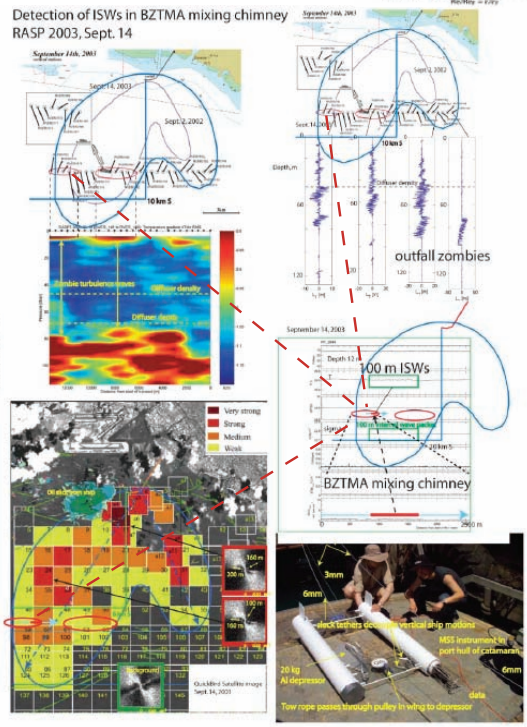

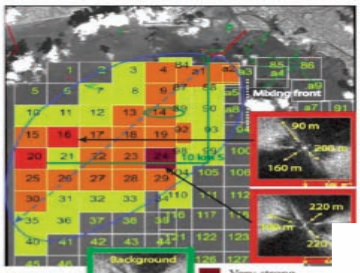

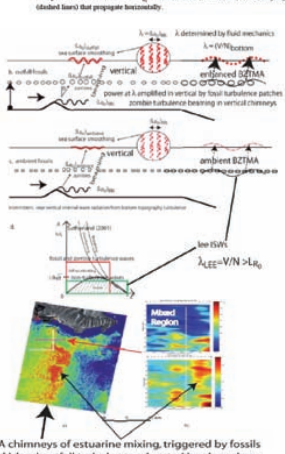

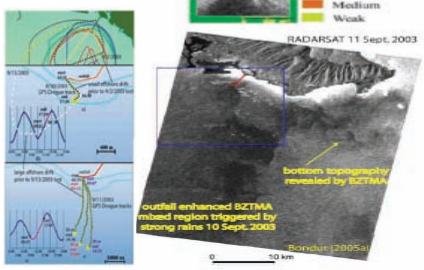

BZTMA chimneys of estuarine mixing, triggered by fossils of Sand Island outfall turbulence advected by alongshore tidal motions and strong offshore flows from Sept. 10 rains
Sept. 11, 2003 RADARSAT radar image

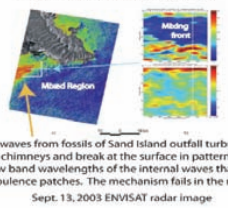

BZTMA waves from fossils of Sand Island outfall turbulence rise in mixing chimneys and break at the surface in patterns that reveal the narrow band wavelengths of the internal waves that power the zombie turbulence patches. The mechanism fails in the mixed regions.
Sept. 13, 2003 ENVISAT radar image

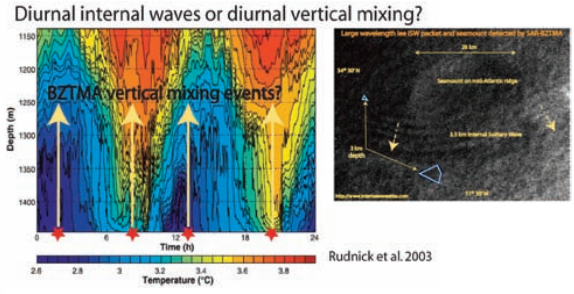

Rudnick et al. 2003

See http://www-acs.ucsd.edu/~ir118

Hydro-Gravitational-Dynamics of Planets and Dark Energy

Carl H. Gibson [1,2]

[1] University of California San Diego, La Jolla, CA 92093-0411, USA
[2] cgibson@ucsd.edu, http://sdcc3.ucsd.edu/~ir118

and

Rudolph E. Schild[3,4]

[3] Center for Astrophysics, 60 Garden Street, Cambridge, MA 02138, USA
[4] rschild@cfa.harvard.edu

Abstract: Self-gravitational fluid mechanical methods termed hydro-gravitational-dynamics (HGD) predict plasma fragmentation 0.03 Myr after the turbulent big bang to form protosuperclustervoids, turbulent protosuperclusters, and protogalaxies at the 0.3 Myr transition from plasma to gas. Linear protogalaxyclusters fragment at 0.003 Mpc viscous-inertial scales along turbulent vortex lines or in spirals, as observed. The plasma protogalaxies fragment on transition into white-hot planet-mass gas clouds (PFPs) in million-solar-mass clumps (PGCs) that become globular-star-clusters (GCs) from tidal forces or dark matter (PGCs) by freezing and diffusion into 0.3 Mpc halos with 97% of the galaxy mass. The weakly collisional non-baryonic dark matter diffuses to > Mpc scales and fragments to form galaxy cluster halos. Stars and larger planets form by binary mergers of the trillion PFPs per PGC on 0.03 Mpc galaxy accretion disks. Star deaths depend on rates of planet accretion and internal star mixing. Moderate accretion rates produce white dwarfs that evaporate surrounding gas planets by spin-radiation to form planetary nebulae before Supernova Ia events, dimming some events to give systematic distance errors misinterpreted as the dark energy hypothesis and overestimates of the universe age. Failures of standard ΛCDM cosmological models reflect not only obsolete Jeans 1902 fluid mechanical assumptions, but also failures of standard turbulence models that claim the cascade of turbulent kinetic energy is from large scales to small. Because turbulence is always driven at all scales by inertial-vortex forces $\vec{v} \times \vec{\omega}$ the turbulence cascade is always from small scales to large.

1. Introduction

Dimness of supernovae Ia (SNe Ia) events for redshift values $0.01 < z < 2$ have been interpreted as an accelerating expansion rate for the universe [1-3]. The acceleration is attributed to mysterious antigravity effects of "dark energy" and a cosmological constant Λ. Dimming is observed at all frequencies by about 30%, with large scatter attributed to uncertainty in the SNe Ia models. Hubble Space Telescope Advanced Camera for Surveys (HST/ACS) images have such high signal to noise ratios that both the scatter and the dimming are statistically significant over the full range of z values. Bright SNe Ia observed for $z \geq 0.46$ exclude "uniform grey dust" systematic errors, supporting flat-universe deceleration until the recent "cosmic jerk" to acceleration for $z \leq 0.46$. The "dark energy" interpretation is a consequence of the commonly accepted Λ-cold-dark-matter (ΛCDM) cosmological theory. However, ΛCDM theory is fluid mechanically untenable. The theory assumes irrotational, collisionless and frictionless flows and neglects viscosity, turbulence[1], diffusion, fossil turbulence and fossil turbulence waves. Hydro-gravitational-dynamics (HGD) is the application of modern fluid mechanics to cosmology [11-16]. As predicted by HGD, primordial planets in protoglobularstarcluster clumps formed at $z = 1100$, $t = 10^{13}$ s comprise the dark matter of galaxies and the source of all stars. Because dying stars may be dimmed by gas planets evaporated near the

[1] Turbulence [4,5] is defined as an eddy-like state of fluid motion where the inertial-vortex forces of the eddies are larger than any other forces that tend to damp the eddies out. Turbulence by this definition always cascades from small scales to large, starting at the viscous-inertial-vortex Kolmogorov scale at a universal critical Reynolds number. The mechanism of this «inverse» cascade is merging of adjacent vortices with the same spin due to induced inertial vortex forces that force eddy mergers at all scales of the turbulence. Such eddy mergers account for the growth of turbulent boundary layers, jets and wakes. A myth of turbulence theory is that turbulence cascades from large scales to small. It never does, and could not be universally similar if it did. Irrotational flows cannot be turbulent by definition. In self-gravitational fluids such as stars and planets, turbulence is fossilized in the radial direction by buoyancy forces. Radial transport is dominated by fossil turbulence waves and secondary (zombie) turbulence and zombie turbulence waves in a beamed, radial, hydrodynamic-maser action.

star, planets provide an alternative to dark energy. New physical laws are not required by HGD but ΛCDM must be discarded. The choice is between planets and dark energy.

The definition of turbulence and its implied small-to-large cascade direction for turbulent energy transfer [5] matches that used [4] to extend the well-known Kolmogorov universal similarity laws of turbulence to stably stratified turbulent mixing of scalar fields like temperature and electron density with variable Prandtl number $\mathrm{Pr} = \alpha/\nu$, where α is thermal diffusivity and ν is kinematic viscosity [6-8]. Substantial evidence supports these similarity laws, the universal constants of second order structure functions and energy spectra, as well as intermittency constants that arise with " Kolmogorov third law" refinements despite claims to the contrary [9]. The direction of the turbulent energy cascade and the definition of turbulence depend on the Navier-Stokes equations written so the nonlinear $\vec{v}\times\vec{\omega}$ term causing turbulence is isolated ($\vec{\omega} = \nabla\times\vec{v}$)

$$\partial\vec{v}/\partial t = \nabla B + \vec{v}\times\vec{\omega} + \vec{F}_{Viscous} + \vec{F}_{Buoyancy} + \vec{F}_{Coriolis} + \vec{F}_{Other} \qquad (1)$$

where $\vec{v}$ is the fluid velocity, B is the Bernoulli group of mechanical energy terms $v^2 + p/\rho + lw$, and the various fluid forces listed tend to damp out turbulent motions driven by $\vec{v}\times\vec{\omega}$. The kinetic energy per unit mass v^2, the specific enthalpy p/ρ and frictional lost work lw in B are generally constant along streamlines in natural hydrodynamic flows so their gradient can be neglected. The ratio of $\vec{v}\times\vec{\omega}$ to the viscous, buoyancy and Coriolis forces defines the Reynolds, Froude and Rossby numbers, respectively. For a flow to be turbulent, universal critical values of Re, Fr and Ro must be exceeded. The direction of the turbulence kinetic energy cascade is not essential to most laboratory studies, but it is crucial to natural flows where fossil turbulence[2] and fossil turbulence waves are important to preserve information about previous turbulence and turbulent fluxes and as components of the dynamical transport mechanism. Most temperature and salinity microstructure in the ocean is fossil turbulence because no mechanism besides molecular diffusion exists to erase these signatures of previous turbulence, even though the kinetic energy of the turbulence at the scale of the fossils has long since radiated away as internal wave motions, termed fossil turbulence waves.

Fossil turbulence patches are identified by means of hydrodynamic phase diagrams Fr_{Patch} versus Re_{Patch}[9]. It is shown that

$$\mathrm{Fr}_{\mathrm{Patch}} = \mathrm{Fr}/\mathrm{Fr}_0 = \left(\varepsilon/\varepsilon_0\right)^{1/3} = \left(\varepsilon/3L_{T0}{}^2N^3\right)^{1/3} \qquad (2)$$

and

$$\mathrm{Re}_{Patch} = \varepsilon/\varepsilon_F = \varepsilon/35\nu N^2, \qquad (3)$$

where dissipation rates ε are normalized by Fr and Re values estimated by fossil turbulence theory assuming the cascade of turbulence is from small scales to large. From (2) we see that the Thorpe overturning scale L_{T0} at the beginning of fossilization in a fossilized microstructure patch may be much larger than the overturning scale at the time of sampling [10]. Without a turbulence definition based on $\vec{v}\times\vec{\omega}$ and a turbulence cascade from small scales to large the signatures of fossil turbulence are not unique. Thousands of hydrodynamic phase diagrams are available from oceanic microstructure studies that demonstrate the dynamics of fossil turbulence formation, contradicting the common oceanographic assumption that fossil turbulence does not exist and the common turbulence assumption that turbulence cascades from large scales to small [4,6,9,10].

[2] Fossil turbulence [4,6,9,10] is a perturbation in any hydrophysical field caused by turbulence that persists after the fluid is no longer turbulent at the scale of the perturbation.

Turbulent kinetic energy dissipates to heat at viscous Kolmogorov scales $L_K = \left(\nu^3/\varepsilon\right)^{1/4}$, so it is reasonable to assume that it cascades down to this scale from some larger scale where it originates. This is the standard turbulence model, expressed by the poem of L. F. Richardson 1922 in all turbulence textbooks. However, the flows from which turbulence extracts energy are irrotational at large scales with $\vec{v}\times\vec{\omega}$ nearly zero, so they are non-turbulent by definition. Turbulent kinetic energy is not only dissipated at the Kolmogorov scale, but is also produced at L_K. Adjacent eddies with the same spin induce $\vec{v}\times\vec{\omega}$ forces on each other in directions that cause the eddies to merge, which is the physical mechanism of the small-to-large turbulent energy cascade.

An example is merging of eddies formed in a boundary layer, which grow and induce $\vec{v}\times\vec{\omega}$ forces away from the boundary layer causing boundary layer separation. Adjacent eddies with opposite spin induce translational and divergence forces that cause ingestion of irrotational external flows into the interstices of the turbulence down to viscous scales where they acquire spin and can be classified as turbulence. In natural flows such as the ocean, atmosphere and galaxy, turbulent flows are limited by buoyancy, Coriolis and other forces at large scales. Most of the turbulent kinetic energy produced at Kolmogorov scales is not dissipated as heat but is radiated or stored as waves. Information about previous turbulence events is stored by a variety of hydrophysical fields such as temperature and electron density by fossil turbulence remnants. Because turbulence events in natural flows are quite brief compared to the persistence time of fossil turbulence, most of the microstructure of the ocean, atmosphere and galaxy are turbulent fossils.

Turbulence is absolutely unstable. A vortex sheet thickens to a Kolmogorov scale L_K starting from zero in a Kolmogorov time $T_K = \left(\nu/\varepsilon\right)^{1/2}$ when the first eddies appear. The cascade of turbulent kinetic energy is to larger scales because the overturn time $T_{Overturn} = L^{2/3}\varepsilon^{-1/3}$ increases with the overturn scale L (from Kolmogorov's second similarity hypothesis). Similarly, self gravitation is absolutely unstable [12]. Starting from a mass perturbation $M'(t_0)$ at the origin of a motionless large body of uniform density fluid with no forces other than gravity, the mass will grow or decrease with time depending on the sign of the perturbation and the gravitational free fall time $\tau_g = \left(\rho G\right)^{-1/2}$, where G is Newton's gravitational constant and ρ is the density. The perturbation

$$M'(t) = \left|M'(t_0)\right|\exp\left[\pm 2\pi\rho G t^2\right] = \left|M'(t_0)\right|\exp\left[\pm 2\pi\left(t/\tau_g\right)^2\right] \qquad (4)$$

suddenly grows exponentially to infinity with time if the perturbation $M'(t_0)$ is positive. If the perturbation $M'(t_0)$ is negative the density suddenly decreases exponentially to zero forming a void at the free fall time. Before either of these singularities are reached, viscous forces or turbulence forces or molecular diffusivity effects will appear to cushion the gravitational collapse or fragmentation. The effect will occur at the largest of three Schwarz scales [11,12]; that is, at

$$L = L_{SX} = \max\left[L_{SV}, L_{ST}, L_{SD}\right] \qquad (5)$$

where $L_{SV} = \left(\nu\gamma/\rho G\right)^{1/2}$, $L_{ST} = \left(\varepsilon/\left[\rho G\right]^{3/2}\right)^{1/2}$, and $L_{SV} = \left(D^2/\rho G\right)^{1/4}$.

A simple demonstration of the direction of the turbulence cascade is to fill a bottle completely with water with a powder (say paprika) to show the small scale motions. It is impossible to make the interior fluid turbulent without spinning the bottle. Large scale motions have no effect, but spin causes turbulence to form from shears at the solid-liquid interface and the turbulence cascade from

small scales to large fills the bottle with turbulent motions. The spectral cascade is illustrated in Fig. 0, where nearly motionless fluid becomes turbulent by spinning the bottle at constant angular velocity. Initially the turbulent kinetic energy spectrum $\phi(k)$ has a small range of wavenumbers k and small mean-square velocity integral $\int \phi(k)dk = \langle v^2 \rangle$, all in a narrow range $k_2 > k_{BL2} = (5L_{K2})^{-1}$. The turbulence of the boundary layer cascades to the bottle scale $L_{bottle} > 5L_K$ at stage 4 and then is damped by viscosity in stages 5 and 6 as the fluid reaches solid body rotation.

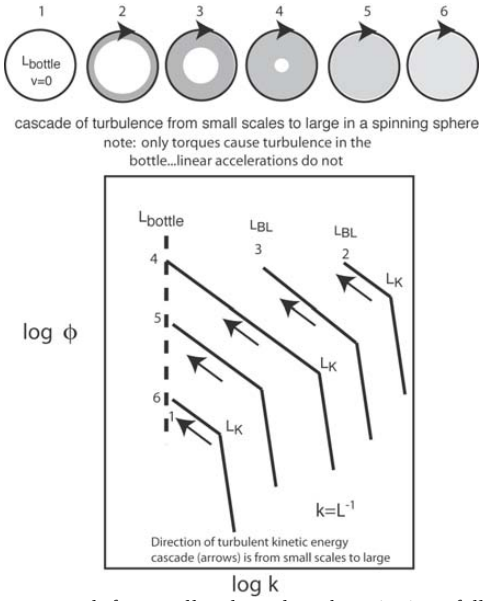

Fig. 0. Demonstration of the turbulence cascade from small scales to large by spinning a full bottle of fluid from rest with constant angular velocity. Turbulence forms at the boundaries of the bottle starting with $L_{BL2} \approx 5L_K$ and grows till the larges scale of the turbulence matches the bottle size. The direction of the energy cascade is shown by arrows.

The most extreme example of the turbulence cascade and turbulence fossilization is that of big bang turbulence [13,14], where turbulence begins at the Planck scale 10^{-35} m and cascades to 10^{-27} m where the turbulent temperature fluctuations are fossilized by inflation stretching them beyond the scale of causal connection $L_H = ct$.

In the following Section 2 we discuss the theories of gravitational structure formation, followed by a review of the observational data in Section 3, a Discussion of Results in Section 4 and finally some Conclusions in Section 5.

2. Theory

The Jeans 1902 linear theory of acoustic gravitational instability [15] predicts only one criterion for structure formation. Fluctuations of density are assumed unstable at length scales larger than the Jeans length $L_J = V_S / (\rho G)^{1/2}$ but stable for smaller scales, where V_S is the speed of sound, ρ is density, G is Newton's gravitational constant, and $(\rho G)^{-1/2}$ is the gravitational free fall time. Because the speed of sound in the plasma epoch after the big bang is nearly the speed of light, the Jeans scale for the plasma is always larger than the scale of causal connection *ct*, where *c* is the speed of light and *t* is the time since the big bang, so no gravitational structures can form in the plasma. Jeans' 1902 fluid mechanical model [15] is the basis of ΛCDM, where an unknown form of collisionless non-baryonic dark matter (NBDM) is assumed to condense

because it is somehow created cold so its sound speed and Jeans length can be assumed smaller than *ct*. The NBDM clumps cluster hierarchically and magically stick together to form potential wells in ΛCDMHC models [1, 2] with dark energy. CDM clumps have been sought but not observed, as predicted by HGD.

It is not true that the primordial plasma is collisionless and it is not true that gravitational instability is linear. Gravitational instability is intrinsically nonlinear and absolute in the absence of viscosity just like the inertial-vortex-force $\vec{v}\times\vec{\omega}$ turbulence instability is nonlinear and absolute in the absence of viscosity. All fluid density fluctuations are unstable to gravity, and in the plasma epoch $10^{11} \le t \le 10^{13}$s structures will form by gravitational forces at all scales less than *ct* unless prevented by diffusion, viscous forces or turbulence forces, as shown in Figure 1 [11].

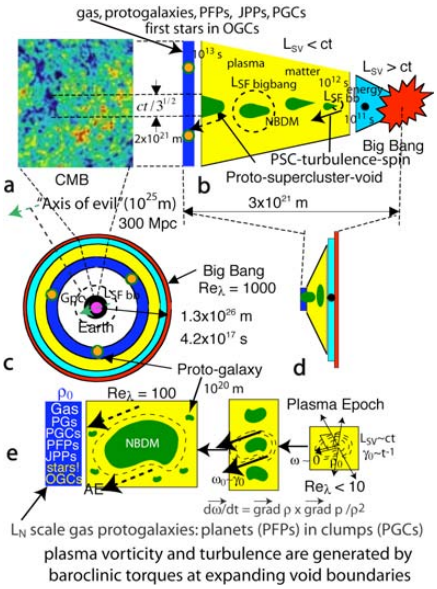

Fig. 1. Formation of gravitational structures according to hydro-gravitational-dynamics (HGD). The entire baryonic plasma universe fragments at the gas Schwarz viscous scale to form planets in Jeans mass clumps in Nomura geometry [9] proto-galaxies at transition. Plasma fossil big bang turbulence density gradients produce "axis of evil" quasar, galaxy and galaxy cluster spin alignments to Gpc scales [11, 22] by baroclinic torques at the expanding void boundaries.

The kinematic viscosity of the plasma is determined by photon collisions with free electrons that drag their protons and alpha particles with them. The photon viscosity of the plasma epoch $\nu_p \approx 4\times10^{26}$ m^2 s^{-1} [5] is so large that the potential wells of CDM halos have Reynold numbers less than one and could not fill with plasma in the available time, and any accoustic oscillations from the filling would be prevented by photon-viscosity. Thus the dominant accoustic peak of the CMB temperature anisotropy spectrum of Fig. 1a is explained by HGD theory from the sonic-speed expansion of protosupercluster voids triggered by plasma density minima as shown in Fig. 1b, but not by CDM theory if viscosity is included in the numerical simulations. The mean free path for photon-electron collisions is less than the horizon scale by two orders of magnitude at the time of first structure from the Thomson scattering cross section and the known electron density, as required by the continuum hypothesis of fluid mechanics.

When the Schwarz viscous-gravitational scale L_{SV} becomes less than the horizon scale $L_H = ct$ then gravitational structure formation begins. The first structures are fragmentations because the rapid expansion of the universe inhibits condensation at density maxima but unhances void formation at density minima. It is

a myth of astrophysics that pressure-support or thermal-support will prevent structure formation at scales smaller than the Jeans scale $L_J = V_s / (\rho G)^{1/2}$. Pressure support occurs in hydrostatics, not hydrodynamics. At the plasma-gas transition the kinematic viscosity decreases by a factor of $\approx 10^{13}$, permitting fragmentation at gas-planetary rather than plasma-galactic scales $L_{SV} = (\gamma\nu / \rho G)^{1/2}$. Viscous forces are no longer able to prevent void growth at density minima so the protogalaxies fragment to form primordial fog particles. From the Bernoulli equation the pressure decreases during the fragmentation process as the specific enthalpy p / ρ decreases to compensate for the increasing kinetic energy per unit mass $v^2/2$ along streamlines toward density maxima or away from density minima. Consider what happens when a cannonball or a vacuum beachball suddenly appears in a uniform motionless gas [5]. In the first case gravity accelerates everything toward the center. In the second case gravity accelerates everything away. Nothing much happens until the gravitational free fall time, at which the density exponentiates to infinity or zero.

In either case the pressure gradient is in the direction of motion, opposite to that required for the fictitious pressure support mechanism. For gravitational condensations after a gravitational free-fall time $\tau_{FF} = (\rho G)^{-1/2}$ the density increases exponentially to form a planet or star with internal stresses to bring the condensation to a halt and allow hydrostatic equilibrium with pressure forces in balance with gravitational forces [5]. For gravitational void formation $\tau_{FF} = (\rho G)^{-1/2}$ is the time required for the rarefaction wave of the growing void to reach its limiting speed at Mach 1 from the Rankine-Hugoniot relations, since rarefaction shocks are impossible from the second law of thermodynamics. This permits the prediction by HGD of the dominant size of CMB temperature anisotropies (Fig. 1a) to be $ct / 3^{1/2}$ or 1.7×10^{21} m at time $t = 10^{13}$ s, as observed.

The density and rate-of-strain of the plasma at transition to gas at 300,000 years (10^{13} s) are preserved as fossils of the time of first structure at 30,000 years (10^{12} s), as shown in Fig. 1e. The plasma turbulence is weak at transition, so the Schwarz viscous scale $L_{SV} = (\gamma\nu / \rho G)^{1/2}$ and Schwarz turbulence scale $L_{ST} = \varepsilon^{1/2} / (\rho G)^{3/4}$ are nearly equal, where γ is the rate-of-strain, ν is the kinematic viscosity, ε is the viscous dissipation rate and ρ is the density. Because the temperature, density, rate-of-strain, composition and thus kinematic viscosity of the primordial gas are all well known it is easy to compute the fragmentation masses to be that of protogalaxies composed almost entirely of $10^{24} - 10^{25}$ kg planets in million-solar-mass 10^{36} kg (PGC) clumps [4]. The NBDM diffuses to diffusive Schwarz scales $L_{SD} = \left(D^2 / \rho G\right)^{1/4}$ much larger than L_N scale protogalaxies, where *D* is the NBDM diffusivity and $D \gg \nu$. The rogue-planet prediction of HGD was promptly and independently predicted by the Schild 1996 interpretation of his quasar microlensing observations [14].

The HGD prediction of $\mathrm{Re}_\lambda \sim 100$ weak turbulence in the plasma epoch is supported by statistical studies of cosmic microwave background (CMB) temperature anisotropy fine structure compared to atmospheric, laboratory and numerical simulation turbulence values [19-21]. Plasma turbulence imposes a preferred direction to the massive plasma objects formed by gravitational instability in the plasma at length scales that reflect fossil temperature turbulence of the big bang [6]. Baroclinic torques produce vorticity at rate $\partial\vec{\omega} / \partial t = \nabla\rho \times \nabla p / \rho^2$ at the boundary of protosupercluster voids as shown in Fig. 1e [11]. Because $\nabla\rho$ is roughly constant over $L_{SF\,\mathrm{bigbang}}$ fossil turbulence scales of the big bang turbulence at strong force freeze-out stretched by inflation, HGD explains observations of quasar polarization matching the direction of the Axis of Evil to Gpc scales approaching the present horizon scale $L_H = ct$ [22]. This direction on the

cosmic sphere is right ascension RA = 202^{o}, declination $\delta = 25^{o}$, which matches the 2-4-8-16 directions of CMB spherical harmonics [23] and galaxy spins to supercluster 30 Mpc scales [24], and is quite unexpected and inexplicable from ΛCDM theory. All temperature fluctuations of big bang turbulence are fossilized by inflation, which stretches space and the fluctuations beyond the scale of causal connection ct at speeds $\approx 10^{25} c$ [6].

3. Observations

Figure 2 (top) shows the Tadpole (VV29, UGC 10214) galaxy merger system imaged by the HST/ACS camera, compared to a Keck Telescope spectroscopic study (bottom) by Tran et al. 2003 [23]. The galaxy dark matter clearly consists of PGCs since the spectroscopy proves the YGCs were formed in place in the galaxy halo and not ejected as a collisionless tidal tail [20]. Quasar microlensing [21] suggests the dark matter PGCs must be composed of frozen planets in metastable equilibrium, as predicted by HGD [11].

Figure 2 (bottom) shows a linear trail of YGCs pointing precisely to the frictional spiral merger of the small blue galaxy VV29c that is embedded in the accretion disk of VV29a, Fig. 2 (top). With tidal agitation from the merger, the planets undergo an accretional cascade to larger and larger planets, and finally form stars within the PGCs that are stretched away by tidal forces to become field stars in the observed star-wakes and dust-wakes. All galaxies originate as protogalaxies at 0.03 Mpc scales L_N reflecting viscous-gravitational fragmentation of weakly turbulent plasma just before its transition to gas. A core of 13.7 Gyr old stars at scale L_N persists in most if not all galaxies bound by PGC-viscosity of its remaining PGC dark matter. Most of the PGC mass diffuses out of the protogalaxy core to form the galaxy dark matter halo, observed to extend to a diameter of 0.3 Mpc in Tadpole, Fig. 1 (top). A more detailed discussion is found elsewhere [20].

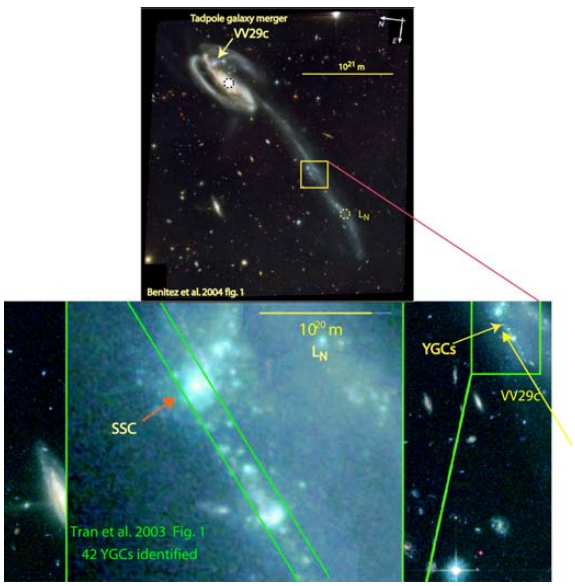

Fig. 2. Tadpole galaxy merger system illustrating the size of the baryonic dark matter system surrounding the central galaxy VV29a and the frictional spiral merger of galaxy VV29c leaving a trail of young-globular-star-clusters (YGCs)

Figure 3 shows a planetary nebula in the Large Magellanic Cloud (LMC) claimed from a recent brightness episode to be on the verge of a SNe Ia event [32], where the central white dwarf and companion

(or possibly just a white dwarf and a JPP accretion disk) have ejected several solar masses of matter in the bright clumps observed. The HGD interpretation is very different [17]. From HGD the bright clumps are formed in place from clumped baryonic-dark-matter frozen planets termed JPPs (Jovian PFP Planets of all sizes form by gassy binary accretional mergers of PFPs and their growing daughters), where some of the multi-Jupiter-mass clumps (globulettes [33]) are accreted by the star, and none are ejected. As the JPPs are accreted the star shrinks, its mass and density increase, and its spin rate increases producing a powerful plasma beam that evaporates the frozen gas planets it encounters.

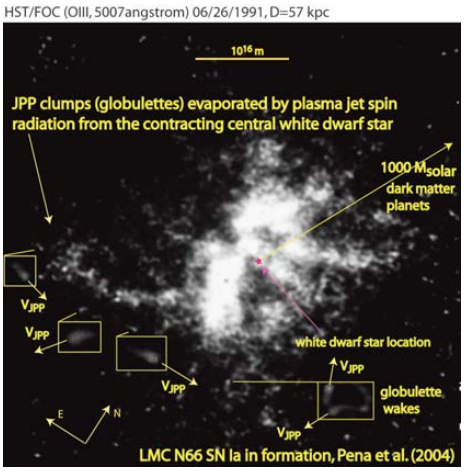

Fig. 3. Planetary nebula LMC N66 suggested by Pena et al. 2004 as a Supernova Ia in formation [25]. From HGD the HST/FOC image reveals globulette clumps [26] of dark matter planets evaporated by the plasma jet of the rapidly spinning, contracting, white dwarf star at the center, burdened by the rain of accreting, evaporating, planets.

Bright wakes can be seen for JPP-PFP globulettes (multi-Jupiter mass planet clumps) in the Fig. 3 magnified images (boxes) showing the objects are moving in random directions with speeds V_{JPP}. Presumably the globulette speed determines the rate of accretion by the central star and the rate of its radial mixing of thermonuclear products [10]. Slow speeds will reduce the size of the JPPs and their clumps, and increase the probability that the central star will die quietly as a helium white dwarf with mass < 1.4 solar. Moderate JPP accretion rates may fail to mix away the carbon core giving a supernova Ia at the Chandresekhar critical mass 1.44 solar. Stronger mixing and accretion may permit an iron core and a supernova II event. Even stronger accretion rates lead to superstars or black holes. Within the PNe size there should be more than a thousand solar masses of dark matter planets, as shown by the arrow toward upper right.

Figure 4 shows the Helix planetary nebula. Helix is much closer (209 pc) and presumably less strongly agitated by tidal forces from other objects than the LMC N66 PNe of Fig. 3.

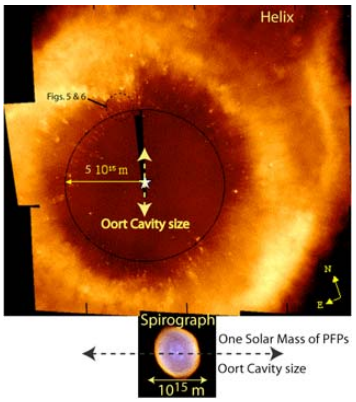

Fig. 4. Helix planetary nebula (top) showing numerous dark matter planets evaporated by the central white dwarf at the outer boundary of the Oort cavity left by the accretion of PFPs to form the star within the PGC. Spirograph PNe (bottom) is young and still growing within its Oort cavity, where apparently no dark matter planets remain unevaporated. Detailed images of Helix dark matter planets are shown in Fig. 5 and Fig. 6 at the indicated location north of the central star.

Thousands of evaporating gas planets can be seen in Fig. 4 (and Fig. 5 and Fig. 6 close-up) HST images. The planets have spacing consistent with the fossil density from the time of first structure at 30,000 years after the big bang; that is, $\rho_0 \sim 10^{-17}$ kg m^{-3}.

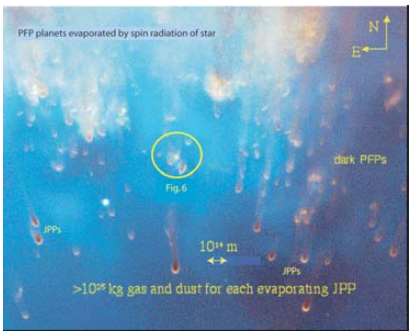

Fig. 5. Closeup image of the region north of the central star shown by the dashed circle in Fig. 4. The central white dwarf spins rapidly because it has shrunk to a density of order 10^{10} kg m^{-3} from the mass of accreted planets. A bipolar plasma beam irradiates and evaporates dark matter planets at the edge of the Oort cavity, creating the planetary nebula.

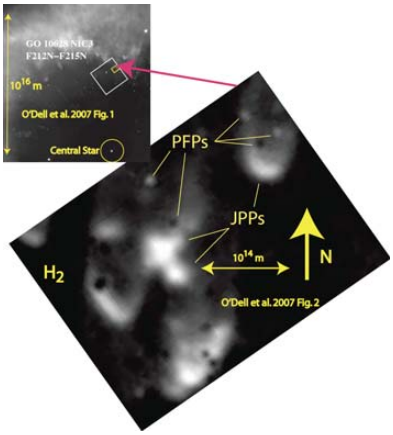

Fig. 6. Detail of location north of central white dwarf star in Helix PNe [35], showing evaporating PFP planets as well as large JPP planets and their atmospheres that can dim a SNe Ia event if it is along the line of sight, Fig. 8.

The mass of white-dwarf-precursor stars are vastly overestimated by ignorance of the existence of dark matter planets. Without PFPs, standard PNe models assume the mass of the nebula originates in the original star and is somehow ejected as clumps and superwinds. Figure 6 shows close-up images of the JPP and partially evaporated PFP planets, illuminated by the spin-radiation of the central star.

Figure 7 shows estimates of the final mass of stars $M_{Final} \le 1.3M_{sun} \le M_{Pulsar} \le M_{SNeIa}$ compared to the initial mass M_{PNE} where the PNe mass is estimated from the nebulae brightness assuming all of the nebula mass originates in the star and none from dark matter planets.

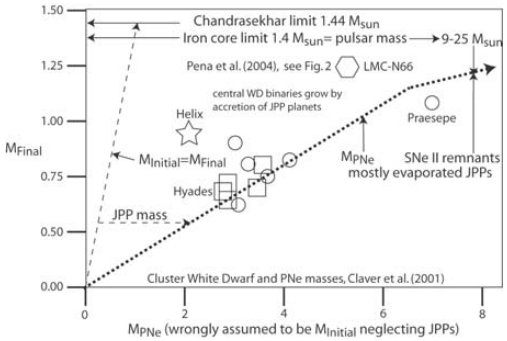

Fig. 7. Star masses compared to assumed PNe and SNe initial star masses neglecting dark matter planet effects such as JPP atmosphere brightness and the mass of evaporated dust and gas [17].

We see from Fig. 7 that final star masses are much smaller than initial masses by standard models of PNe and SNe. Pulsar masses $M_{Pulsar} = 1.4M_{sun}$ are less than the Chandrasekhar white dwarf limit $M_{Chandrasekhar} = 1.44M_{sun}$.

Figure 8 shows that an alternative to dark energy is dark matter planets. Fig. 8 (top) is dimness of SNe Ia events vesus redshift z for uniform-grey-dust, dark-energy (nonlinear-grey-dust) and no-dark-energy models. The uniform-grey-dust model fails at large z. Dark matter planets provide a nonlinear-grey-dust effect if SNe Ia events take place in PNe surroundings such as the Helix, Fig. 8 (bottom) where spin-radiation of a white dwarf creates JPP atmospheres that may dim or not dim depending on the line of sight.

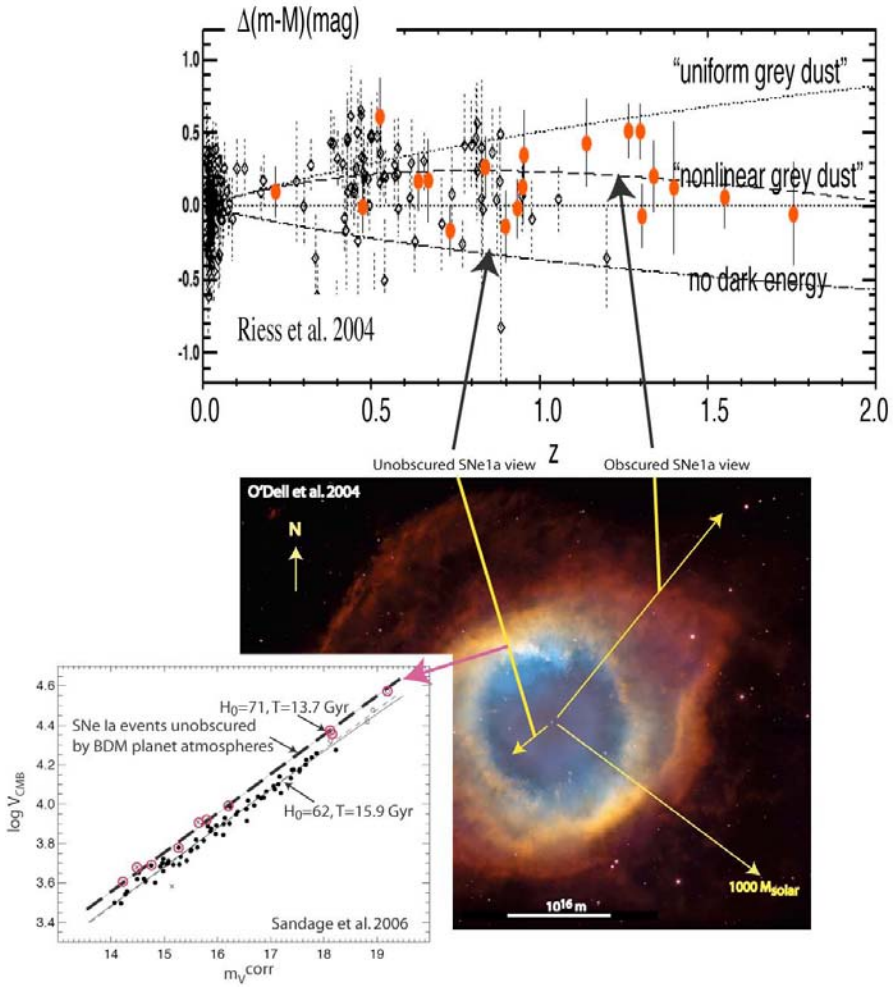

Fig. 8. Helix planetary nebula showing the effect of JPP planetary atmospheres along the line of sight to SNe Ia events is to produce a systematic dimming error that can masquerade both as dark energy (top) or as increased Hubble constants and ages of the universe (left insert). Open circles (red) are bright SNe Ia events of the Sandage 2006 data set taken to be unobscured by evaporated planetary atmospheres, and supporting the CMB universe age T = 13.7 Gyr.

The brightest SNe Ia events agree with the no-dark-energy curve of Fig. 8 (top) and can be interpreted as lines of sight that do not intersect dense dark matter planet atmospheres. A similar interpretation is given to the Sandage 2006 [27] SNe Ia global Cepheid Hubble-Constant H_0 = 62.3 km s^{-1} Mpc^{-1} estimates that disagree with the WMAP H_0 = 71 km s^{-1} Mpc^{-1} value and estimate of the age of the universe T to be 15.9 Gyr rather than the CMB value of 13.7 Gyr. Taking the least dim SNe Ia values measured to be correct removes the systematic error of dark matter planet atmosphere dimming (non-linear grey dust), so discrepancies in T and H_0 are removed.

Figure 9 shows luminosity scales for gamma-ray-burst GRB events extrapolated with the SNe Ia events of Fig. 8 top. GRB power can exceed that of 10^{23} stars or a trillion galaxies, permitting detection at redshifts z>5.8. Such events imply the formation of dense central objects in protogalaxies, contrary to ΛCDM cosmology where galaxies should not be formed at such redshifts, let alone central objects. At large redshifts luminosity distances can exceed Hubble distances depending on the cosmology assumed, but the GRB luminosity distances exceed maximum possible ratios for any

cosmology. Squares and a dashed line indicate maximum D_L / L_H for a flat universe with no Λ-dark-energy. The data suggest both the SNe Ia events and the GRB events have been dimmed by evaporated planets-in-clumps surrounding the central powerful events. Small values below the curve suggest clear lines of sight and a slightly closed universe, as expected from necessary frictional losses of big bang turbulence [14].

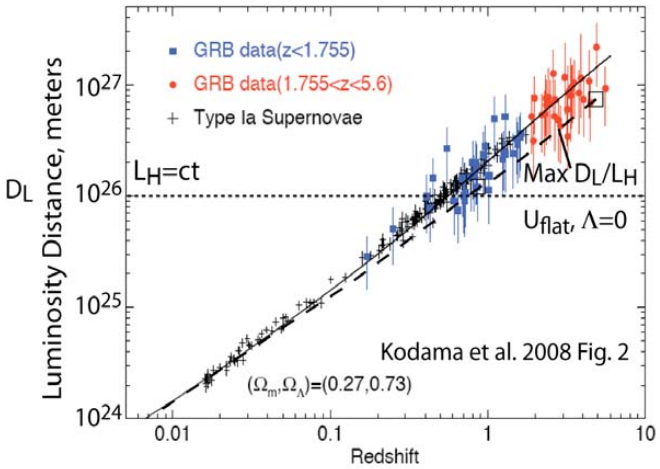

Fig. 9. Gamma ray burst data of Kodama et al. 2008 [36] are calibrated with SNe Ia data of Fig. 8. Luminosity distance scales are larger than physically possible values because both the SNe Ia events and the GRB events are dimmed by intervening partially evaporated galaxy-dark-matter planets-in-clumps. The dashed line with squares indicate the maximum possible D_L / L_H ratio for a flat universe with no dark energy or Λ.

4. Discussion

An accumulation of evidence in a variety of frequency bands from a variety of very high resolution and highly sensitive modern telescopes leaves little doubt that the dark matter of galaxies is primordial planets in proto-globular-star-cluster clumps, as predicted from HGD by Gibson 1996 [11] and inferred from quasar microlensing by Schild 1996 [21]. All stars form from these planets so all star models and planetary nebulae models must be revised to take the effects of planets and their brightness and dimness effects into account. Turbulence produces post-turbulence (fossil turbulence) with structure in patterns that preserve evidence of previous events such as big bang turbulence and plasma epoch turbulence. Post-turbulence perturbations [6] guide the evolution of all subsequent gravitational structures. Numerous fatal flaws in the standard ΛCDMHC cosmology have appeared that can be traced to inappropriate and outdated fluid mechanical assumptions [22] that can be corrected by HGD [11-21]. A critically important advance in the understanding of fluid mechanics is the correct definition of turbulence and the realization that all turbulence cascades from small scales to large [4-10]. Failure to recognize this advance has hampered the field of oceanography, which is therefore blind to the importance of fossil turbulence, fossil turbulence waves, zombie turbulence and zombie turbulence waves as the dominant physical mechanism of vertical transport of hydrophysical fields and for the preservation of information about previous turbulence [37-39].

5. Conclusions

Dark matter planet dimming errors account for the SNe Ia overestimate (T=15.9 Gyr) of the age of the universe [27] and dark energy dimming of SNe Ia events, as described by Fig. 8. Dark energy is an unecessary and incorrect hypothesis from HGD. Thus we need not modify any physical laws nor predict the

end of cosmology because evidence of cosmological beginnings are being swept out of sight by an accelerating vacuum-antigravity-powered expansion of the universe [40,41].

From HGD and the second law of thermodynamics, the frictional non-adiabatic big bang turbulence beginning of the universe [11] implies the universe is closed, not open. Because the big bang was extremely hot, the big bang turbulence produced little entropy so the departures from a flat universe should be small, as observed. Fossil strong-force freeze-out scale density turbulence explains the Gpc scales of quasar polarization vectors in alignment with the CMB axis of evil [29, 31, 18], as shown by the dashed circles in Fig. 1. Negative big bang turbulence stresses and negative gluon viscous stresses are candidates to drive the exponential inflation of space during and at the end of the big bang. An inflationary event is indicated by observations showing similar galaxy patterns exist in regions outside each others causal connection scales.

Star formation models and planetary nebulae formation models must be corrected to account for the effects of dark matter planets [24]. Initial star masses have been vastly overestimated from the brightness of evaporating planets formed around dying central stars by spin radiation, as shown by Fig. 7. Red giant and asymptotic giant branch (AGB) excursions of brightness on the Hertzsprung-Russell color-magnitude diagram for star evolution must be reexamined to account for the fact that all stars are formed and grow by the accretion of planets that have first order effects on both the color and magnitude of stars as they evolve. Planetary nebulae are apparently not dust clouds ejected by AGB superwind events as usually assumed but are partially evaporated and brightly illuminated dark matter planets, as shown by Figs. 3-6, and Fig. 8.

References

1. Riess, A. G., Filippenko, A.V. et al. 1998. Observational evidence from supernovae for an accelerating universe and a cosmological constant AJ, 116, 1009.
2. Perlmuter, S., Aldering, G. et al. 1999. Measurements of Ω and Λ from 42 high-redshift supernovae ApJ, 517, 565.
3. Chernin, A.D., Karachentsev, I.D. et al. 2007. Detection of dark energy near the Local Group with the Hubble Space Telescope, arXiv:astro-ph/0706.4068v1.
4. Gibson, C.H. (1991). Kolmogorov similarity hypotheses for scalar fields: sampling intermittent turbulent mixing in the ocean and galaxy, Proc. Roy. Soc. Lond. A, 434, 149-164.
5. Gibson, C. H. (2006). Turbulence, update of article in Encyclopedia of Physics, R. G. Lerner and G. L. Trigg, Eds., Addison-Wesley Publishing Co., Inc., pp.1310-1314.
6. Gibson, C. H. (1981). Buoyancy effects in turbulent mixing: Sampling turbulence in the stratified ocean, AIAA J., 19, 1394.
7. Gibson, C. H. (1968a). Fine structure of scalar fields mixed by turbulence: I. Zero-gradient points and minimal gradient surfaces, Phys. Fluids, 11: 11, 2305-2315.
8. Gibson, C. H. (1968b). Fine structure of scalar fields mixed by turbulence: II. Spectral theory, Phys. Fluids, 11: 11, 2316-2327.
9. Gibson, C. H. (1986). Internal waves, fossil turbulence, and composite ocean microstructure spectra," J. Fluid Mech. 168, 89-117.
10. Gibson, C. H. (1999). Fossil turbulence revisited, J. of Mar. Syst., 21(1-4), 147-167, astro-ph/9904237
11. Gibson, C.H. (1996). Turbulence in the ocean, atmosphere, galaxy and universe, Appl. Mech. Rev., 49, no. 5, 299–315.
12. Gibson, C.H. (2000). Turbulent mixing, diffusion and gravity in the formation of cosmological structures: The fluid mechanics of dark matter, J. Fluids Eng., 122, 830–835.
13. Gibson, C.H. (2004). The first turbulence and the first fossil turbulence, Flow, Turbulence and Combustion, 72, 161–179.
14. Gibson, C.H. (2005). The first turbulent combustion, Combust. Sci. and Tech., 177: 1049–1071, arXiv:astro-ph/0501416.
15. Gibson, C.H. (2006). The fluid mechanics of gravitational structure formation, astro-ph/0610628.
16. Gibson, C.H. (2008). Cold dark matter cosmology conflicts with fluid mechanics and observations, J. Applied Fluid Mech., Vol. 1, No. 2, pp 1-8, 2008, arXiv:astro-ph/0606073.
17. Gibson, C.H. & Schild, R.E. (2007). Interpretation of the Helix Planetary Nebula using Hydro-Gravitational-Dynamics: Planets and Dark Energy, arXiv:astro-ph/0701474.
18. Schild, R.E & Gibson, C.H. (2008). Lessons from the Axis of Evil, axXiv[astro-ph]:0802.3229v2.
19. Gibson, C.H. & Schild, R.E. (2007). Interpretation of the Stephan Quintet Galaxy Cluster using Hydro-Gravitational-Dynamics: Viscosity and Fragmentation, arXiv[astro-ph]:0710.5449.
20. Gibson, C.H. & Schild, R.E. (2002). Interpretation of the Tadpole VV29 Merging Galaxy System using Hydro-Gravitational Theory, arXiv:astro-ph/0210583.
21. Schild, R. 1996. Microlensing variability of the gravitationally lensed quasar Q0957+561 A,B, ApJ, 464, 125.
22. Jeans, J. H. 1902. The stability of spherical nebula, Phil. Trans., 199A, 0-49.
23. Tran, H. D., Sirianni, M., & 32 others 2003. Advanced Camera for Surveys Observations of Young Star Clusters in the Interacting Galaxy UGC 10214, ApJ, 585, 750.
24. Toomre, A., & Toomre, J. 1972. Galactic Bridges and Tails, ApJ, 178, 623.

25. Gibson, C.H. & Schild, R.E. (2002). Interpretation of the Tadpole VV29 Merging Galaxy System using Hydro-Gravitational Theory, arXiv:astro-ph/0210583.
26. Bershadskii, A. 2006. Isotherms clustering in cosmic microwave background, Physics Letters A, 360, 210-216.
27. Bershadskii, A., and Sreenivasan, K.R. 2002. Multiscaling of cosmic microwave background radiation, Phys. Lett. A, 299, 149-152.
28. Bershadskii, A., and Sreenivasan, K.R. 2003. Extended self-similarity of the small-scale cosmic microwave background anisotropy Phys. Lett. A, 319, 21-23.
29. Hutsemekers, D. et al. 2005. Mapping extreme-scale alignments of quasar polarization vectors, A&A 441, 915–930.
30. Land, K. & Magueijo, J. 2005. Phys. Rev. Lett. 95, 071301.
31. Longo, M. J. 2007. Evidence for a Preferred Handedness of Spiral Galaxies arXv:0707.3793.
32. Pena, M. et al. 2004. A high resolution spectroscopic study of the extraordinary planetary nebula LMC-N66, A&A, 419, 583-592.
33. Gahm, G. et al. 2007. Globulettes as seeds of brown dwarfs and free-floating planetary-mass objects, AJ, 133, 1795-1809.
34. Sandage, A. et al. 2006. The Hubble constant: a summary of the HST program for the luminosity calibration of Type Ia supernovae by means of Cepheids, ApJ, 653, 843.
35. O'Dell, C.R., Henney, W. J. & Ferland, G. J. 2007. Determination of the physical conditions of the knots in the Helix nebula from optical and infrared observations, AJ, 133, 2343-2356, astro-ph/070163.
36. Kodama, Y., Yonetoku, D. et al. 2008. Gamma-ray bursts in 1.8<z<5.6 suggest that the time variation of the dark energy is small, for MNRAS, arXiv0802.3428.
37. Keeler, R. N., V. G. Bondur, and C. H. Gibson 2005. Optical Satellite Imagery Detection of Internal Wave Effects from a Submerged Turbulent Outfall in the Stratified Ocean, Geophysical Research Letters, Vol. 32, L12610.
38. Gibson, C. H., Bondur, V. G., Keeler, R. N. and Leung, P. T. (2006). Remote sensing of submerged oceanic turbulence and fossil turbulence, International Journal of Dynamics of Fluids, Vol. 2, No. 2, 171-212.
39. Gibson, C. H., Bondur, V. G., Keeler, R. N. and Leung, P. T. (2008). Energetics of the beamed zombie turbulence maser action mechanism for remote detection of submerged oceanic turbulence, Journal of Applied Fluid Mechanics, Vol. 1, No. 1, 11-42.
40. Krauss, L. M. and Scherrer, R. J. 2008. The end of cosmology, Scientific American, 298 (3), 46-53.
41. Krauss, L. M. and Scherrer, R. J. 2007. The return of a static universe and the end of cosmology, J. Gen. Rel. and Grav., 39, 10, 1545-1550, arXv:0704.0221.

astro-ph/0701474v4 Nov 2

Interpretation of the Helix Planetary Nebula using Hydro-Gravitational-Dynamics: Planets and Dark Energy

Carl H. Gibson[1]

Departments of Mechanical and Aerospace Engineering and Scripps Institution of Oceanography, University of California, San Diego, CA 92093-0411

cgibson@ucsd.edu

and

Rudolph E. Schild

Center for Astrophysics, 60 Garden Street, Cambridge, MA 02138

rschild@cfa.harvard.edu

ABSTRACT

Hubble Space Telescope (HST/ACS) images of the Helix Planetary Nebula (NGC 7293) are interpreted using the hydro-gravitational-dynamics theory (HGD) of Gibson 1996-2006. HGD claims that baryonic-dark-matter (BDM) dominates the halo masses of galaxies (Schild 1996) as Jovian (Primordial-fog-particle [PFP]) Planets (JPPs) in proto-globular-star-cluster (PGC) clumps for all galaxy halo diameters bounded by stars. From HGD, supernova Ia (SNe Ia) events always occur in planetary nebulae (PNe) within PGCs. The dying central star of a PNe slowly accretes JPP mass to grow the white-dwarf to $1.44M_{\odot}$ instability from $\geq 1000M_{\odot}$ BDM within luminous PNe diameters. Plasma jets, winds and radiation driven by contraction and spin-up of the carbon star evaporate JPPs revealing its Oort accretional cavity. SNe Ia events may thus be obscured or not obscured by radiation-inflated JPP atmospheres producing systematic SNe Ia distance errors, so the otherwise mysterious "dark energy" concept is unnecessary. HST/ACS and WFPC2 Helix images show $> 7,000$ cometary globules and SST/IRAC images show $> 20,000 - 40,000$, here interpreted as gas-dust

[1]Center for Astrophysics and Space Sciences, UCSD

cocoons of JPPs evaporated by the spin powered radiation of the PNe central white-dwarf. Observed JPP masses $\approx 3 \times 10^{25}$ kg with spacing $\approx 10^{14}$ m for galaxy star forming regions give a density ρ that fossilizes the primordial density $\rho_0 \approx 3 \times 10^{-17}$ kg m^{-3} existing for times $10^{12} \leq t \leq 10^{13}$ s when the plasma universe fragmented into proto-superclusters, proto-clusters, and proto-galaxies. Pulsar scintillation spectra support the postulated multi-planet atmospheres.

Subject headings: ISM: structure – Planetary Nebula: general – Cosmology: theory – Galaxy: halo, dark matter, turbulence

1. Introduction

Brightness values of Supernovae Ia (SNe Ia) events, taken as standard candles for redshift values $0.01 < z < 2$, depart significantly from those expected for the decelerating expansion rate of a flat universe (Riess et al. 2004). Departures indicate a recent dimming at all frequencies by about 30%, but with large scatter attributed to uncertainty in the SNe Ia models. For ≥15 years of study such evidence has accumulated with no explanation other than an accelerating(!) expansion rate of the universe, presumed to reflect a negative pressure from a time dependent $\Lambda(t)$ "cosmological constant" component of the Einstein equations termed "dark-energy" (Bean et al. 2005). Hubble Space Telescope Advanced Camera for Surveys (HST/ACS) images have such high signal to noise ratios that both the scatter and the dimming are statistically significant over the full range of z values. Bright SNe Ia observed for $z \geq 0.46$ exclude "uniform grey dust" systematic errors, supporting a flat universe deceleration of expansion rate until the recent "cosmic jerk" to an accelerated expansion rate for $z \leq 0.46$. This physically mysterious "dark energy" interpretation is made from SNe Ia observations because no alternative exists in the commonly accepted (but fluid mechanically untenable) Λ-cold-dark-matter (ΛCDM) hierarchically clustering cosmological theory (ΛCDMHCC, Table 2). In the following we suggest that the primordial exoplanets of HGD provide just the fluid-mechanically-correct alternative demanded by the observed intermittent SNe Ia brightness dimming. New physical laws are not required by HGD but ΛCDMHCC must be discarded. The choice is between planets and dark energy.

When a massive primordial-planet (exoplanet, rogue-planet, planemo, Jovian) population comprised of plasma-fossil-density (ρ_0 frozen H-He) PGC clumps of JPPs is recognized as the baryonic dark matter (BDM) and the interstellar medium (ISM), new scenarios are required for planetary nebulae (PNe) formation and for star formation, star evolution, and star death. From HGD the average galaxy BDM-ISM mass is ≈ 30× the luminous mass of stars and ≫ the more diffusive NBDM-ISM (CDM) mass. The million trillion-planet-PGCs

per galaxy each have fossil-density $\rho_0 \approx \rho_{PGC} \approx 10^4$ greater than the $\langle\rho_g\rangle \approx 10^{-21}$ kg m^{-3} galaxy average and $\approx 10^9\langle\rho_U\rangle$, where $\langle\rho_U\rangle \approx 10^{-26}$ kg m^{-3} is the flat universe average density at the present time. All stars and all JPP planets are thus born and grown within such $10^6 M_\odot$ PGCs by mergers and accretions of PFP and JPP planets from the large PGC supply. By gravity the planets collect and recycle the dust and water of exploded stars to explain solar terrestrial planets and life. Application of fluid mechanics to the big bang, inflation, and the plasma- and gas- self-gravitational structure formation epochs (Table 1) is termed hydo-gravitational-dynamics (HGD) theory (Gibson 1996, 2000, 2001, 2004, 2005). Viscosity, density and expansion-rate fix plasma gravitational fragmentation scales with a linear-spiral weak-turbulence protogalaxy geometry (Gibson 2006a; Nomura & Post 1998). Voids between the $10^{46} - 10^{43}$ kg ρ_0 supercluster-to-protogalaxy fragments first fill in the plasma epoch and later empty in the gas epoch by diffusion of a more massive neutrino-like population ($\Omega_{NB} + \Omega_B = 1, \Omega_\Lambda = 0; \Omega = \langle\rho\rangle/\langle\rho_U\rangle$). Instead of concordance cosmology values ($\Omega_{NB} = 0.27, \Omega_B = 0.024, \Omega_\Lambda = 0.73$) commonly used (Wise & Abel 2007), HGD gives ($\Omega_{NB} = 0.968, \Omega_B = 0.032, \Omega_\Lambda = 0$). Supercluster voids with radio-telescope-detected scales $\geq 10^{25}$ m at redshift $z \leq 1$ (Rudnick et al. 2007) confirm this prediction of HGD, but decisively contradict ΛCDMHC where superclustervoids form last rather than first.

Many adjustments to standard cosmological, astrophysical, and astronomical models are required by HGD (Gibson 2006a, Gibson 2006b) and many puzzling questions are answered. For example, why are most stars binaries and why are population masses of small stars larger than population masses of larger stars ($m_{SS} \geq m_{LS}$)? From HGD it is because all stars form and grow by a frictional-clumping binary-cascade from small PFP planets. Where do planetary nebulae and supernova remnants get their masses? From HGD these masses are mostly evaporated ambient BDM planets, just as the masses for many stars assumed larger than $2M_\odot$ can be attributed mostly to the brightness of the huge ($\geq 10^{13}$ m) dark-matter-planet atmospheres they evaporate (§3 Fig. 3). Masses of supergiant OB and Wolf-Rayet stars are vastly overestimated neglecting evaporated JPP brightness (Maund et al. 2004; Shigeyama & Nomoto 1990). Because stars form from planets the first stars must be small and early. Large $\geq 2M_\odot$ population III stars forming directly from $10^6 M_\odot$ Jeans mass gas clouds in CDM halos never happened and neither did re-ionization of the gas-epoch back to a second plasma-epoch. CDM halos never happened. There were no dark ages because the first stars formed immediately from merging PFP planet-mass clouds before the luminous hot gas cooled (at $\approx 10^{13}$ s). All big stars were once little stars. All little stars were once planets. The mystery of massive low surface brightness galaxies (O'Neil et al. 2007) is solved. From HGD these are protogalaxies where, despite maximum tidal agitation, the central PGCs have remained in their original starless BDM state. All proto-galaxies were created simultaneously without stars at the end of the plasma epoch (at $\approx 3 \times 10^5$ y).

Jovian rogue planets dominating inner halo galaxy mass densities (Gibson 1996) matches an identical, but completely independent, interpretation offered from Q0957+561A,B quasar microlensing observations (Schild 1996). Repeated, continuous, redundant observations of the Q0957 lensed quasar for > 20 years by several observers and telescopes confirm that the mass of galaxies within all radii containing the stars must be dominated by planets (Colley & Schild 2003; Schild 2004a; Schild 2004b; Gibson 2006a; Gibson 2006b). The non-baryonic dark matter (NBDM) is probably a mix of neutrino flavors, mostly primordial and sterile (weakly collisional) with mass $m_{NBDM} \approx 30 m_{BDM}$. NBDM is super-diffusive and presently forms large outer galaxy halos and galaxy cluster halos. From HGD, the function of NBDM is to continue the decelerating expansion of the universe toward zero velocity (or slightly less) by large scale gravitational forces. A matter dominated $\Lambda = 0$ flat expanding universe monotonically decelerates from general relativity theory. The entropy produced by its big bang turbulent beginning (Gibson 2005) implies a closed contracting fate for the universe, not an open accelerating expansion driven by dark energy (Busa et al. 2007).

According to HGD, SNe Ia explosions always occur in PNes within PGC massive dense clumps of frozen primordial planets where virtually all stars form and die. Planetary nebulae are not just brief puffs of illuminated gas and dust ejected from dying stars in a vacuum, but are manifestations of $\approx 3 \times 10^7$ primordial dark matter planets per star in galaxies of 3% bright and 97% dark PGCs. When the JPP supply-rate of H-He gas is too small, stars die and cool as small helium or carbon white dwarfs. With modest internal stratified turbulent mixing rates from larger JPP rates, gravity compresses the carbon core, the angular momentum, and the magnetic field giving strong axial plasma jets and equatorial stratified turbulent plasma winds (Gibson et al. 2007). Nearby JPP planets heated by the star and illuminated by the jets and winds evaporate and become visible as a PNe with a white-dwarf central star. PNes thus appear out of the dark whenever white-dwarf (WD) carbon stars are gradually growing to the Chandrasekhar limit of $1.44 M_\odot$ (Hamann et al. 2003; Pena et al. 2004; Hachisu & Kato 2001). Gradual star growth is dangerous to the star because its carbon core may collapse from inadequate radial mass mixing, giving a SNe Ia event. Modest star growth may be even more dangerous because enhanced turbulence may mix and burn the carbon core but not mix the resulting incombustible iron core, which explodes at $1.4 M_\odot$ to form a neutron star in a supernova II event. Rapid stably stratified turbulent mixing within a star forced by a strong JPP rain may mix away both carbon core and iron core instabilities to form $\gg 2 M_\odot$ superstars (Keto & Wood 2006).

Thus when JPPs in a PGC are agitated to high speed V_{JPP}, the rapid growth of its stars will inhibit formation of collapsing carbon cores so that fewer carbon white dwarfs and fewer SNe Ia result. More stars with $M_{Fe[Crit]} \approx 1.4 M_\odot < 1.44 M_\odot$ will centrally mix and explode as supernova II (SNe II) due to iron core collapse to form neutron stars

manifested as $1.4M_{\odot}$ pulsars (Thorsett & Chakrabarty 1999). Supernova II remnants such as the Crab are mostly evaporated or evaporating JPPs. The speed V_{JPP} of planets and planet clumps within a PGC, their spin, and the size and composition of their gas-dust atmospheres are critical parameters to the formation of larger planets, stars, and PNe, and will be the subject of future studies (see Fig. 2 below). These parameters are analogous to the small protein chemicals used for bacterial quorum sensing in symbiotic gene expressions (Loh & Stacey 2003) by providing a form of PGC corporate memory. Numerous dense, cold, water-maser and molecular-gas-clumps detected by radio telescopes in red giants and PNe (Miranda et al. 2001; Tafoya et al. 2007) are massive ($\geq M_{Jup}$) JPPs and should be studied as such to reveal important JPP parameters such as V_{JPP}.

A gentle rain of JPP comets permits the possibility that a WD may grow its compressing carbon core to deflagration-detonation at the Chandrasekhar limit (Ropke & Niemeyer 2007). As the core mass and density grow, the angular momentum increases along with the strength of plasma beams and winds, giving strong increases in the WD surface temperature, photon radiation, and observable PNe mass M_{PNe}. Strong JPP rains lead to Wolf-Rayet (C, N and O class) stars cloaked in massive envelopes of evaporating JPPs misinterpreted as super-wind ejecta. With larger accretion rates, radially beamed internal wave mixing driven by buoyancy damped turbulence (Keeler et al. 2005; Gibson et al. 2006a; Gibson et al. 2006b) prevents both SNe II detonation at $1.4M_{\odot}$ and SNe Ia detonation at $1.44M_{\odot}$. Turbulence and internal waves cascade from small scales to large, mix and diffuse. With strong forcing, turbulent combustion can be quenched (Peters 2000). With moderate JPP accretion rates, white-dwarfs can gradually burn gas to precisely enough carbon to collapse, spin up, and explode within the PNes they produce.

It is known (Padoan et al. 2005) that Pre-Main-Sequence (PMS) star formation is not understood. Numerical simulations from gas clouds and the Bondi-Hoyle-Littleton model of wake gas accretion show the larger the star the larger the gas accretion rate. By conventional models of stars collapsing from clouds of molecular gas without planets there should be more large (supersolar) stars than small (brown dwarf BD, red dwarf RD) stars, contrary to observations (Calchi-Novati et al. 2005; Alcock et al. 2000; Gahm et al. 2007) that globulette-star-population-mass m_{GS} decreases as globulette-star-mass M_{GS} increases; that is, $m_G \geq m_{BD} \geq m_{RD} \geq m_{\odot}$. Such a monotonic decrease in m_{GS} with M_{GS} giving $m_{PFP} \geq m_{JPP} \geq m_{BD} \geq m_{RD}$ is expected from HGD where all stars and planets form by hierarchical accretion from $10^{-3}M_{Jup}$ PFP dark matter planets within 3×10^{15} m Oort cavities in the ISM. Because $m = NM$, the decrease in m_{GS} with M_{GS} is also supported by observations of exo-planet numbers N showing $dN/dM \sim M^{-1.2}$ for $M = (0.04 - 15)M_{Jup}$ (Butler et al. 2006), contrary to conventional planet formation models (Ida & Lin 2004; Boss 2001) where stars form mostly giant $\geq M_{Jup}$ planets within $\leq 10^{12}$ m (10 AU) of the protostar.

Aging WR-stars, neutron stars, pulsars, and C-stars are most frequently identified in spiral-galaxy-disks (SGD) where tidal agitation is maximum for the $\approx 10^{18}$ planets of galaxy BDM halos. From HGD, SGDs reflect PGC accretion from the halo. As the initially gaseous PGCs of protogalaxies freeze they become less sticky and collisional, so they diffuse out of their protogalaxy cores (with Nomura scale $L_N \approx 10^{20}$ m ≈ 2 kpc) in growing orbits to form the present $\geq 30L_N$ baryonic dark matter halos (Gibson 2006a). Some tidally agitated PGCs become luminous as they are captured and accreted back toward the original core region, forming SGD accretion disks. Dark or nearly dark PGCs leave thin great circle metal-free star wakes about the Galaxy center to $(2-3)L_N$ radii, triggered and stretched away by tidal forces (Grillmair 2006; Belokurov et al. 2006; Odenkirchen et al. 2001), where the mass in these ancient star "streams" typically exceeds that of their sources (eg.: the "Orphan Stream"). Dwarf galaxy clumps of PGCs in orbits out to $7L_N$ leave streams of stars and globular clusters (Ibata et al. 2002) and high-velocity-clouds of gas (HVCs) at the $15L_N$ distance of the Magellanic cloud stream (Ibata & Lewis 2007). Observations and HGD contradict suggestions of a non-baryonic dark matter origin or a capture origin for these recently discovered Galactic objects. Thousands of PGCs and their wakes covering $\approx 20\%$ of the sky may be identified with anomalous velocity HVC objects and ≈ 200 isolated compact CHVCs covering $\approx 1\%$ from their neutral hydrogen signatures, masses $10^{4-5}M_\odot$, distances up to 6×10^{21} m $(60L_N)$, and sizes $\approx 10^{17-18}$ m (Putnam et al. 2002). Stars should form slowly enough to make white dwarfs with intermittently dimmed SNe Ia events in such gently agitated PGCs with small V_{JPP} values. Pulsars, however, always twinkle because lines of sight always intersect fossil electron density turbulence (Gibson et al. 2007) atmospheres of planets powerfully evaporated by the SN II event and the pulsar (see Fig. 12 §4, §5).

From HGD, SNe Ia events will be intermittently dimmed by Oort-rim-distant JPP-atmospheres evaporated by the increasing radiation prior to the event that has ionized and accreted all JPPs in the Oort cloud cavity. Evidence of a massive (several $M_\odot$) H-rich circumstellar medium at distances of up to nearly a light year (10^{16} m) after the brightness maximum is indicated by slow fading SNe Ia events (Woods-Vasey et al. 2004). Our scenario of SNe Ia formation by gradual carbon WD growth of $\leq M_\odot$ size stars fed by JPP comets contradicts the standard model for SNe Ia events (see §2.3.1) where superwinds dump most of the mass of $(3-9)M_\odot$ intermediate size stars into the ISM. Few SNe Ia events are seen at large redshifts because billions of years are needed to grow a $1.44M_\odot$ star. In §2.3.1 we question PNe models involving intermediate size stars, their envelopes, and their superwinds. Stars formed by a gassy merging planet clump binary cascade is supported by observations in star forming regions of $(10^{26}-10^{29}$ kg) spherical globulette objects with mass distributions dominated by the small mass globulettes (Gahm et al. 2007).

Theories describing the death of small to intermediate mass stars $(0.5M_\odot - 9M_\odot)$ to form

white-dwarfs and planetary nebulae are notoriously unsatisfactory (Iben 1984). Neglecting the ambient JPPs of HGD, observations of PNe mass and composition indicate that most of the matter for such stars is inexplicably expelled (Knapp et al. 1982) when they form dense carbon cores and die. Models of PNe formation have long been admittedly speculative, empirical, and without meaningful theoretical guidance (Iben 1984). Multiple dredge-up models reflect complex unknown stellar mixing processes. A counter-intuitive 1975 "Reimer's Wind" expression gives stellar mass loss rates $\dot{M} \sim LR/M$ inversely proportional to the mass M of the star dumping its mass, where L is its huge luminosity (up to $10^6 L_\odot$) and R is its huge radius (up to $10^2 R_\odot$). Why inversely? "Superwinds" must be postulated (§2.3) to carry away unexpectedly massive stellar envelopes of surprising composition by forces unknown to fluid mechanics and physics in unexpectedly dense fragments in standard numerical models of star evolution (Paxton 2004). Massive $\geq 2M_\odot$ main sequence stars with mass inferred from gravitational-cloud-collapse luminosity-models (Iben 1965) rather than JPP brightness are highly questionable. Mass and species balances in star, PNe and supernova formation models without HGD are uniformly problematic (Shigeyama & Nomoto 1990).

Radiation pressure, even with dust and pulsation enhancement, is inadequate to explain the AGB superwind (Woitke 2006). Shock wave effects cannot explain the large densities of the Helix cometary knots (§3). All these surprises vanish when one recognizes that the interstellar medium consists of primordial H-He planets rather than a hard vacuum. From HGD, planetary nebulae contain $\geq 1000M_\odot$ of unevaporated JPPs from observed PNe radii 3×10^{16} m assuming the BDM density in star forming regions is 3×10^{-17} kg m^{-3}. Less than 1% of these JPPs must be evaporated and ionized to form the unexpectedly massive stellar envelopes in place rather than ejected as superwinds. Why is it credible that a star can dump 94% of its mass into the ISM when it forms a carbon core? From HGD, the AGB-envelope-superwind concepts are failed working hypotheses like CDM, Λ and dark energy.

By coincidence, the direction opposite to the peak Leonid meteoroid flux in November 2002 matched that of the closest planetary nebula (PNe) Helix (NGC 7293), so that the Hubble Helix team of volunteers could devote a substantial fraction of the 14 hour Leonid stand-down period taking photographs with the full array of HST cameras, including the newly installed wide angle Advanced Camera for Surveys (ACS). A composite image was constructed with a 4 m telescope ground based image mosaic (O'Dell et al. 2004) to show the complete system. Helix is only 219 (198-246) pc $\approx 6.6 \times 10^{18}$ m from earth (Harris et al. 2007) with one of the hottest and most massive known central white dwarf stars (120,000 K, $M_{WD} \approx M_\odot$), and is also the dimmest PNe (Gorny et al. 1997). With either a close (dMe) X-ray companion (Guerrero et al. 2001) or just a JPP accretion disk (Su et al. 2007) it powerfully beams radiation and plasma into the interstellar medium (ISM) surroundings. Thus Helix provides an ideal laboratory to test our claims from theory and

observation (Gibson 1996; Schild 1996) that both the ISM of star forming regions of galaxies and the baryonic-dark-matter (BDM) of the universe are dominated by dense collections of volatile primordial frozen-gas planets.

In §3 we compare HST/ACS Helix and other PNe observations with HGD and standard explanations of cometary globule and planetary nebula formation. Planetary nebulae from HGD are not just transient gas clouds emitted by dying stars, but baryonic dark matter brought out of cold storage. A new interpretation of Oort cloud comets and the Oort cloud itself appears naturally, along with evidence (Matese et al. 1999) of Oort comet deflection by an $\approx 3 \times 10^{27}$ kg solar system $\geq$Jupiter-mass JPP at the Oort cavity distance $\approx 3 \times 10^{15}$ m. The first direct detection of PFPs in Helix (O'Dell et al. 2007) is discussed in §4 and the detection of 40,000 infrared Helix JPP atmospheres (Hora et al. 2006) in §5, consistent with pulsar evidence (§4, §5).

In the following §2 we review hydro-gravitational-dynamics theory and some of the supporting evidence, and compare the PNe predictions of HGD with standard PNe models and the observations in §3. We discuss our "nonlinear grey dust" alternative to "dark energy" in §4 and summarize results in §5. Finally, in §6, some conclusions are offered.

2. Theory

2.1. HGD structure formation

Standard CDMHC cosmologies are based on flawed concepts about turbulence, ill-posed, over-simplified fluid mechanical equations, an inappropriate assumption that primordial astrophysical fluids are collisionless, and the assumption of zero density to achieve a solution of the equations. This obsolete Jeans 1902 theory neglects non-acoustic density fluctuations, viscous forces, turbulence forces, particle collisions, differences between particles, and the effects of multiparticle mixture diffusion on gravitational structure formation, all of which can be crucially important in some circumstances where astrophysical structures form by self gravity. Jeans did linear perturbation stability analysis (neglecting turbulence) of Euler's equations (neglecting viscous forces) for a completely uniform ideal gas with density ρ only a function of pressure (the barotropic assumption) to reduce the problem of self-gravitational instability to one of gravitational acoustics. Diffusivity effects were not considered.

To satisfy Poisson's equation $\nabla^2\phi = 4\pi G\rho$ for the gravitational potential ϕ of a collisionless ideal gas, Jeans assumed the density ρ was zero in a maneuver appropriately known as the "Jeans swindle". The only critical wave length for gravitational instability with all

these questionable assumptions is the Jeans acoustical length scale L_J where

$$L_J \equiv V_S/(\rho G)^{1/2} \gg (p/\rho^2 G)^{1/2} \equiv L_{JHS}, \quad (1)$$

G is Newton's gravitational constant and $V_S \approx (p/\rho)^{1/2}$ is the sound speed.

The Jeans hydrostatic length scale $L_{JHS} \equiv (p/\rho^2 G)^{1/2}$ in Eq. 1 has been misinterpreted by Jeans 1902 and others as an indication that pressure can somehow prevent the formation of structures by gravity at length scales smaller than L_J. Viscosity, turbulence and diffusivity can prevent small scale gravitational structure formation at Schwarz scales (Table 1). Pressure cannot. In a hydrodynamic description, ratio $h = p/\rho$ is the stagnation specific enthalpy for gravitational condensation and rarefaction streamlines. The appropriate reference enthalpy h_0 is zero from Bernoulli's equation $B = p/\rho + v^2/2 = constant$ from the first law of thermodynamics for adiabatic, isentropic, ideal gas flows at the beginning of structure formation, where $v = 0$ is the fluid speed. In an expanding universe where $v = r\gamma$ the positive rate of strain γ is important at large radial values r and favors fragmentation. In the initial stages of gravitational instability, pressure is a slave to the velocity and is irrelevant because it drops out of the momentum equation. "Where the speed is greatest the pressure is least" with B constant quotes the usual statement of Bernoulli's law. For supersonic real gases and plasmas at later stages the specific enthalpy term p/ρ acquires a factor of $\approx 5/2$ famously neglected by Newton in his studies of acoustics without the second law of thermodynamics (Pilyugin & Usov 2007). Turbulence concepts of HGD are necessary (Gibson et al. 2007).

Pressure support and thermal support are concepts relevant only to hydrostatics. For hydrodynamics, where the velocity is non-zero, pressure appears in the Navier-Stokes momentum equation only in the $\nabla B \approx 0$ term. Non-acoustic density extrema are absolutely unstable to gravitational structure formation (Gibson 1996; Gibson 2000). Minima trigger voids and maxima trigger condensates at all scales not stabilized by turbulent forces, viscous forces, other forces, or diffusion (see Eqs. 3-5 and Table 1 below). The Jeans acoustic scale L_J is the size for which pressure can equilibrate acoustically without temperature change in an ideal gas undergoing self gravitational collapse or void formation, smoothing away all pressure forces and all pressure resistance to self gravity. The Jeans hydrostatic scale L_{JHS} is the size of a fluid blob for which irreversibilities such as frictional forces or thermonuclear heating have achieved a hydrostatic equilibrium between pressure and gravitation in a proto-Jovian-planet or proto-star. L_{JHS} is generically much smaller than L_J and has no physical significance until gravitational condensation has actually occurred and a hydrostatic equilibrium has been achieved.

When gas condenses on a non-acoustic density maximum due to self gravity a variety of results are possible. If the amount is much larger than the Eddington limit 110 $M_\odot$ permitted by radiation pressure, a turbulent maelstrom, superstar, and possibly a black hole

(or magnetosphere eternally collapsing object MECO) may appear. If the amount is small, a gas planet can form in hydrostatic equilibrium as the gravitational potential energy is converted to heat by turbulent friction, and is radiated. The pressure force $F_P \approx p \times L^2$ matches the gravitational force of the planet at $F_G \approx \rho^2 G L^4$ at the hydrostatic Jeans scale L_{JHS}. Pressure p is determined by a complex mass-momentum-energy balance of the fluid flow and ambient conditions. A gas with uniform density is absolutely unstable to self gravitational structure formation on non-acoustic density perturbations at scales larger and smaller than L_J and is unstable to acoustical density fluctuations on scales larger than L_J (Gibson 1996). Pressure and temperature cannot prevent structure formation on scales larger or smaller than L_J. Numerical simulations showing sub-Jeans scale instabilities are rejected as "artificial fragmentation" based on Jeans' misconceptions (Truelove et al. 1997). The fragmentation is real, and the rejection is a serious mistake.

Density fluctuations in fluids are not barotropic as assumed by Jeans 1902 except rarely in small regions for short times near powerful sound sources. Density fluctuations that triggered the first gravitational structures in the primordial fluids of interest were likely non-acoustic (non-barotropic) density variations from turbulent mixing of temperature and chemical species concentrations reflecting big bang turbulence patterns (Gibson 2001, 2004, 2005) as shown by turbulence signatures (Bershadskii and Sreenivasan 2002; Bershadskii 2006) in the cosmic microwave background temperature anisotropies. From Jeans' theory without Jeans' swindle, a gravitational condensation on an acoustical density maximum rapidly becomes a non-acoustical density maximum because the gravitationally accreted mass retains the (zero) momentum of the motionless ambient gas. The Jeans 1902 analysis was ill posed because it failed to include non-acoustic density variations as an initial condition.

Fluids with non-acoustic density fluctuations are continuously in a state of structure formation due to self gravity unless prevented by diffusion or fluid forces (Gibson 1996). Turbulence or viscous forces can dominate gravitational forces at small distances from a point of maximum or minimum density to prevent gravitational structure formation, but gravitational forces will dominate turbulent or viscous forces at larger distances to cause structures if the gas or plasma does not diffuse away faster than it can condense or rarify due to gravity. The concepts of pressure support and thermal support are artifacts of the erroneous Jeans criterion for gravitational instability. Pressure forces could not prevent gravitational structure formation in the plasma epoch because pressures equilibrate in time periods smaller that the gravitational free fall time $(\rho G)^{-1/2}$ on length scales smaller than the Jeans scale L_J, and L_J in the primordial plasma was larger than the Hubble scale of causal connection $L_J > L_H = ct$, where c is light speed and t is time. Therefore, if gravitational forces exceed viscous and turbulence forces in the plasma epoch at Schwarz scales L_{ST} and L_{SV} smaller than L_H (Table 1) then gravitational structures will develop, independent of the

Jeans criterion. Only a very large diffusivity (D_B) could interfere with structure formation in the plasma. Diffusion prevents gravitational clumping of the non-baryonic dark matter (cold or hot) in the plasma epoch because $D_{NB} \gg D_B$ and $(L_{SD})_{NB} \gg L_H$. Diffusion does not prevent fragmentation of the baryonic material at 30,000 years when $(L_{SD})_B \leq L_H$.

Consider the gravitational response of a large motionless body of uniform density gas to a sudden change at time $t = 0$ on scale $L \ll L_J$ of a rigid mass perturbation $M(t)$ at the center, either a cannonball or vacuum beach ball depending on whether $M(0)$ is positive or negative (Gibson 2000). Gravitational forces cause all the surrounding gas to accelerate slowly toward or away from the central mass perturbation. Integrating the radial gravitational acceleration $dv_r/dt = -GM/r^2$ gives the radial velocity

$$v_r = -GM(t)tr^{-2} \tag{2}$$

so the central mass increases or decreases at a rate

$$dM(t)/dt = -v_r 4\pi r^2 \rho = 4\pi\rho G M(t)t \tag{3}$$

substituting the expression for v_r. Separating variables and integrating gives

$$M(t) = M(0)exp(\pm 2\pi\rho G t^2), t \ll t_G \tag{4}$$

respectively, where nothing much happens for time periods less than the gravitational free fall time $t_G = (\rho G)^{-1/2}$ except for a gradual build up or depletion of the gas near the center. Note that the classic Bondi-Hoyle-Littleton accretion rate $dM_{BH}/dt \approx 4\pi\rho[GM]^2 V_S^{-3}$ (Krumholz et al. 2006; Padoan et al. 2005; Edgar 2004) on point masses M in a gas of density ρ is contradicted. The sound speed V_S is irrelevant to point mass accretion rates for the same reasons V_S is irrelevant to gravitational structure formation for times $t \ll t_G$.

For condensation, at $t = 0.43t_G$ the mass ratio $M(t)/M(0)$ for $r < L$ has increased by only a factor of 2.7, but goes from 534 at $t = t_G$ to 10^{11} at $t = 2t_G$ during the time it would take for an acoustic signal to reach a distance L_J. Hydrostatic pressure changes are concentrated at the Jeans hydrostatic scale $L_{JHS} \ll L_J$. Pressure support and the Jeans 1902 criterion clearly fail in this exercise, indicating failure of CDMHC cosmology.

The diffusion velocity is D/L for diffusivity D at distance L (Gibson 1968a; Gibson 1968b) and the gravitational velocity is $L(\rho G)^{1/2}$. The two velocities are equal at the diffusive Schwarz length scale

$$L_{SD} \equiv [D^2/\rho G]^{1/4}. \tag{5}$$

Weakly collisional particles such as the hypothetical cold-dark-matter (CDM) material cannot possibly form clumps, seeds, halos, or potential wells for baryonic matter collection

because the CDM particles have large diffusivity and will disperse, consistent with observations (Sand et al. 2002). Diffusivity $D \approx V_p \times L_c$, where V_p is the particle speed and L_c is the collision distance. Because weakly collisional particles have large collision distances with large diffusive Schwarz lengths the non-baryonic dark matter (possibly neutrinos) is the last material to fragment by self gravity and not the first as assumed by CDM cosmologies. The first structures occur as proto-supercluster-voids in the baryonic plasma controlled by viscous and weak turbulence forces, independent of diffusivity ($D \approx \nu$). The CDM seeds postulated as the basis of CDMHCC never happened because $(L_{SD})_{NB} \gg ct$ in the plasma epoch. Because CDM seeds and halos never happened, hierarchical clustering of CDM halos to form galaxies and their clusters never happened (Gibson 1996, 2000, 2001, 2004, 2005, 2006a, 2006b).

Cold dark matter was invented to explain the observation that gravitational structure formed early in the universe that should not be there from the Jeans 1902 criterion that forbids structure in the baryonic plasma because $(L_J)_B > L_H$ during the plasma epoch (where sound speed approached light speed $V_S = c/\sqrt{3}$). In this erroneous CDM cosmology, non-baryonic particles with rest mass sufficient to be non-relativistic at their time of decoupling are considered "cold" dark matter, and are assumed to form permanent, cohesive clumps in virial equilibrium that can only interact with matter and other CDM clumps gravitationally. This assumption that CDM clumps are cohesive is unnecessary, unrealistic, and fluid mechanically untenable. Such clumps are unstable to tidal forces because they lack particle collisions necessary to produce cohesive forces to hold them together (Gibson 2006a).

Numerical simulations of large numbers of falsely cohesive CDM clumps show a tendency for the clumps to clump further due to gravity to form "dark matter halos", falsely justifying the cold dark matter hierarchical clustering cosmology (CDMHCC). The clustering "halos" grow to $10^6 M_\odot$ by about $z = 20$ (Abel et al. 2002) as the universe expands and cools and the pre-galactic clumps cluster. Gradually the baryonic matter (at 10^{16} s) falls into the growing gravitational potential wells of the CDM halos, cools off sufficiently to form the first (very massive and very late at 300 Myr) Population III stars whose powerful supernovas reionized all the gas of the universe (O'Shea & Norman 2006). However, observations show this never happened (Aharonian et al. 2006; Gibson 2006a). Pop-III photons are not detected, consistent with the HGD prediction that they never existed and that the first stars formed at 10^{13} s (0.3 Myr) and were quite small except at the cores of PGCs at the cores of the protogalaxies. The missing hydrogen cited as ("Gunn-Peterson trough") evidence for reionization is actually sequestered as PGC clumps of frozen JPP planets. As we have seen, CDMHCC is not necessary since the Jeans 1902 criterion is incorrect. Baryons (plasma) begin gravitational structure formation during the plasma epoch when the horizon scale exceeds the largest Schwarz scale (Gibson 1996; Gibson 2000).

Clumps of collisionless or collisional CDM would either form black holes or thermalize in time periods of order the gravitational free fall time $(\rho G)^{-1/2}$ because the particles would gravitate to the center of the clump by core collapse where the density would exponentiate, causing double and triple gravitational interactions or particle collisions that would thermalize the velocity distribution and trigger diffusional evaporation. For collisional CDM, consider a spherical clump of perfectly cold CDM with mass M, density ρ, particle mass m and collision cross section σ. The clump collapses in time $(\rho G)^{-1/2}$ to density $\rho_c = (m/\sigma)^{3/2} M^{-1/2}$ where collisions begin and the velocity distribution thermalizes. Particles with velocities greater than the escape velocity $v \approx 2MG/r$ then diffuse away from the clump, where $r = (M/\rho)^{1/3}$ is the initial clump size. For typically considered CDM clumps of mass $\approx 10^{36}$ kg and CDM particles more massive than 10^{-24} kg (WIMPs with $\sigma \approx 10^{-42}$ m^2 small enough to escape detection) the density from the expression would require a collision scale smaller than the clump Schwarzschild radius so that such CDM clumps would collapse to form black holes. Less massive motionless CDM particles collapse to diffusive densities smaller than the black hole density, have collisions, thermalize, and diffuse away. From the outer halo radius size measured for galaxy cluster halos it is possible to estimate the non-baryonic dark matter particle mass to be of order 10^{-35} kg (10 ev) and the diffusivity to be $\approx 10^{30}$ m^2 s^{-1} (Gibson 2000). Thus, CDM clumps are neither necessary nor physically possible, and are ruled out by observations (Sand et al. 2002). It is recommended that the CDMHC scenario for structure formation and cosmology be abandoned.

The baryonic matter is subject to large viscous forces, especially in the hot primordial plasma and gas states existing when most gravitational structures first formed (Gibson 2000). The viscous forces per unit volume $\rho\nu\gamma L^2$ dominate gravitational forces $\rho^2 G L^4$ at small scales, where ν is the kinematic viscosity and γ is the rate of strain of the fluid. The forces match at the viscous Schwarz length

$$L_{SV} \equiv (\nu\gamma/\rho G)^{1/2}, \tag{6}$$

which is the smallest size for self gravitational condensation or void formation in such a flow. Turbulent forces may permit larger mass gravitational structures to develop; for example, in thermonuclear maelstroms at galaxy cores to form central black holes. Turbulent forces $\rho\varepsilon^{2/3} L^{8/3}$ match gravitational forces $\rho^2 G L^4$ at the turbulent Schwarz scale

$$L_{ST} \equiv \varepsilon^{1/2}/(\rho G)^{3/4}, \tag{7}$$

where ε is the viscous dissipation rate of the turbulence. Because in the primordial plasma the viscosity and diffusivity are identical and the rate-of-strain γ is larger than the free-fall frequency $(\rho G)^{1/2}$, the viscous and turbulent Schwarz scales L_{SV} and L_{ST} will be larger than the diffusive Schwarz scale L_{SD}, from (3), (4) and (5).

The criterion for structure formation in the plasma epoch is that both L_{SV} and L_{ST} become less than the horizon scale $L_H = ct$. Reynolds numbers in the plasma epoch were near critical, with $L_{SV} \approx L_{ST}$. From $L_{SV} < ct$, gravitational structures first formed when ν first decreased to values less than radiation dominated values $c^2 t$ at time 30,000 years or $t \approx 10^{12}$ seconds (Gibson 1996), well before 10^{13} seconds which is the time of plasma to gas transition (300,000 years). Because the expansion of the universe inhibited condensation but enhanced void formation in the weakly turbulent plasma, the first structures were proto-supercluster-voids in the baryonic plasma. At 10^{12} s

$$(L_{SD})_{NB} \gg L_{SV} \approx L_{ST} \approx 5 \times L_K \approx L_H = 3 \times 10^{20}\mathrm{m} \gg (\mathrm{L_{SD}})_{\mathrm{B}}, \tag{8}$$

where $(L_{SD})_{NB}$ refers to the non-baryonic component and L_{SV}, L_{ST}, L_K, and $(L_{SD})_B$ scales refer to the baryonic (plasma) component. Acoustic peaks inferred from CMB spectra reflect acoustic signatures of the first gravitational structure formation and the sizes of the voids (see §4 Fig. 9). These supercluster voids are cold spots on the CMB and completely empty at 10^{25} m scales from radio telescope measurements (Rudnick et al. 2007). Because such scales require impossible clustering speeds, this strongly contradicts ΛCDMHCC.

As proto-supercluster mass plasma fragments formed, the voids filled with non-baryonic matter by diffusion, thus inhibiting further structure formation by decreasing the gravitational driving force. The baryonic mass density $\rho \approx 3 \times 10^{-17}$ kg/m^3 and rate of strain $\gamma \approx 10^{-12}$ s^{-1} were preserved as hydrodynamic fossils within the proto-supercluster fragments and within proto-cluster and proto-galaxy objects resulting from subsequent fragmentation as the photon viscosity and L_{SV} decreased prior to the plasma-gas transition and photon decoupling (Gibson 2000). As shown in Eq. 6, the Kolmogorov scale $L_K \equiv [\nu^3/\varepsilon]^{1/4}$ and the viscous and turbulent Schwarz scales at the time of first structure matched the horizon scale $L_H \equiv ct \approx 3 \times 10^{20}$ m, freezing in the density, strain-rate, and spin magnitudes and directions of the subsequent proto-cluster and proto-galaxy fragments of proto-superclusters. Remnants of the strain-rate and spin magnitudes and directions of the weak turbulence at the time of first structure formation are forms of fossil vorticity turbulence (Gibson 1999).

The quiet condition of the primordial gas is revealed by measurements of temperature fluctuations of the cosmic microwave background radiation that show an average $\delta T/T \approx 10^{-5}$ too small for much turbulence to have existed at that time of plasma-gas transition (10^{13} s). Turbulent plasma motions were strongly damped by buoyancy forces at horizon scales after the first gravitational fragmentation time 10^{12} s. Viscous forces in the plasma are inadequate to explain the lack of primordial turbulence ($\nu \geq 10^{30}$ m^2 s^{-1} is required but, after 10^{12} s, $\nu \leq 4 \times 10^{26}$, Gibson 2000). The observed lack of plasma turbulence proves that large scale buoyancy forces, and therefore self gravitational structure formation, must have begun in the plasma epoch $\approx 10^{11} - 10^{13}$ s.

The gas temperature, density, viscosity, and rate of strain are all precisely known at transition, so the gas viscous Schwarz mass $L_{SV}^3\rho$ is 10^{24-25} kg, the mass of a small planet (Mars-Earth), or about $10^{-6}M_\odot$, with uncertainty a factor of ten. From HGD, soon after the cooling primordial plasma turned to gas at 10^{13} s (300,000 yr), the entire baryonic universe condensed to a fog of hot planetary-mass primordial-fog-particle (PFPs) clouds, preventing collapse at the accoustic Jeans mass. In the cooling universe these gas-cloud objects cooled and shrank, formed H-He rain, and froze solid to become the BDM and the basic material of construction for stars and everything else, presently $\approx 30 \times 10^6$ rogue planets per star in trillion-planet Jeans-mass (10^{36} kg) PGC clumps.

The Jeans mass $L_J^3\rho$ of the primordial gas at transition was about $10^6 M_\odot$, also with $\approx \times 10$ uncertainty, the mass of a globular-star-cluster (GC). Proto-galaxies fragmented at the PFP scale but also at this proto-globular-star-cluster PGC scale L_J, although not for the reasons given by the Jeans 1902 theory. Density fluctuations in the gaseous proto-galaxies were absolutely unstable to void formation at all scales larger than the viscous Schwarz scale L_{SV}. Pressure can only remain in equilibrium with density without temperature changes in a gravitationally expanding void on scales smaller than the Jeans scale. From the second law of thermodynamics, rarefaction wave speeds are limited to speeds less than the sonic velocity. Density minima expand due to gravity to form voids subsonically. Cooling could therefore occur and be compensated by radiation in the otherwise isothermal primordial gas when the expanding voids approached the Jeans scale. Gravitational fragmentations of proto-galaxies were then accelerated by radiative heat transfer to these cooler regions, resulting in fragmentation at the Jeans scale and isolation of proto-globular-star-clusters (PGCs) with the primordial-gas-Jeans-mass.

These PGC objects were not able to collapse from their own self gravity because of their internal fragmentation at the viscous Schwarz scale to form $\approx 10^{24}$ kg PFPs. The fact that globular star clusters have precisely the same density $\approx \rho_0$ and primordial-gas-Jeans-mass from galaxy to galaxy proves they were all formed simultaneously soon after the time of the plasma to gas transition 10^{13} s. The gas has never been so uniform since, and no mechanism exists to recover such a high density, let alone such a high uniform density, as the fossil turbulent density value $\rho_0 \approx 3 \times 10^{-17}$ kg/m^3. Young globular cluster formation in BDM halos in the Tadpole, Mice, and Antennae galaxy mergers (Gibson & Schild 2003a) show that dark PGC clusters of PFPs are remarkably stable structures, persisting without disruption or star formation for more than ten billion years.

2.2. Observational evidence for PGCs and PFPs

Searches for point mass objects as the dark matter by looking for microlensing of stars in the bulge and the Magellanic clouds produced a few reliable detections and many self-lenses, variable stars and background supernova events, leading to claims by the MACHO/OGLE/EROS consortia that this form of dark matter has been observationally excluded (Alcock et al. 1998). These studies have all assumed a uniform ("Gaussian") density rather than the highly clumped ("log-Gaussian") density (Gibson & Schild 1999) with a non-linear frictional accretion cascade for the MAssive Compact Halo Objects (MACHOs) expected from HGD. Sparse sampling reduces detection sensitivity to small clumped planetary mass objects. Since PFPs within PGC clumps must accretionally cascade over a million-fold mass range to produce JPPs and stars their statistical distribution becomes an intermittent lognormal that will profoundly affect an appropriate sampling strategy and microlensing data interpretation. This rules out the exclusion of PFP mass objects as the baryonic dark matter (BDM) of the Galaxy by MACHO/OGLE/EROS (Gibson & Schild 1999). OGLE campaigns focusing on large planetary mass ($10^{-3}M_{\odot}$) to brown dwarf mass objects have revealed 121 transiting and orbiting candidates, some with orbits less than one day (Udalski et al. 2003). More recent observations toward M31 give 95% confidence level claims that brown dwarf MACHOs comprise ≈20% of the combined MW-M31 dark matter halo (Calchi-Novati et al. 2005). Estimates for the MW halo of $\approx 0.2M_{\odot}$ lenses from LMC stars have increased to ≈16% (Alcock et al. 2000; Bennett 2005). Both of these estimates increase by a large factors ($\gg 5$) from HGD when JPP clumping into PGCs is taken into account since microlensing by a JPP planet requires a line of sight passing through a PGC and PGCs (as CHVCs) occupy a small fraction of the sky ($\approx 1\%$) with HVC wakes ($\approx 20\%$).

Evidence that planetary mass objects dominate the BDM in galaxies has been gradually accumulating and has been reviewed (Gibson & Schild 2003b). Cometary knot candidates for PFPs and JPPs appear whenever hot events like white dwarfs, novas, plasma jets, Herbig-Haro objects, and supernovas happen, consistent with the prediction of HGD that the knots reveal Jovian planets that comprise the BDM, as we see for the planetary nebulae in the present paper. However, the most convincing evidence for our hypothesis, because it averages the dark matter over much larger volumes of space, is provided by one of the most technically challenging areas in astronomy; that is, quasar microlensing (Schild 1996). Several years and many dedicated observers were required to confirm the Schild 1996 measured time delay of the Q0957 lensed quasar images so that the twinkling of the subtracted light curves could be confirmed and the frequency of twinkling interpreted as evidence that the dominant point mass objects of the lensing galaxy were of small planetary mass.

By using multiple observatories around the Earth it has now been possible to accurately

establish the Q0957 time delay at 417.09 ± 0.07 days (Colley et al. 2002, 2003). With this unprecedented accuracy a statistically significant microlensing event of only 12 hours has now been detected (Colley & Schild 2003) indicating a 7.4×10^{22} kg (moon-mass) PFP. An additional microlensing system has been observed (Schechter et al. 2003) and confirmed, and its time delay measured (Ofek and Maoz 2003). To attribute the microlensing to stars rather than planets required Schechter et al. 2003 to propose relativistic knots in the quasar. An additional four lensed quasar systems with measured time delays show monthly period microlensing. These studies support the prediction of HGD that the masses of their galaxy lenses are dominated by small planetary mass objects as the baryonic dark matter (Burud et al. 2000, 2002; Hjorth et al. 2002) that may produce intermittent systematic dimming errors rather than dark energy (Schild & Dekker 2006).

Flux anomalies in four-quasar-image gravitational lenses have been interpreted as evidence (Dalal and Kochanek 2002) for the dark matter substructure predicted by CDM halo models, but the anomalies may also be taken as evidence for concentrations of baryonic dark matter such as PGCs, especially when the images are found to twinkle with frequencies consistent with the existence of planetary mass objects. Evidence that the small planetary objects causing high frequency quasar image twinkling are clumped as PGCs is indicated by the HE1104 (Schechter et al. 2003) damped Lyman alpha lensing system (DLA $\equiv$ neutral hydrogen column density larger than $10^{24.3}$ m^{-2}), suggesting PGC candidates from the evidence of gas and planets. Active searches are underway for quasar lensing DLAs with planetary frequency twinkling that can add to this evidence of PGCs. Twenty $10^5 - 10^6 M_\odot$ (PGC-PFP) galaxy halo objects have been detected $\geq 10^{21}$ m from M31 (Thilker et al. 2004).

Perhaps the most irrefutable evidence for galaxy inner halos of baryonic PGC-PFP clumps is the HST/ACS image showing an aligned row of $42 - 46$ YGCs (see §2.3.2 and Fig. 1) precisely tracking the frictionally merging galaxy fragments VVcdef in the Tadpole system (Gibson & Schild 2003a). Concepts of collisionless fluid mechanics and collisionless tidal tails applied to merging galaxy systems are rendered obsolete by this image. Numerous YGCs are also seen in the fragmenting galaxy cluster Stephan's Quintet-HGC 92 (Gibson & Schild 2003c). The mysterious red shifts of this dense Hickson Compact Galaxy Cluster (HGC) support the HGD model of sticky beginnings of the cluster in the plasma epoch, where viscous forces of the baryonic dark matter halo of the cluster have inhibited the final breakup due to the expansion of the universe to about 200 million years ago and reduced the transverse velocities of the galaxies to small values so that they appear aligned in a thin pencil by perspective. Close alignments of QSOs with bright galaxies (suggesting intrinsic red shifts) have been noted for many years (Hoyle et al. 2000), but are easily explained by the HGD concept that proto-galaxies formed in the plasma epoch by viscous-gravitational fragmentation of larger objects termed proto-galaxy-clusters (Gibson 2000).

2.3. Planetary Nebula formation

2.3.1. The standard model

According to the standard model of white dwarf and planetary nebula formation, an ordinary star like the sun burns less than half of its hydrogen and helium to form a hot, dense, carbon core (Busso et al. 1999; Iben 1984). White dwarf masses are typically $0.6M_{\odot}$ or less even though the initial star mass is estimated from the increased brightness at WD formation to be $8M_{\odot}$ or more. Are intermediate stars really so massive? If so, how does all this mass escape? Radiation pressures are much too small for such massive ejections either as winds, plasma beams, or clumps, even assisted by dust and pulsations (Woitke 2006). Most of the large mass inferred from the brightness probably just reflects the bright JPP atmospheres as the massive frozen planets near the new white-hot dwarf evaporate and ionize, incleasing the JPP entrainment rate by friction. Claims of red-blue supergiant stripping (Maund et al. 2004) are highly questionable. The brightness of the JPP atmospheres masquerades as huge central stellar masses and envelopes. Friction from the gas and dust of evaporated JPPs accelerates the formation of the PNe and the growth of central carbon white dwarf(s) toward either a SNe Ia event or a bypass of the event by enhanced mixing of the carbon core giving critical mass $1.4M_{\odot}$ iron-nickel cores and SNe II events. How much of the $9 - 25M_{\odot}$ mass of SNe II remnants can be attributed to the precursor star?

Interpretation of nuclear chemistry from spectral results to describe the physical processes of stellar evolution to form white dwarfs (Herwig 2005) is limited by a poor understanding of modern stratified turbulent mixing physics. Methods that account for fossil and zombie turbulence radial internal wave transport in mixing chimneys are required (Keeler et al. 2005; Gibson et al. 2006a; Gibson et al. 2006b; Gibson et al. 2007) focusing on the smallest scales (Wang & Peters 2006). New information about carbon stars is available at the critical infrared spectral bands of cool AGB stars from the *Spitzer Space Telescope* (Lagadec et al. 2006) but the mass loss problem remains unsolved. Crucial contributions of mass and luminosity from the ISM are not taken into account in the standard models of PNe formation and evolution and in standard models of star formation and evolution.

From standard star models, the neutral atmosphere of a dying red giant with approximate density $\rho \approx 10^{-17}$ kg m^{-3} (Chaisson & McMillan 2001) is somehow expelled to the ISM along with a very massive (but unobserved and likely mythical) envelope by (unexplained) dynamical and photon pressures when the hot, $T \approx 10^5$ K, dense, $\rho \approx 10^{10}$ kg m^{-3}, carbon core is exposed as a white dwarf star with no source of fuel unless accompanied by a donor companion. The density of this 10^{16} kg atmosphere expanded to the distance of the inner

Helix radius is trivial ($\approx 10^{-29}$ kg m^{-3}). At most this could bring the PNe ejected atmosphere density to a small fraction ($\approx 10^{-15}$) of $\rho \approx 10^{-14}$ kg m^{-3} values observed in the knots (Meaburn et al. 1998). Why are small and intermediate mass main sequence stars ($1-9M_{\odot}$) so inefficient that they burn only a small fraction of their initial mass before they die to form ($0.5-1.44M_{\odot}$) white dwarfs? We suggest small stars are likely to be more efficient than large stars in their burning of gravitationally collected mass. What they don't burn is returned as helium and carbon white dwarfs, neutron stars (if the small star gets large) and SNe ashes, not superwinds. The ashes are collected gravitationally by the $\geq 1000M_{\odot}$ of ambient PFPs and JPPs influenced by an average star in its evolution from birth to death, and a small fraction returned to the stars as the dust of comets. From HGD, most intermediate mass stars and superwinds are obsolete working hypotheses used to explain unexpected brightness of JPP atmospheres formed from the ISM and not ejected (Herwig 2005).

From radio telescope measurements (Knapp et al. 1982) large stars up to $9M_{\odot}$ form white dwarfs and companions with huge envelopes that have complex histories with superwind Asymptotic Giant Branch (AGB) periods where most of the assumed initial mass of the star is mysteriously expelled into the ISM (Busso et al. 1999). The possibility is not mentioned in the literature that the ISM itself could be supplying the unexpectedly large, luminous, envelope masses and superwind mass losses inferred from radio and infrared telescope measurements (Knapp et al. 1982), OH/IR stars (de Jong 1983), and star cluster models (Claver et al. 2001). It has been speculated in versions of the standard model that shock wave instabilities somehow produce cometary knots ejected by PNe central stars (Vishniac 1994; Vishniac 1983), or that a fast wind impacts the photo-ionized inner surface of the dense ejected envelope giving Rayleigh-Taylor instabilities that somehow produce the cometary globules and radial wakes observed (Garcia-Segura et al. 2006; Capriotti 1973). Such models produce cometary globule densities much smaller than observed, and require globule wake densities much larger than observed.

Several other problems exist for standard PNe models without HGD. Huge ($3-9M_{\odot}$) H-He masses observed in PNe are richer in other species and dust than one would expect to be expelled as stellar winds or cometary bullets during any efficient solar mass star evolution, where most of the star's H-He fuel should presumably be converted by thermonuclear fusion to carbon in the core before the star dies. More than a solar mass of gas and dust is found in the inner nebular ring of Helix, with a dusty H-He-O-N-CO composition matching that of the interstellar medium rather than winds from the hydrogen-depleted atmosphere of a carbon star, but up to $11M_{\odot}$ may be inferred for the total PNe (Speck et al. 2002). The cometary globules are too massive and too dense to match any Rayleigh-Taylor instability model. Such models (Garcia-Segura et al. 2006) give cometary globule densities of only $\rho \approx 10^{-19}$ kg m^{-3} compared to $\rho \approx 10^{-14}$ kg m^{-3} observed.

The closest AGB C star is IRC+10216 (Mauron & Huggins 1999). It is brighter than any star at long wavelengths, but invisible in the blue from strong dust absorption. Loss rates inferred from its brightness are large ($2 \times 10^{-5} M_{\odot}$/yr). The possibility that the mass indicated by the brightness could have been brought out of the dark in place has not been considered. Multiple, fragmented and asymmetric rings are observed, indicating a central binary. The rings are irregular and extend to 4×10^{15} m, with central brightness of the envelope confined to 2×10^{14} m. The observed ring structures appear to be wakes of Jovian orbital planets evaporating in response to the red giant growth and powerful radiation from the central star(s). Rather than superwinds outward we see the effects of enhanced JPP accretion inward, clearing the Oort cloud cavity prior to PNe formation.

The density increase due to maximum expected Mach 6 hypersonic shock waves in astrophysical gases is only about a factor of six, not 10^5. Rayleigh-Taylor instability, where a low density fluid accelerates a high density fluid, causes little change in the densities of the two fluids. Turbulence dispersion of nonlinear thin shell instabilities (Vishniac 1994; Vishniac 1983) should decrease or prevent shock induced or gravitational increases in density. The masses of the inner Helix cometary globules are measured and modeled to be $\gg 10^{25}$ kg, much larger than expected for PFP planets that have not merged with other PFPs to form globulette clumps and JPPs. No mechanism is known by which such massive dense objects can form or exist near the central star. Neither could they be ejected without disruption to the distances where they are observed. Measurements of proper motions of the cometary knots provide a definitive test of whether the knots are in the gas and expanding at the outflow velocity away from the central binary, as expected in the standard model, or moving randomly with some collapse component toward the center. Proper motion measurements to date (O'Dell et al. 2002) suggest they are mostly moving randomly with approximately virial PGC speeds (also see Fig. 2 below in §3).

2.3.2. The HGD model

According to HGD, all stars are formed by accretion of PFP planets, larger Jovian PFP planets (JPPs), and brown and red dwarf stars within a primordial PGC interstellar medium. The accretion mechanism is likely to be binary with clumping, where two JPPs experience a near collision so that internal tidal forces and frictional heating of their atmospheres produces evaporation of the frozen H-He planets and an increase in the amount of gas in their atmospheres. Smaller JPP and PFP planets within the atmospheres are collected as comets or merging moons. Increased size and density of planet atmospheres from collisions, tidal forces, or star radiation results in "frictional hardening" of binary planets

until they fragment, evaporate, merge and then shrink and refreeze by radiation. The binary accretion cascade to larger mass clumps of planet-binaries and star-binaries continues until inhibited by thermonuclear processes. Hence "3 out of every 2 stars is a binary" (personal communication to RES from Cecilia Helena Payne-Gaposchkin, pioneer astronomer). This classic astronomical overstatement could actually be true if one of the "stars" is a binary and the other a binary of binaries or a triplet of two binaries and a rogue. Small binary stars with lots of moons and planets is the signature of star formation from planets. Large single stars with no planets and no moons is what you get from the large clouds of gas collected by CDM halos (Abel et al. 2002; O'Shea & Norman 2006).

Exotic clumped binary-star and binary-planet systems are highly likely from the non-linear nature of HGD star and JPP planet formation. Heating from a binary PFP merger results in a large atmosphere for the double-mass PFP-binary that will increase its cross section for capture of more PFPs in growing clumps. Evidence is accumulating that most PNe central stars are binaries as expected from HGD (De Marco et al. 2004; Soker 2006; Moe & De Marco 2006). One of the brightest stars in the sky is Gamma Velorum in Vela, with two binaries and two rogues all within 10^{16} m of each other, the nominal size of a PNe. One of the binaries is a WR star and a blue supergiant B-star with 1.5×10^{11} m (1 AU) separation. From aperture masking interferometry using the 10-m aperture Keck I telescope, another WR-B binary is the pinwheel nebula Wolf-Rayet 104 in Sagitarrius, where the stars are separated by only 3×10^{11} m (3 AU) and are 10^5 brighter than the sun (Tuthill et al. 1999). How much of the apparent brightness and apparent masses of these systems is provided by evaporating JPPs? The pinwheel nebula dust clouds are surprising this close to large hot stars ($\approx$ 50kK) that should reduce dust to atoms. Complex shock cooling induced dust models from colliding superwinds (Usov 1991; Pilyugin & Usov 2007) to explain the dust of pinweel nebulae are unnecessary if the stars are accreting a rain of dusty evaporating JPPs. When one member of the binary dies to become a shrinking white-dwarf it appears that the smaller star begins to eat the larger one (creating a brown dwarf desert). Few WD binaries are found with large mass ratios (Hoard et al. 2007). Either the WD binary has an equal mass companion or just a JPP accretion disk (Su et al. 2007).

Large PFP atmospheres from mergers and close encounters increase their frictional interaction with other randomly encountered ambient PFP atmospheres. This slows the relative motion of the objects and increases the time between their collisions and mergers. Radiation to outer space will cause the PFP atmospheres to cool and eventually rain out and freeze if no further close encounters or collisions occur, leading to a new state of metastable equilibrium with the ambient gas. To reach Jupiter mass, $10^{-6} M_\odot$ mass PFPs and their growing sons and daughters must pair 10 times ($2^{10} \approx 10^3$). To reach stellar mass, 20 PFP binary pairings are required ($2^{20} \approx 10^6$). Because of the binary nature of PFP structure

formation through JPPs, it is clear that matched double stars and complex systems will result, as observed, and that the stars will have large numbers of large gassy planets with many moons that the stars capture in orbit or absorb as comets, as observed.

Rocky and nickel-iron cores of planets like the Earth and rock-crusted stainless-steel Mercury in this scenario are simply the rocky and iron-nickel cores of rogue interstellar Jupiters that have processed the SiO dust, water, organics, iron and nickel particles accumulated gravitationally from supernova remnants in their cores and in the cores of the thousands of PFPs that they have accreted to achieve their masses. Rather than being accreted as comets by the growing star, these massive JPPs were captured in orbits and their gas layers evaporated as their orbits decayed to leave terrestrial planets (Vittone & Errico 2006). They were not created by any star as often assumed (Boss 1995; Boss 2004). A hot-Saturn exoplanet observed in orbit at only 6×10^9 m with a 4×10^{26} kg rocky-metal core conflicts with such stellar Jeans gravitational instability models (Sato et al. 2005) as well as with core accretion-gas capture models (Kornet et al. 2002) and proto-star dynamical fragmentation models (Bodenheimer et al. 2000). From HGD this size core implies a multi-Jupiter or red dwarf that has already lost most of its atmosphere to the central star or stars.

Without PFPs, the existence of rocks and unoxidized iron-nickel cores of planets are mysteries. It has been known since the end of the bronze age that very high temperatures are needed for carbon to reduce iron oxides to metalic iron, as will happen in supernovas IIab where hydrogen, silicon and carbon will form oxides by reducing oxides of iron and nickel to metal particles. All this stardust will be swept up by gravitational fields of the PFPs, which should by now be deeply crusted with dry magnetic talcum powder after their ≈13 billion years in existence as interstellar gravitational vacuum cleaners. Samples of cometary material confirm large quantities of stardust in comet tails and in comet bodies. Crashing a 364 kg object into Jupiter comet Tempel 1 revealed a ≫ 10m deep crust of 1-100 micron particle size low strength powder (A'Hearn et al. 2005; Feldman et al. 2006; Sunshine et al. 2006). Exotic refractory dust particles lacking carbonates or hydrates as collected by NASA's *Stardust* mission to Jupiter comet Wild 2 require high temperatures of formation (≫800-1400 K) and no wetness (Brownlee et al. 2006). Unexpectedly powerful mixing from creation in sub-Mercury orbits with transport far beyond Jupiter must be postulated for such comets to be created as the sun formed. The comets are easy to understand as pieces of PFP crust if stars, large planets and comets all form from dusty primordial planets in primordial PGC molecular clouds.

Large gas planets from PFP accretion cascades may form gently over long periods, with ample time at every stage for their atmospheres to readjust with ambient conditions and return to metastable states of random motion. These are probably the conditions under

which the old globular star clusters (OGCs) in the halo of the Milky Way Galaxy formed their small long-lived stars, and their large ancient planets (Sigurdsson et al. 2003). However, if the PFP accretional cascade is forced by radiation or tidal forces from passing stars or ambient supernovae, a more rapid cascade will occur where the PFP atmospheres become large and the relative motions in a PGC become highly turbulent. The turbulence will mix the PFPs and their large planet descendants and inhibit large average density increases or decreases. In this case another instability becomes possible; that is, if the turbulence weakens the creation of large central density structures but enhances accretion and clumping to form large planets and brown dwarfs, the increase of density at an accretion center can become so rapid that buoyancy forces may develop from the density gradients. This will suddenly damp the turbulence at the Schwarz turbulence scale L_{ST} (see Table 1) to produce fossil turbulence (Gibson 1999) in a volume containing $> M_{\odot}$ of gas, PFPs, JPPs, and a complex of binary stars in formation.

Turbulence fossilization due to buoyancy then creates a gravitational collapse of an accretion center of the resulting non-turbulent gas and PFPs from the sudden lack of turbulence resistance. A fossil turbulence hole in the ISM will be left with size determined by the turbulence levels existing at the beginning of fossilization. The accretion of the planets and gas within the hole will be accelerated by the rapidly increasing density. The total mass of the stars produced will be the volume of the "Oort cloud" hole (Oort cavity) times the ISM density. If the mass is many solar masses then the superstars formed will soon explode as supernovae, triggering a sequence of ambient PFP evaporations, accretional cascades, and a starburst that may consume the entire dark PGC and its PFPs to produce a million stars and a young globular cluster (YGC) or a super-star cluster (Tran et al. 2003).

Numerous YCCs are triggered into star formation by galaxy mergers, such as the merging of two galaxies and some fragments revealing a 130 kpc (4×10^{21} m) radius baryonic dark matter halo in the VV29abcdef Tadpole complex imaged by HST/ACS immediately after installation of the ACS camera (Benitez et al. 2004). Figure 1 shows an SSC dwarf galaxy, revealed in the baryonic dark matter halo of the central Tadpole galaxy VV29a by a dense narrow trail of YGCs pointing precisely to the spiral star wake produced as the dwarf blue galaxy VV29c and companions VV29def merged with VV29a (Gibson & Schild 2003a).

Planetary nebulae form when a small star formed by gradual PFP accretion uses up all its H-He fuel to form a dense white dwarf carbon core with temperature less than 8×10^8 K. The high exposed core temperature and spin enhanced radiation of plasma in jets and winds from the white dwarf evaporate JPPs remaining nearby from its red giant phase giving an AGB (asymptotic giant branch) red giant star (eg: Arcturus) that appears to be a massive envelope from its brightness. As discussed previously for the standard model, red giant stars

have envelope diameter $\approx 10^{12}$ m, atmosphere density $\approx 10^{-17}$ kg m^{-3} and a 6×10^6 m diameter $\rho \approx 10^{10}$ kg m^{-3} carbon star core (Chaisson & McMillan 2001). The total mass expelled is thus only $\approx 10^{16}$ kg, or $\approx 10^{-8} M_\odot$, much less than the gas mass values $(3-1) \times M_\odot$ claimed to be observed in planetary nebulae from their luminosity. Without HGD, this much gas is mysterious.

Because white dwarfs have close companion stars and continuous JPP accretion, as observed for Helix and Cats-Eye and easily inferred for many other PNe's (O'Dell et al. 2002), the companions and JPP accretion disk will contribute to the WD growth. Spinning magnetic field lines at the white dwarf poles and magnetohydrodynamic turbulence at its equator capture the incoming plasma and magnetic fields to produce powerful plasma jets, plasma winds, and photon radiation. The accretion disk of the white dwarf may shield some of its radiation and broadly beam some of its radiation. The following observations show the effects of such plasma beams and radiation in PNe.

3. Observations

Figure 2 is an HST image of the Large Magellanic Cloud PNe N66 (SMP 83, WS 35, LM1-52) at a distance of 1.7×10^{21} m (57 pc), taken on 06/26/1991 with the European Space Agency Faint Object Camera (FOC) filtered for 540 seconds at the 5007 Å doubly ionized oxygen emission line (O III). This remarkable object is the only confirmed PNe where the central star is classified as a Wolf-Rayet of the nitrogen sequence type (WN). LMC-N66 has recently exhibited highly variable brightness, with an indicated mass loss rate increase from 1983 to 1995 by a factor of 40 (Pena et al. 1997). Its central binary is surrounded by a looped $\approx 6 M_\odot$ mass PNe of bright cometary globules, interpreted in Fig. 2 as partially evaporated clumping JPPs in multi-Jupiter mass globulettes (Gahm et al. 2007). From spectal analysis and modeling the central binary system is a $1.2 M_\odot$ white dwarf with a non-degenerate companion that is building the WD toward the Chandrasekhar limit and a SN Ia event in $\approx 10^5$ years (Pena et al. 2004; Hamann et al. 2003) along with the rain of JPP comets. Part of the mass stream to the WD is ejected as a nutating plasma beam that evaporates JPPs in the looped arcs shown in Fig. 2. The mass M_{PNe} of the observed nebular material is more than $5 M_\odot$. From HGD this implies about 0.5% of the $1000 M_\odot$ PFPs and JPPs of the interstellar medium within the 2.5×10^{16} m luminous range of the PNe have been brought out of the dark by radiation and plasma jets from the central star system.

Some of the JPPs in Fig. 2 have detectable O III emission (5007 Å) wakes that indicate JPP velocities V_{JPP} are in random directions with at least virial values, as expected from HGD. The virial velocity $V_{vir} = (2MG/r)^{1/2}$ for a PGC is about 1.7×10^4 m/s, where M

is the PGC mass, G is Newton's constant, and r is the PGC radius. In PGC metastable equilibrium the PFP speed should slow to less than V_{vir} due to gas friction, so that the growth of JPPs and the rate of star formation are low. Most PGCs will never develop a star. Some have developed a million.

Wolf-Rayet (WR) stars are very bright, red, and until recently have been claimed to be very massive ($\geq 20M_{\odot}$) with large mass loss rates ($\geq 10^{-5}M_{\odot}$/yr). Star mass models derived from the increased luminosity with mass of gas cloud collapse (Iben 1965) are unreliable if stars form from planets. WR stars are often found with surrounding nebulae (Morgan et al. 2003), generally in galaxy disks where PGCs are accreted and where V_{JPP} values should be large. High He, C, N, and O concentrations suggest final stages of evolution toward white dwarf status for at least one of the central stars. HST images reveal most WRs to be binary or in multiple star systems, with numerous dense clumps in their envelopes that appear to be evaporating globulette-JPPs as in Fig. 2. Most of their claimed mass and most of their claimed large mass loss rates are likely the result of bright evaporating JPPs spin-radiated by a central dying star and misinterpreted as massive stellar envelopes and superwinds. For example, see WR124 in nebula M1-67, STSci-1998-38 in the HST archives. From the 1998 news release nebular clumps have mass 2×10^{26} kg and scale 10^{14} m, giving a density 10^{-16} kg m^{-3}. How can such massive dense objects be ejected from a star? From HGD the clumps are clearly bright JPP planet atmospheres evaporated from the PGC-ISM. Vast overestimates result for WR star masses, SN II precursor star masses (Maund et al. 2004; Podsialowski et al. 1993), and initial White-Dwarf star masses. To explain the extreme brightness of SN 1993J with a single star without JPPs requires a $40M_{\odot}$ precursor mass (Aldering et al. 1994).

Figure 3 shows a standard stellar-model white dwarf mass evolution diagram for planetary nebulae in Praesepe (circles) and Hyades (squares) star clusters (Claver et al. 2001), compared to Helix and LMC-N66 and our pulsar precursor model. In an 80 PNe collection (Gorny et al. 1997), Helix has the most massive central white dwarf. It is also the dimmest, and therefore has the smallest estimated PNe mass M_{PNe} (shown as an open star in Fig. 3). From HGD, $M_{Initial} \approx M_{PNe}$ masses are vastly overestimated from the brightness of evaporated JPPs that dominate M_{PNe}. Observed M_{PNe} should therefore not be interpreted as the initial masses $M_{Initial}$ of central white dwarfs, as assumed using the standard PNe model (Weidemann 2000). Masses of WR stars and SNe II precursors are overestimated from their extreme JPP atmosphere brightness and implied super-massive Hayashi tracks (Iben 1965) by even larger factors. Rather than $9 - 25M_{\odot}$ (Gelfand et al. 2007; Maund et al. 2004; Shigeyama & Nomoto 1990) such stars are likely no larger than $1.4M_{\odot}$ since neutron stars have mass $1.4M_{\odot}$ (Thorsett & Chakrabarty 1999) precisely known from pulsar timing. Any central WD of a PNe has the possibility to grow

to the SNe Ia size by accretion of JPPs, as shown by the LMC-N66 (hexagon) point in Fig. 3. If the WD is fed by a companion red giant (RB) accretion disk (Hachisu & Kato 2001) as well as by JPP rain the probability of a SN Ia or SN II event increases. In the final stages of growth, the WD will likely be surrounded by a PNe similar to that of Helix, where the central Oort cavity sphere has been depleted of JPPs by gravity to form the central star and its JPP accretion disk (Su et al. 2007) and the PNe is formed by radiative evaporation of JPPs to form large atmospheres by plasma jets and plasma and photon radiation powered by JPP accretion and the rapid spinning and complex magnetohydrodynamics of the central white dwarf. Supernova Ia events will always be subject to intermittent dimming depending on the line of sight. PNe can appear around hot central stars at any time during the life of the star, which is more than 10^{10} years for the small stars leading to SNe Ia events, not 10^4 years as assumed in the standard PNe model.

Figure 4 shows a mosaic of nine HST/ACS images from the F658N filter (H_α and N II) that enhances the ionized cometary globules and their hydrogen tails (http://archive.stsci.edu /hst/helix/images.html). A sphere with radius 5×10^{15} m is shown. A much smaller sphere will give an adequate supply of primordial-fog-particles (PFPs) with PGC primordial mass density $\rho_0 = 3 \times 10^{-17}$ kg m^{-3} to form two central solar mass stars. The large comets closest to the central stars must be evaporating massive planets (Jupiters) to survive measured evaporation rates of $2 \times 10^{-8} M_\odot$ year^{-1} (Meaburn et al. 1998) for the 20,000 year kinematic age of Helix. Massive planets are formed in the accretional cascade of PFPs to form stars according to HGD. The younger (2,000 year old) planetary nebula Spirograph (IC 418) shown below shows shock wave patterns from the supersonic stellar winds but no cometary PFP candidates within its fossil turbulence accretion sphere corresponding to the Oort cloud source of long period comets.

Is the sun surrounded by an Oort cavity of size $L_{Oort} \approx (M_{star}/\rho_{ISM})^{1/3} \approx 4 \times 10^{15}$ m reflecting its $1 M_\odot$ of accretion in a PFP dominated interstellar medium with primordial density ρ_0? Rather than an Oort cloud of comets, are long period "Oort Cloud Comets" actually PFP and JPP planets accreting from the inner boundary of the Oort cavity? In a remarkable application of celestial mechanics to Oort cloud comets ("Cometary evidence of a massive body in the outer Oort cloud") a multi-Jupiter (JPP) mass perturber within 5° of the Galactic plane has been inferred (Matese et al. 1999). Out of 82 "new" first-time entrant long period comets with orbit scales less than 10^{16} m, 29 have aphelion directions on the same great circle, suggesting that the galactic-tide-Saturn-Jupiter loss cylinder has been smeared inward along the track of the perturber. An apparently independent 99.9% detection (Murray 1999) gives the object a retrograde orbit with period of 5.8×10^6 years assuming it is gravitationally bound to the sun, and excludes a variety of explanations (eg: star encounter, solar system ejection) for its existence as extremely unlikely. The object is

easy to explain from HGD as one of many JPPs at distance $\geq 2\times10^{15}$ m on the inner surface or our Oort cavity as in Figs. 4 for Helix, Fig. 7 for Eskimo and Fig. 8 for Dumbbell PNes.

Assuming density ρ_0, the inner spherical nebular shell for Helix contains $\approx 20M_\odot$ of dark PFPs, from which $1.5 \times M_\odot$ has been evaporated as gas and dust (Speck et al. 2002). Evidence for bipolar beamed radiation is shown by the brighter regions of the nebula in Fig. 4 at angles 10 and 4 o'clock, and by the light to dark transition after 11:30 suggesting the bipolar beam is rotating slowly clockwise. Note that the tails of the comets are long ($\approx 10^{15}$ m) before 11:30 and short or nonexistent afterward. Rayleigh-Taylor instability as a mechanism to produce the globules (Capriotti 1973) gives densities much too low. The WD plasma beams appear to have started rotation at about 1 o'clock with deep penetration of the radiation on both sides, revolved once, and is observed with bright edge at 11:30 having completed less than two revolutions to form the Helix spiral.

Figure 5 shows a Hubble Space Telescope Helix WFPC2 1996 image to the northeast in Helix where the closest comets to the center are found (O'Dell & Handron 1996). The cometary globules have size about 6×10^{13} m and measured atmospheric mass $(2-11)\times10^{25}$ kg (Meaburn et al. 1992; O'Dell & Handron 1996; Huggins et al. 2002), with spacing $\approx 3 \times 10^{14}$ m, as expected for $\approx 8 \times 10^{26}$ kg evaporating JPP gas planets in a relic concentration corresponding to the primordial (ρ_0) plasma density 3×10^{-17} kg m^{-3} at the time of first structure 30,000 years after the big bang. These largest cometary globules must have much larger mass planets than PFPs at their cores to have survived the 20,000 year lifetime of the Helix planetary nebula with measured mass loss rates of order $10^{-8}M_\odot$ year^{-1} (Meaburn et al. 1998). The spacing of the cometary knots becomes closer for distances farther from the central stars, consistent with these objects having PFPs or small JPPs at their cores (see Fig. 11 below).

Figure 6 shows an example of the new ACS/WFPC composite images from the northern region of Helix nebula confirming the uniform density of the cometary globules. From HGD this reflects the uniform ambient distribution of virialized, dark-matter, frozen PFPs and JPPs expected in PGCs with primordial density $\rho_0 \approx 3\times10^{-17}$ kg m^{-3}. Thus planets provide raw material to produce and grow the central white dwarf of a PNe by binary hierarchical clustering and clumping. Once clustering and clumping begins the star formation is highly non-linear. The more clustering the more gas. The more gas the more clustering. Thus the larger JPPs and globulettes of PFPs in the Jupiter mass range are more likely to be found at Oort cavity distances and the brown dwarfs near the center or merged as stars and close binaries. Within the ionized cavity of the PNe accreted JPPs are evaporated by radiation from the white dwarf and absorbed or captured in orbits. Images and properties of "knots" in Helix, Eskimo, Dumbbell and other PNe (O'Dell et al. 2002) are consistent with

this PFP-JPP-globulette star formation interpretation.

Figure 7 shows the Eskimo planetary nebula (NGC 2392), which at 7.2×10^{19} m (2.4 kpc) is 11 times more distant from earth than Helix (Gorny et al. 1997), but is still close enough for numerous cometary globules to be resolved by HST cameras. The PNe is smaller than Helix and has a central shocked region with no comets, just like the small, even younger, Spirograph nebula shown at the bottom of Fig. 4. Eskimo PNe has a few very large widely separated cometary globules dominating its brightness, suggesting these may be evaporating JPPs with multi-Jupiter masses. Note the large gas wakes without cometary globules at the 6 o'clock position (in the beard). Presumably these were even brighter while their JPPs were evaporating.

Figure 8 shows details of the central region of the Dumbbell planetary nebula featuring numerous cometary globules and knots. The spacing of the objects is consistent with PFP and JPP planets with average mass density $\approx 10^4$ times the average 10^{-21} kg m^{-3} for the Galaxy. Because of their primordial origin, planets with this same density ρ_0 dominate the mass and species content of the ISM in all galaxies, fossilizing the primordial baryonic density from the time of first structure in the plasma epoch 30,000 years after the big bang as predicted by HGD. The dumbbell morphology reflects the existence of a binary central star system and its plasma beam jet to evaporate JPPs at the Oort cavity edge.

4. The "Nonlinear Grey Dust" Systematic Error of "Dark Energy"

Figure 9 summarizes the hydro-gravitational-dynamics (HGD) theory of gravitational structure formation leading to the formation of baryonic dark matter and the resulting dark energy misconception (Gibson 2005). A Planck scale quantum-gravitational instability triggers big bang turbulent combustion. The resulting turbulent temperature patterns are fossilized by nucleosynthesis in the energy epoch as random H-He density fluctuations, which seed the first gravitational formation of structure by fragmentation at the horizon and Schwarz viscous scale and Schwarz turbulent scale in the plasma epoch ($L_H \approx L_{SV} \approx L_{ST}$, Table 1). The first gravitational structures are super-cluster-voids starting at 10^{12} seconds and growing with sonic ($c/3^{1/2}$) speed until the plasma-gas transition at 10^{13} s (300,000 years). An observed -73 μK CMB cold spot reflects a 10^{25} m void for $z \leq 1$ (Rudnick et al. 2007) as expected from HGD. The maximum probability for such a large void from ΛCDMHCC is much less than 10^{-9} (Hoyle & Vogeley 2004).

The smallest gravitational fragments from the plasma epoch are proto-galaxies formed by fragmentation with the 10^{20} m Nomura scale ($L_N \approx L_{ST} \geq L_{SV} \approx L_K$, Table 1) and

chain-clump spiral-clump morphology (Gibson 2006b) along stretching turbulent vortex lines and compressing spirals of the weak plasma turbulence. The kinematic viscosity reduction by a factor of 10^{13} gives two fragmentation scales and structures in the primordial gas; that is, the $10^6 M_\odot$ Jeans acoustic scale and PGCs, and the $10^{-6} M_\odot$ viscous Schwarz scale and the PFPs. With time the planetary mass PFPs freeze to form the baryonic dark matter. Some small fraction accrete to form JPPs and stars. Because SNe Ia occur surrounded by evaporating PFPs and JPPs, a random "nonlinear grey dust" dimming of the supernova brightness is likely.

Figure 10 shows the proposed interpretation of the ground based (open circle) and (Riess et al. 2004) HST/ACS (solid circle) SNe Ia dimming for red shifts $0.01 \leq z \leq 2$. The wide scatter of the amount of SNe Ia dimming appears to be real, and is consistent with our "nonlinear grey dust" model, where a random amount of absorption should be expected depending on the line of sight to the supernova and the degree of evaporation of the baryonic dark matter interstellar medium. A "uniform grey dust" systematic dimming increases with z contrary to observations. The "dark energy" concept seems unlikely because it requires a radical change in the physical theory of gravity. HGD requires changes in the standard (CDMHCC) model of gravitational structure formation and the interpretation of planetary nebulae. The slight random dimming found in the observations is just what one expects from "nonlinear grey dust" formed as the growing hot carbon star evaporates Oort cavity and rim planets to form large, cold, dusty atmospheres that may be on the line of sight to the SNe Ia that eventually occurs. Planetary nebulae such as the Helix and other PNe described above illustrate the process we are suggesting. Radiation from the proto-SNe Ia can be directly from the shrinking carbon star or from plasma jets and winds formed as any companion stars or just a JPP accretion disk (Su et al. 2007) feeds its carbon growth.

Figure 11 shows a closeup view of clumped JPPs and PFPs in the northern rim of the Helix Oort cavity imaged in molecular hydrogen H_2 at 2.12 microns (O'Dell et al. 2007). The distance scales are derived from the new O'Dell et al. images and a trigonometric parallax estimate of 219 (198-246) pc for the distance to Helix (Harris et al. 2007). O'Dell et al. 2007 conclude H_2 is in local thermodynamic equilibrium, as expected for evaporated planet atmospheres produced by intense radiation and not by any shock phenomenon.

Figure 12 shows a collection of interstellar medium electron density spectral estimates often referred to as the "Great Power Law on the Sky" from the remarkable agreement with the same $q^{-11/3}$ Kolmogorov, Corrsin, Obukhov spectral form over 11 decades of wavenumber q (Armstrong et al. 1981; Gibson 1991; Armstrong et al. 1995). An 'inner scale' at $\approx 10^{12}$ m from pulsar scintillations can be understood as the Obukhov-Corrsin scale $L_C \equiv (D/\varepsilon)^{1/4}$ marking the beginning of a fossil turbulence inertial-diffusive spectral subrange $q^{-15/3}$ (shown

in Fig. 12), where electron density is a strongly diffusive passive scalar property with diffusity $D \approx 30\times$ larger than the kinematic viscosity ν (Gibson 1968a; Gibson 1968b; Gibson et al. 2007). Evidence that observed pulsar scintillation spectra (You et al. 2007) represent forward scattering from discrete features is provided by observations of parabolic scintillation arcs (Trang & Rickett 2007; Hill et al. 2005). The observed scintillations with small inner scales $\leq 10^{10}$ m and possibly $\leq 10^{7}$ m indicate turbulent partially ionized atmospheres evaporated from dark matter planets by neutron star supernova and pulsar plasma jets and radiation. The $\varepsilon \approx 1$ m^2 s^{-3} and Reynolds number $\approx 10^5$ values implied by the spectra indicate fossilized strong turbulent mixing driven by the planet evaporation. For a gas to be a fluid and produce the observed scintillations with strong turbulence and turbulent mixing spectra requires gas density $\rho \geq 10^{-14}$ kg m^{-3} in the scintillation regions; that is, higher than average in the Galaxy by $\geq 10^7$. Such a large density matches that measured for the cometary globules of Helix, also interpreted as dark matter planet atmospheres. The well-studied Crab supernova II remnant at 6×10^{19} m shows strong evidence of evaporated dark matter planets with wakes pointing to the path of the pulsar and its close companions, revealing powerful pulsar jets and evaporated JPP atmospheres in a series of HST images. Atmosphere diameters (1 arc sec 'knots') as large as 3×10^{14} m are reported (Schaller & Fessen 2002), $\approx \times 10$ larger than those in Helix.

Extreme scattering events (ESE), multiple images of radio pulsars and quasars, and other indications of small $\approx 10^{13}$ m dense $\approx 10^{-12}$ kg m^{-3} refractors are detected frequently using the $\leq 10^{-3}$ arc sec resolution of radio telescopes. From the detection frequency and the size and $\approx 10^{27}$ kg mass of the ionized and neutral clouds observed, authors have suggested the objects may provide most of the Galaxy mass (Walker & Wardle 1998; Hill et al. 2005). We agree. From HGD, these radio telescope detections manifest gas atmospheres of Galaxy disk primordial dark matter Jovian planets. No other explanation seems plausible.

5. Discussion of results

HGD theory combined with high-resolution multi-frequency space telescope observations require major changes in the standard models of cosmology, star formation, star death, and planetary nebulae formation. Trails of young globular clusters in merging galaxies and bright gases of clumpy nebulae and dense masers surrounding white-dwarf stars, Wolf-Rayet stars and neutron stars provide a growing body of clear evidence for the existence of the millions of frozen primordial planets (PFPs and JPPs) per star in metastable-planet-clusters (PGCs) suggested (Gibson 1996; Schild 1996) as the baryonic dark matter and interstellar medium. Even though the primordial planets are dark and distant they make their presence

known because of their enormous total mass, the brightness and scattering properties of their evaporated atmospheres, and because they are the raw material for everything else. PFPs are now individually detectable in the Helix PNe from their H_2 signal at 2.12 microns (Fig. 11). JPPs with molecular atmospheres in great abundance ($\geq$ 20,000-40,000) are detected in Helix from their 5.8 and 8 micron purely rotational lines of molecular hydrogen from the infrared array camera IRAC on the *Spitzer* space telescope with Helix resolution of 6×10^{13} m (Hora et al. 2006). Since these JPP atmospheres are mostly evaporated by spin-powered beamed plasma jets and winds of the white dwarf, they represent a small fraction of the $> 1000 M_{\odot}$ of JPPs in its range. Similar results are obtained from the NICMOS NIC3 camera with the 2.12 micron molecular hydrogen filter from HST (Meixner et al. 2005).

When disturbed from equilibrium by tidal forces or radiation, JPP planets grow to stellar mass by binary accretion with neighbors where friction of close encounters causes growth of planetary atmospheres, more friction, merger, reprocessing and cooling to a new state of metastable equilibrium with shrinking planetary atmospheres as the gases refreeze. This non-linear binary cascade to larger size gas planets in pairs and pairs of pairs leads to star formation as stellar binaries within the PGC clumps. It explains the presence of the massive JPPs that persist in Helix in the shells closest to the central stars, as shown in Figs. 4, 5, 6, 10 and 11. HGD theory explains why most stars are binaries and why most galaxies and galaxy clusters are not. Stars are formed by hierarchical clustering of planets, not condensation within gas clouds, and galaxies and galaxy clusters are formed in strings and spirals by gravitational fragmentation of weakly turbulent plasma, not by hierarchical clustering of CDM halos. Measured supervoid sizes are so large they must have begun growth by gravitational fragmentation in the plasma epoch as predicted by HGD. The CDMHCC paradigm should be abandoned along with Λ and dark energy. Supernova models based on supergiant stars and their $9 - 25 M_{\odot}$ envelopes are highly questionable along with PNe models and estimates of WD and SNe II precursor star masses (Fig. 3).

Hundreds of PNe are observed in the LMC and SMC galaxies, interpreted from HGD as tidally agitated star forming clumps of PGCs in the BDM halo of the Milky Way equivalent to the super-star-clusters (SSCs) of YGCs formed in the BDM halo of the Tadpole (VV29) merger (Fig. 1). Fig. 1 (Tran et al. 2003; Gibson & Schild 2003a) shows the SSC as a linear string of $\geq$ 42 young globular star clusters with star formation triggered by passage of one of the merging galaxy fragments (VV29cdef) passing through the BDM halo of VV29a. The YGCs have 3-10 My ages, showing they must have been formed in place and not ejected as a frictionless tidal tail in this 500 My old merging system. Collisionless fluid mechanical modeling of galactic dynamics with frictionless tidal tails instead of star trails in the baryonic dark matter is highly misleading and should be abandoned.

One of the LMC PNe (LMC-N66) has recently shown strong brightness variation and appears to be in the final stages of white-dwarf growth leading to a SNE Ia event (Pena et al. 2004). Fig. 2 shows an archive HST image at the 5007 Å wavelength OIII emission line. The heavy rain of JPPs on the central star(s) appears to be adding carbon to the WD and fueling a powerful plasma beam that brings JPPs and their O III wakes out of the dark to diameters $\approx 5 \times 10^{16}$ m, a region containing $\geq 1000 M_{\odot}$ of JPPs using the primordial density $\rho_0 \approx 3 \times 10^{-17}$ kg m^{-3} from HGD. The wakes point in random directions, indicating that the evaporating JPP velocities V_{JPP} are large and random, consistent with a rapid JPP accretion rates and rapid white-dwarf growth. Will the C-N core of the WD be mixed away by this rapid accretion to give Fe and a SN II event?

From HGD and the observations it seems clear that most stars form as binary star systems from Jovian primordial planets that grow by binary accretion within dark primordial PGC clumps of such planets. Unless the JPPs are strongly agitated the stars formed will be small. The white dwarf and its companion can then both slowly grow toward the Chandrasekhar limit drawing mass from accreted JPPs and possibly each other. Because SNe Ia events result from dying small stars that have very long lives, we can understand why it took nearly 10 billion years with red shift $z = 0.46$ for "dark energy" effects to appear, and why SNe Ia events are not seen at red shifts much larger than 1.

Why do all pulsars twinkle? It is because the progenitors of neutron stars form in PGCs surrounded and generously fed by partially evaporated planets with large atmospheres. Over 50 pulsar binaries and doubles in complex dense systems including exo-planets have been detected (Sigurdsson et al. 2003; Bisnovatyi-Kogan 2006; Lyne et al. 2004; Thorsett & Chakrabarty 1999). The supernovae IIab in agitated Galaxy disk PGCs where pulsars usually occur generate so many large atmosphere JPPs that all lines of sight to pulsars pass through at least one large turbulent or previously turbulent planet atmosphere (Fig. 12). It should therefore be no surprise that less strongly agitated PGCs forming poorly mixed carbon stars that explode as SNe Ia events will occasionally have unobscured and occasionally obscured lines of sight (Fig. 10), calling the dark energy hypothesis into question.

6. Conclusions

High resolution wide angle HST/ACS images and 4m ground based telescope images (O'Dell et al. 2004) confirm and extend the previous WFPC2 HST picture of the Helix planetary nebula (O'Dell & Handron 1996) showing thousands of closely-spaced cometary globules. Slow comet rains on central white dwarfs in dense primordial metastable molecular clouds of planets are interpreted from HGD as generic features of PNes. Frozen BDM planets

(PFPs and JPPs sometimes in globulettes) evaporated by spin driven plasma beams and plasma winds from the central white dwarf form the PNe. A slow rain of planet-comets grow the WD to Chandrasekhar instability. Evaporation rates from the largest cometary globules suggest they possess ≥Jupiter mass cores (Meaburn et al. 1998), consistent with background radiation absorption masses $(2-11)10^{25}$ kg for the Helix cometary globule atmospheres (Meaburn et al. 1992; O'Dell & Handron 1996; Huggins et al. 2002). From their spacing and HGD, the largest cometary globules have multiple Jupiter masses (Fig. 5) and are termed JPPs. From HGD, all SN Ia events should occur in PNes subject to random dimming by JPP atmospheres, as observed (Fig. 10) and misinterpreted as dark energy.

Models are questioned for planetary nebula formation where Rayleigh-Taylor instabilities of a postulated (unexplainably) dense and massive superwind outer shell are triggered by collision with a later, rapidly expanding, less-dense, inner shell to form the globules (Capriotti 1973; Garcia-Segura et al. 2006). Such two wind PNe models cannot account for the morphology, regularity, and large observed densities and masses of the globules. Speculations that accretional shocks or variable radiation pressures in stars can trigger gravitational instabilities (Vishniac 1994; Vishniac 1983) to achieve such large density differences underestimate powerful turbulence, radiation, and molecular dispersion forces existing in stellar conditions that would certainly smooth away any such dense globules. From HGD, superwinds are not necessary to explain PNes and never happen. Star mass overestimates indicating superwinds have neglected the brightness of evaporated JPP atmospheres (Fig. 3). Luminous galaxy masses have probably been overestimated for the same reason and should be reexamined. Stars with mass $2M_{\odot} \rightarrow 100M_{\odot}$ may exist, but require strong turbulent mixing from exceptionally large JPP accretion rates.

No convincing mechanism exists to produce or expel dense objects from the central stars of PNe. Dense OH and SiO maser cloudlets near red giants observed by high resolution radio telescopes (Alcock & Ross 1986a; Alcock & Ross 1986b) are interpreted as evaporating JPPs from their high densities $\rho \geq 10^{-9}$ kg m^{-3}. Such densities cannot be achieved by shocks in the relatively thin red giant atmospheres. Shock fronts can be seen to exist in younger PNe than Helix (Figures 4 and 7) but are not accompanied by any cometary globules. Models for white dwarf and planetary nebula formation (Busso et al. 1999; Iben 1984) cannot and do not explain either the cometary globules or the tremendous loss of mass for stars with initial mass $M_{Initial} = (1-9)M_{\odot}$ by superwinds to form white dwarfs with final mass $M_{Final} = (0.5-1)M_{\odot}$ (Fig. 3). Observations of post AGB stars with multiple masers and bipolar flows reflect JPP evaporation and accretion, not envelope formation (Zijlstra et al. 2001).

We conclude that a better model for interpreting the observations is provided by hydro-gravitational-dynamics theory (HGD, Fig. 9), where the brightest cometary globules in

PNe are indeed comets formed when radiation and plasma jets from the white dwarf and its companion evaporate and reveal volatile frozen gas planets of the ISM at Oort cavity distances. Observed Oort cavity sizes (Figs. 4, 7, 10) $L_{Oort} \approx 3 \times 10^{15}$ m produced when a star forms from accreting planets in a PGC confirms the the primordial density ρ_0 of HGD for the first gravitational structures from the expression $L_{Oort} \approx (M_\odot/\rho_0)^{1/3} = 4 \times 10^{15}$ m. The planets are JPP Jovian accretions of primordial-fog-particle (PFP) frozen H-He proto-planets formed at the plasma to gas transition 300,000 years after the big bang in proto-globular-star-cluster (PGC) clumps (Gibson 1996), consistent with quasar microlensing observations showing a lens galaxy mass dominated by rogue planets "likely to be the missing mass" (Schild 1996). All stars are formed from primordial planets in these dense primordial clumps.

From HGD and all observations, PFPs and JPPs in PGCs dominate the mass and gases of the inner halo mass of galaxies within a radius of about 100 kpc (3×10^{21} m) as most of the dark matter. Proto-galaxies formed during the plasma epoch fragmented after transition to gas at primordial Jeans and Schwarz scales (Table 1) to form PGC clouds of PFPs that comprise the BDM and ISM of all inner galaxy halos. From HST/ACS Helix images and previous observations, the density of the Galaxy disk ISM is that of proto-superclusters formed 30,000 years after the big bang; that is, $\rho_0 \approx 3 \times 10^{-17}$ kg/m^3, preserved as a hydrodynamic fossil and revealed by the $(10-4) \times 10^{13}$ m separations of the PFP candidates (cometary globules) observed in Helix that imply this density (Fig. 11).

HST images of other nearby planetary nebula support our interpretation. Cometary globules brought out of the dark by beamed and other spin enhanced radiation from a shrinking central white dwarf is a generic rather than transient feature of planetary nebulae. Thus, the ISM is dominated by small frozen accreting planets with such small separations that the indicated mass density is that of a PGC; that is, $\rho \approx \rho_{PGC} \approx \rho_0$, which is $\approx 10^4$ larger than that of the Galaxy. Standard PNe models that suggest planetary nebulae are brief (10^4 year) puffs of star dust from dying white dwarfs by superwinds from massive envelopes (Fig. 3) must be discarded. Large PNe masses M_{PNe} formed by the evaporation of JPPs (Fig. 2) must not be confused with $M_{Initial}$ for the white dwarf (Fig. 3). Infrared detections of dense molecular hydrogen clumps in Helix from both HST and *Spitzer* space telescopes provide $\approx$ 40,000 JPP and PFP clump (globulette) candidates (O'Dell et al. 2007; Meixner et al. 2005; Hora et al. 2006) from the $\geq 1000 M_\odot$ mass of JPPs and PFPs expected to exist in the observed 2.5×10^{16} m radius of Helix from HGD. JPPs should form within globulette clumps of PFPs from the stickiness of PFP atmospheres (Gahm et al. 2007).

From HGD, most stars form as binary pairs from the binary and globulette accretion of baryonic dark matter PFP and JPP planets in PGC clumps leaving Oort cloud size holes in the ISM. When one of the stars in a binary forms a white dwarf it can draw on the fuel

of its companion and accreted JPPs to form a PNe of cometary globules (Fig. 2) and a proto-SNe Ia from the growing central stars (Fig. 3). Radiation from the pair can be seen as precessing plasma jets that evaporate rings of cometary globules as in the Helix PNe (Figs. 4, 5, 6, 10, 11) and in other planetary nebulae (Figs. 2, 7, 8). These JPP atmospheres give the "nonlinear grey dust" random-systematic-error-dimming indicated in Fig. 10. Pulsar scintillation spectra (Fig. 12) require stratified turbulence and turbulent mixing in dense weakly ionized gases (Gibson et al. 2007), strongly indicating large evaporated Jovian planet atmospheres agitated by the supernova and pulsar winds as seen in HST images of the Crab nebula and inferred for PNe in Fig. 10. Both the dark energy concept and the ΛCDM cosmology required to justify dark energy seem hopelessly problematic.

Critically important information in this paper would not be available without the heroic work and dedication of astronaut John Mace Grunsfeld whose amazing preparation and skills in the fourth space telescope repair mission made HST/ACS images possible.

REFERENCES

Abel, T., Bryan, G. L., Norman, M. L. 2002, Science, 295, 93

Aharonian et al. 2006, Nature, 440, 1018

A'Hearn, M. F. 2005, Science, 310, 258

Alcock, C. & Ross, R. 1986a, ApJ, 305, 837-851

Alcock, C. & Ross, R. 1986b, ApJ, 310, 828-841

Alcock, C., et al. 1998, ApJ, 499, L9

Alcock, C., et al. 2000, ApJ, 542, 281

Aldering, G., Humphreys, R. H. & Richmond, M. 1994, AJ, 107, 662-672

Armstrong, J.W., Cordes, J.M., & Rickett, B.J. 1981, Nature, 291, 561

Armstrong, J. W., Rickett, B.J., & Spangler, S. R. 1995, ApJ, 443, 209

Bean, R., Carroll, S. & Trodden, M. 2005, astro-ph/0510059

Belokurov, V. et al. 2006, astro-ph/0608448

Belokurov, V. et al. 2007, ApJ, in press, astro-ph/0605705v2

Benitez, N. et al. 2004, ApJS, 150, 1-18

Bennitt, D., ApJ, 633, 906-913

Bershadskii, A. 2006, Physics Letters A, 360, 210-216

Bershadskii, A., and K.R. Sreenivasan, 2002, Phys. Lett. A, 299, 149

Bisnovatyi-Kogan, G. S., 2006, Physics-Uspekhi, 49(1), 53-61, astro-ph/0611398v1

Bodenheimer, P. et al. 2000, Protostars and Planets IV, ed. Mannings, V. et al., U. Ariz. Press, Tucson, 675

Boss, A. P. 1995, Science, 267, 360

Boss, A. P. 2001, ApJ, 551, L167

Boss, A. P. 2004, ApJ, 610:456463

Brownlee et al. 2006, Science, 314, 1711-1716

Burud, I. et al., 2000, ApJ, 544, 117

Burud, I. et al., 2002, A&A, 391, 451

Busa, M. T., Evard, A. E. & Adams, F. C. 2007, ApJ, 665, 1-13

Butler, R. P. et al. 2006, ApJ, 646, 505

Busso, M., Gallino, R., and Wasserburg, G. J. 1999, Annu. Rev. Astron. Astrophys. 1999. 37:239-309

Calchi-Novati, S. et al. 2005, A&A, 443, 911-928

Capriotti, E. R. 1973, ApJ, 179, 495

Chaisson, E. and McMillan, S. 2001, Astronomy, Prentice Hall, NJ.

Claver, C.F. et al. 2001, ApJ, 563, 987-998

Colley, W. et al., 2002, ApJ, 565, 105

Colley, W. et al., 2003, ApJ, 587, 71

Colley, W. & Schild, R., 2003, ApJ, 594, 97 astro-ph/0303170

Dalal, N. and Kochanek, C. 2002, ApJ, 572, 25, astro-ph/0111456

de Jong, T. 1983, ApJ, 274, 252-260

De Marko, O. et al. 2004, ApJ, 602, L93-L96

Edgar, R., NewA Rev., 48, 843-859

Feldman, P. D. et al. 2006, astro-ph/0608487

Gahm, G. et al. 2007, AJ, 133, 1795

Garcia-Segura, G. et al. 2006, ApJ, 646, L61-L64

Gelfand, J. D. et al. 2007, ApJ, 663, 468-486

Gibson, C.H. 1968a, Phys. Fl., 11, 2305-2315

Gibson, C.H. 1968b, Phys. Fl., 11, 2316-2327

Gibson, C.H. 1991, Proc. Roy. Soc. Lon. A, 434, 149-169

Gibson, C. H. 1996, Appl. Mech. Rev., 49, 299, astro-ph/9904260

Gibson, C. H. 1999, J. of Mar. Systems, 21, 147, astro-ph/9904237

Gibson, C. H. 2000, J. Fluids Eng., 122, 830, astro-ph/0003352

Gibson, C. H. 2001, Proc. ICME 2001, Vol. 1, BUET, 1, astro-ph/0110012

Gibson, C. H. 2003, astro-ph/0304441

Gibson, C. H. 2004, Flow, Turbulence and Combustion, 72, 161179

Gibson, C. H. 2005, Combust. Sci. and Tech., 177, 1049-1071

Gibson, C. H. 2006a, J. Appl. Fluid Mech. (in press 2008, 2(1), 1-8, www.jafmonline.net), astro-ph/0606073v3

Gibson, C. H. 2006b, astro-ph/0610628

Gibson, C. H., Bondur, V. G., Keeler, R. N., & Leung, P. T. 2006a, Int. J. Dyn. Fluids, 2(2), 171-212

Gibson, C. H., Bondur, V. G., Keeler, R. N., & Leung, P. T. 2006b, J. Appl. Fluid Mech., 1, 1, 11-42

Gibson, C. H. and Schild, R. E. 1999, astro-ph/9904362

Gibson, C. H. and Schild, R. E. 2003a, astro-ph/0210583v3

Gibson, C. H. and Schild, R. E. 2003b, astro-ph/0304483v3

Gibson, C. H. and Schild, R. E. 2003c, astro-ph/0304107

Gibson, C. H. and Schild, R. E. 2003d, astro-ph/0306467

Gibson, C. H. et al. 2007, SPIE 6680-33, Aug. 27, arXiv:0709.0074v2

Gorny, S. K., Stasinska, G., & Tylenda, R. 1997, A&A, 318, 256

Grillmair, C. 2006, ApJ, 645, L37-L40

Guerrero, M. A., You-Hau Chu, Gruendl, R. A., Williams, R. M. 2001, ApJ, 553, L55

Hachisu, I. & Kato, M. 2001. ApJ, 558, 323-350

Hamann, W.-R. et al. 2003, A&A, 409, 969-982

Harris, H. C. et al. 2007, astro-ph/06011543

Herwig, F. 2005, Annu. Rev. Astron. Astrophys.. 43:435-479

Hill, A. et al. 2005, ApJ, 619, L171

Hjorth, J. et al. 2002, ApJ, 572 (2002) L11-L14

Hoard, D. W. et al. 2007, AA, 134, 26-42

Hoyle, F., Burbidge, G., & Narlikar, J. V. 2000, A Different Approach to Cosmology, Cambridge U. Press

Hora, J. L. et al. 2006, astro-ph/0607541

Hoyle, F. & Vogeley, M. S. 2004. ApJ, 607, 751

Huggins, P. J., T. Forveille, R. Bachiller, P. Cox, N. Ageorges, and J. R. Walsh 2002, ApJ, 573:L55L58

Ibata, R. A., Lewis, G. F., Irwin, M. J., & Quinn, T. 2002, MNRAS, 332, 915-920

Ibata, R. & Lewis, B. 2007, Sci. Amer., 296. 40

Iben, I. 1965, ApJ, 141, 993

Iben, I., 1984, ApJ, 277, 333-354

Ida, S. & Lin, D. N. C. 2004, ApJ, 604, 388

Jeans, J. H. 1902, Phil. Trans. R. Soc. Lond. A, 199, 1

Keeler, R. N., Bondur, V. G., & Gibson, C. H. 2005, GRL, 32, L12610

Keto, E. & Wood, K. 2006, ApJ, 637, 850-859

Knapp, T.G., Leighton, K.Y., Wannier, P.G., Wooten, H.A., Huggins, P.J. 1982, ApJ, 252, 616-634

Kornet, K. et al. 2002, A&A, 396, 977

Krumholz, M. R., McKee, C. F. & Klein, R. I. 2006, ApJ, 638, 369-381

Lagadec, E. et al. 2006, astro-ph/060611071v1

Lineweaver, C. H. & Grether, D. 2002, astro-ph/0201003v2

Loh, J. & Stacey, G. 2003, Appl. and Env. Microbiol., 69(1), 10-17

Lyne, A. G. et al. 2004, Science, 303, 1154

Matese J. J., Whitman P. G., Whitmire D. P. 1999, Icarus, 141, 354

Maund, J. et al. 2004, Nature, 427, 129-131

Mauron, N. & Huggins, P.J. 1999, A&A, 349, 1203-208

Meaburn, J., Clayton, C. A., Bryce, M., Walsh, J. R., Holloway, A. J., and Steffen, W. 1998, MNRAS, 294, 201

Meaburn, J., Walsh, J. R., Clegg, R. E. S., Walton, N. A., Taylor, D., & Berry, D. S. 1992, MNRAS, 255, 177

Meaburn, J. et al. 2005, MNRAS, 360, 963-973

Meixner, M. et al. 2005, AJ, 130, 1784-1794

Miranda, L. F. et al. 2001, Nature, 414, 284

Moe, M., & De Marco, O. 2006, ApJ, 650, 916-932

Morgan, D.H., Parker, Q.A., Cohen, M. 2003, A&A, 346, 719-730

Murray J. B. 1999, MNRAS, 309, 31

Nomura, K. K. & Post, G. K. 1998, JFM, 377, 65-97

O'Dell, C. R. and Handron, K. D. 1996, ApJ, 111, 1630

O'Dell, C. R., Balick, B., Hajian, A., Henney, W. & Burkert, A. 2002, AJ, 123, 3329

O'Dell, C.R.,McCullough, P.R., & Meixner, M. 2004, AJ, 128, 2339-2356

O'Dell, C.R., Henney, W. J. & Ferland, G. J. 2007, AJ, 133, 2343-2356, astro-ph/070163

Odenkirchen, M. et al. 2001, ApJ, 548, L165

Ofek, E. O., Maoz D. 2003, in press ApJ, astro-ph/0305200

O'Neil, K., Oey, M. S., Bothun, G. 2007, AJ, 134, 547-565

O'Shea, B. W., & Norman, M. L. 2006, ApJ, 648, 31-46

Padoan, P., Kritsuk, A., & Norman, M. L. 2005, ApJ, 622, L61

Paxton, B. 2004, PASP, 116, 699, astro-ph/0405130

Pena, M. et al. 1997, ApJ, 491, 233-241

Pena, M. et al. 2004, A&A, 419, 583-592

Peters, N. 2000, Turbulent Combustion, Camb. Univ. Press

Pilyugin, N. N. & Usov, V. V. 2007, ApJ, 655, 1002-1009

Podsialowski, P. et al. 1993, Nature, 364, 509

Putnam, M. et al. 2002, AJ, 123, 873

Riess, A. G., Strolger, L.G., Tonry, J. and others 2004, ApJ, 607, 665-687, astro-ph/00402512

Ropke, F. K. & Niemeyer, J. C. 2007, astro-ph/0703378

Rudnick, L., Brown, S., Williams, L. R. 2007. ApJ, in press, astro-ph/0704.0908v2

Sand, D. J., Treu, T., & Ellis, R. S. 2002, ApJ, 574, L129

Sato, B. et al. 2005, ApJ, 633, 465-473

Schaller, E. & Fesen, R. A. 2002, AJ, 123, 941-947

Schechter, P. et al. 2003, ApJ, 584, 657

Schild, R. 1996, ApJ, 464, 125

Schild, R. 2004a, astro-ph/0406491

Schild, R. 2004b, astro-ph/0409549

Schild, R. & Dekker, M. 2006, Astronomische Nachrichten, Vol.327, Issue 7, p.729-732, astro-ph 0512236

Schild, R. & Vakulik, V., 2003, astro-ph/0303356

Shigeyama, T. & Nomoto, K. 1990, ApJ, 360, 242-256

Sigurdsson, S., Richer, H. B., Hansen, B. M., Stairs, I. H. and Thorsett, S. E. 2003, Science, 301, 193

Soker, N., PASP, 118, 260

Speck, A. K., Meixner, M, Fong, D., McCullogh, P. R., Moser, D. E., Ueta, T. 2002, AJ, 123, 346-361

Su, K. Y. L. et al. 2007, astro-ph/0702296

Sunshine, J. M. et al. 2006, 311, 1453

Tafoya, D. et al. 2007, A. J., 133, 364-369

Thilker, D. et al. 2004, ApJ, 601, L39-L42

Thorsett, S. E. & Chakrabarty, D. 1999, ApJ, 512, 288-299

Tran, H. D., Sirianni, M., & 32 others 2003, ApJ, 585, 750

Trang, F.S., & Rickett, B. J., astro-ph/0702210

Truelove, J., Klein, R.I., McKee, C., Holliman, J.H., Howell, L., & Greenough, J., 1997, ApJL, 489, L179

Tuthill, P., Morrier, J., & Danchi, W. 1999, Nature, 398, 487-489.

Udalski, A. , O. Szewczyk, K. Zebrun, G. Pietrzynski, M. Szymanski, M. Kubiak, I. Soszynski, L. Wyrzykowski 2002, Acta Astronomica (2002) 52, 317, astro-ph/0301210

Usov, V. V. 1991, MNRAS, 252, 49-52

Vishniac, E. 1983, ApJ, 274, 152-167

Vishniac, E. 1994, ApJ, 428, 186

Vittone, A. A. & Errico, L. 2006, Ch. J. Astron. Astro., 6, 132-136

Walker, M.A. & Wardle, M. 1998, ApJ, 498, L125

Wang, L. & Peters, N. 2006, J. Fluid Mech., 554, 457-475

Weidemann, V. 2000, A&A, 363, 647-656

Wise, J. H.. & , Abel, T. 2007, ApJ, 665, 899-910

Woitke, P. 2006, A&A, 460, L9-L12

Woods-Vasey, W. M., Wang, L., Aldering, G. 2004, ApJ, 616, 339-345

You, X. P. et al., astro-ph/0702366

Zijlstra, A. et al., MNRAS, 322, 280-308

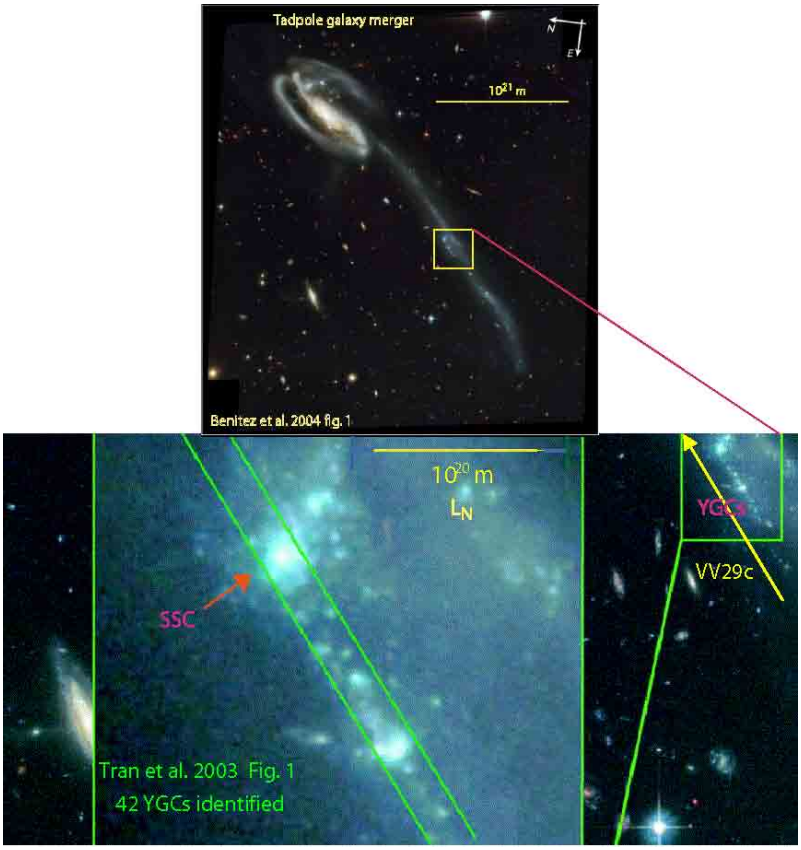

Fig. 1.— Trail of 42 young-globular-star-clusters (YGCs) in a dark dwarf galaxy examined spectroscopically by Tran et al. 2003 using the Keck telescope. The 1 ″ Echellette slit and a loose super-star-cluster (SSC arrow) are shown at the left. Ages of the YGCs range from 3-10 Myr. The aligned YGC trail is extended by several more YGGs (arrow on right) and points precisely to the beginning, at 2×10^{21} m distance, of the spiral star wake of VV29c in its capture by VV29a. The baryonic dark matter halo of Tadpole is revealed by a looser trail of YGCs extending to a radius of 4×10^{21} m from VV29a, or 130 kpc (Gibson & Schild 2003a).

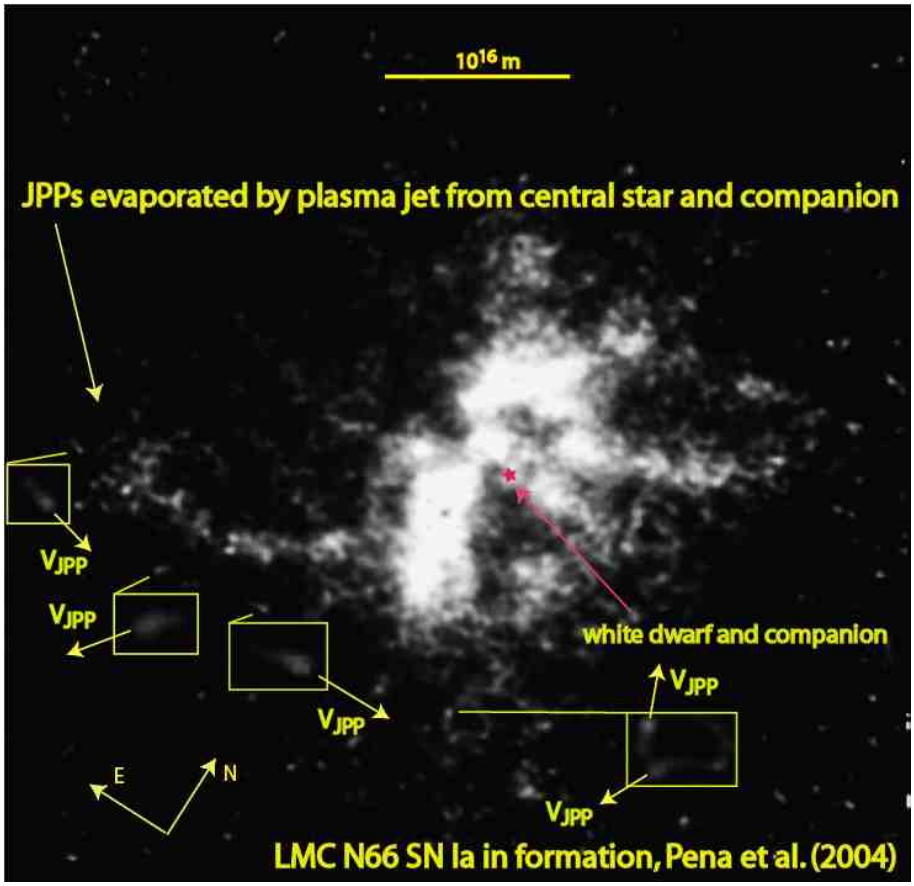

Fig. 2.— HST/FOC 5007 Å image (HST archives, 6/26/1991) of distant (1.7×10^{21} m) LMC/N66 PNe with a central $1.2M_{\odot}$ WD-companion close binary rapidly growing toward SN Ia formation (Pena et al. 2004). Wakes in O III emission (magnified inserts) show random velocities V_{JPP} of the evaporating planets in globulette clumps of PFPs (Gahm et al. 2007). From its spectrum the central star is a Wolf-Rayet of class WN. Arc-like patterns show strong nutating plasma beams from the binary have evaporated $\approx 5M_{\odot}$ of the ambient JPPs (Fig. 3) . From HGD and ρ_0 the 2.5×10^{16} m radius nebular sphere for LMC/N66 should contain $\geq 1000M_{\odot}$ of PFP and JPP Jovian planets.

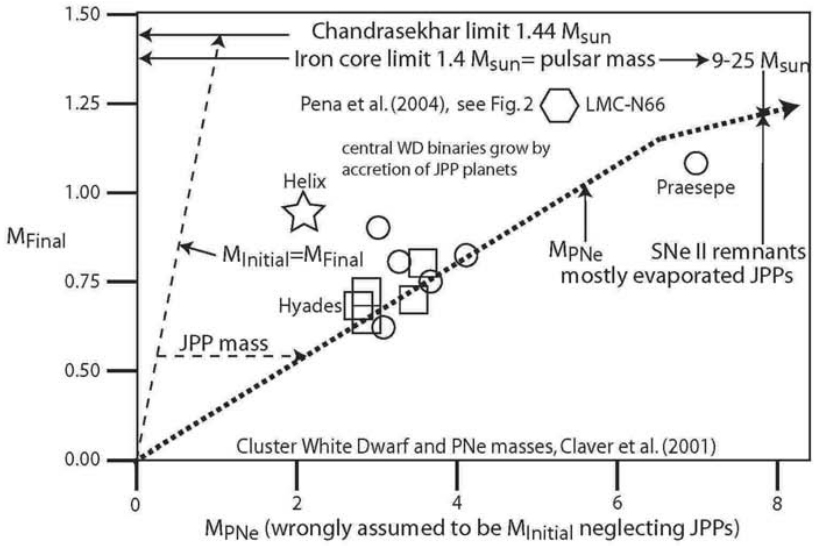

Fig. 3.— Mass evolution of white dwarf stars to the Chandrasekhar limit by accretion of JPPs. The standard PNe model incorrectly estimates the initial white dwarf mass $M_{Initial}$ to be the total PNe mass M_{PNe}, but this includes the brightness mass of evaporated JPPs. Measurements for the N66 PNe of Fig. 2 (hexigon) and the Helix PNe of Figs. 4-6 (star) are compared to star cluster PNe of Praesepe (circles) and Hyades (squares) (Claver et al. 2001). Infrared detection of JPP atmospheres in Helix indicate $M_{PNe} \geq 40 M_{\odot}$ (Hora et al. 2006). Neutron star precursor masses (upper right) should be $\leq 1.4 M_{\odot}$ pulsar masses, and much less than SN II remnant masses of $(9 - 25) M_{\odot}$ (Gelfand et al. 2007; Maund et al. 2004).

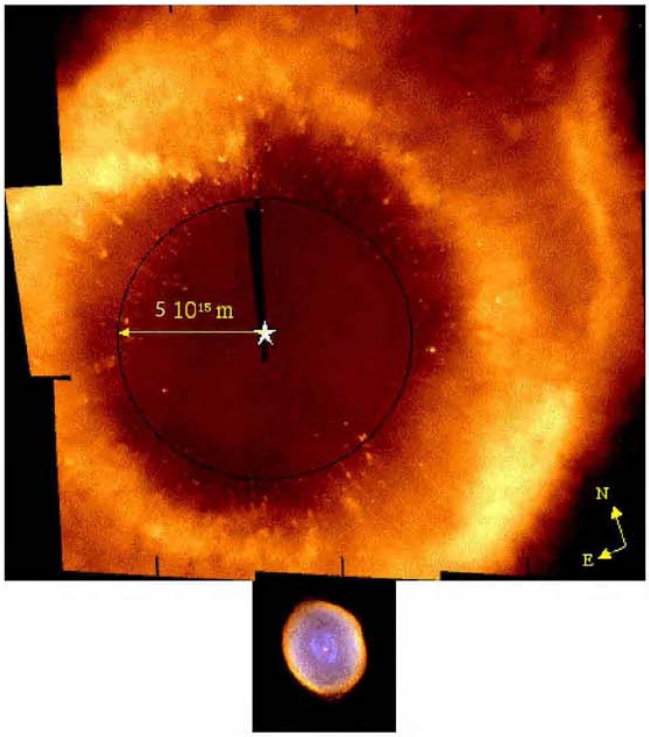

Fig. 4.— Helix Planetary Nebula HST/ACS/WFC F658N image mosaic. A sphere with radius 3×10^{15} m corresponds to the volume of primordial-fog-particles (PFPs) with mass density $\rho_0 = 3 \times 10^{-17}$ kg m^{-3} required to form two central stars by accretion. The comets within the sphere are from large gas planets (Jupiters, JPPs) that have survived evaporation rates of $2 \times 10^{-8} M_\odot$/year (Meaburn et al. 1998) for the 20,000 year kinematic age of Helix. The younger planetary nebula Spirograph (IC 418) shown below with no PFPs is within its accretion sphere. From HGD the 2.5×10^{16} m radius nebular sphere for Helix contains $\geq 1000 M_\odot$ of dark PFP and JPP planets, from which $1.5 \times M_\odot$ has been evaporated as detectable gas and dust (Speck et al. 2002).

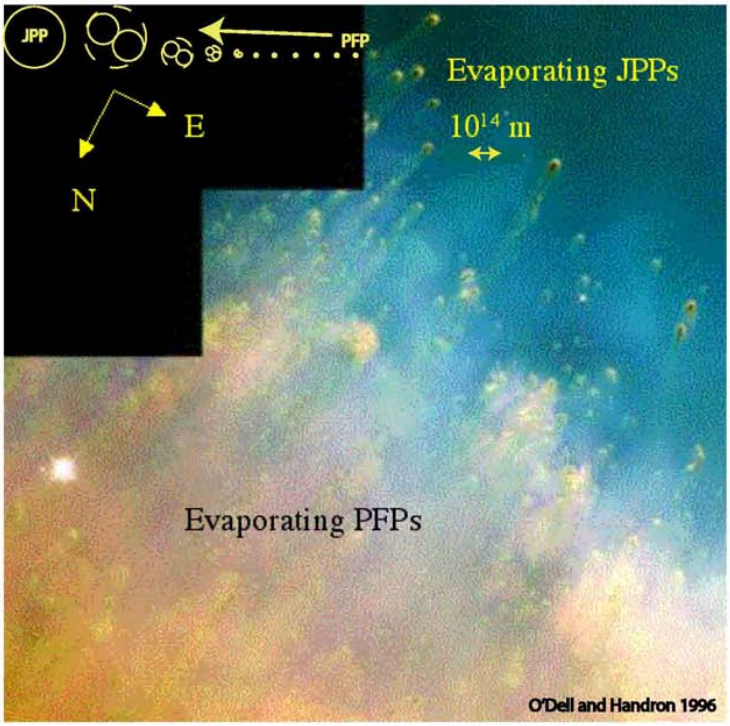

Fig. 5.— Helix Planetary Nebula HST/WFPC2 1996 image (O'Dell & Handron 1996) from the strongly illuminated northeast region of Helix containing massive JPP comets close to the central stars ($\approx 4 \times 10^{15}$ m) with embedded ≥ 0.4 Jupiter-mass planet atmospheres. The largest JPPs have about Jupiter mass 1.9×10^{27} kg from their spacing $\approx 4 \times 10^{14}$ m assuming primordial density $\rho_0 = 3 \times 10^{-17}$ kg m^{-3}. The 2^{10} stage binary cascade from Earth-mass to Jupiter-mass is shown in upper left.

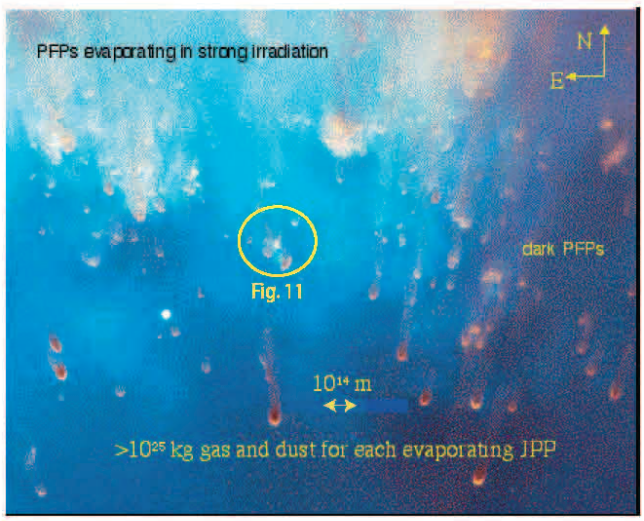

Fig. 6.— Detail of closely spaced cometary globules to the north in Helix from the 2002 HST/ACS images at the dark to light transition marking the clockwise rotation of the beamed radiation from the binary central star. Comets (evaporating JPPs) in the dark region to the right have shorter tails and appear smaller in diameter since they have recently had less intense radiation than the comets on the left. Two puffs of gas deep in the dark region suggest gravitational collection by planet gravity occured during the several thousand years since their last time of strong irradiation. Dark PFPs are detected in Fig. 11 (circle).

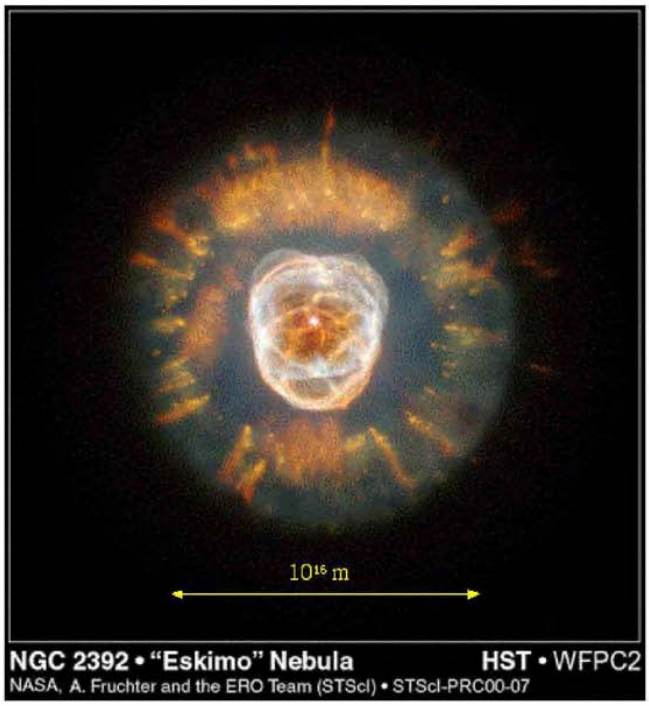

Fig. 7.— The Eskimo planetary nebula (NGC 2392) is ≈ 12 times more distance from earth than Helix, but still shows numerous evaporating PFP and JPP candidates in its surrounding interstellar medium in the HST/WFPC images. The nebula is smaller and younger than Helix, with a central shocked region like that of Spirograph in Fig. 4.

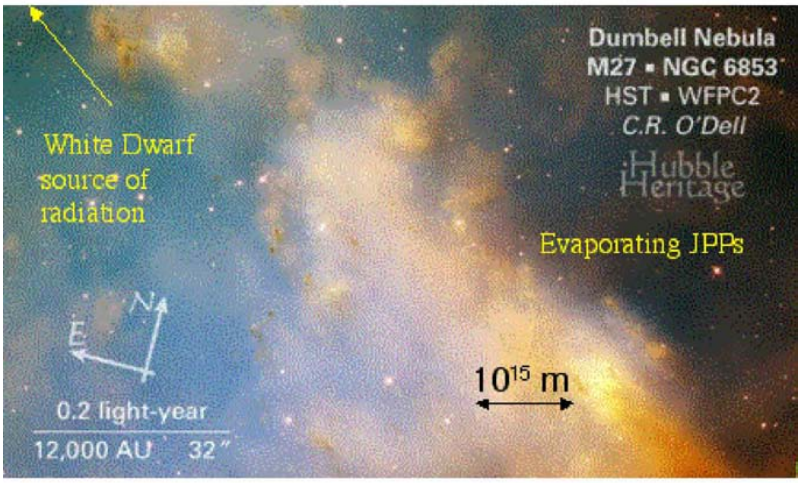

Fig. 8.— Close-up image of the Dumbbell planetary nebula (M27, NGC 6853) shows numerous closely spaced, evaporating, irradiated PFP and JPP candidates in its central region. The PNe is at a distance $\approx$ 500 pc, with diameter $\approx 2 \times 10^{16}$ m. The white dwarf central star appears to have a companion from the double beamed radiation emitted to produce the eponymous shape. The lack an apparent accretional hole may be the result of a different viewing angle (edgewise to the binary star plane of radiation) than the face-on views of Ring, Helix (Fig. 4) and Eskimo (Fig. 7).

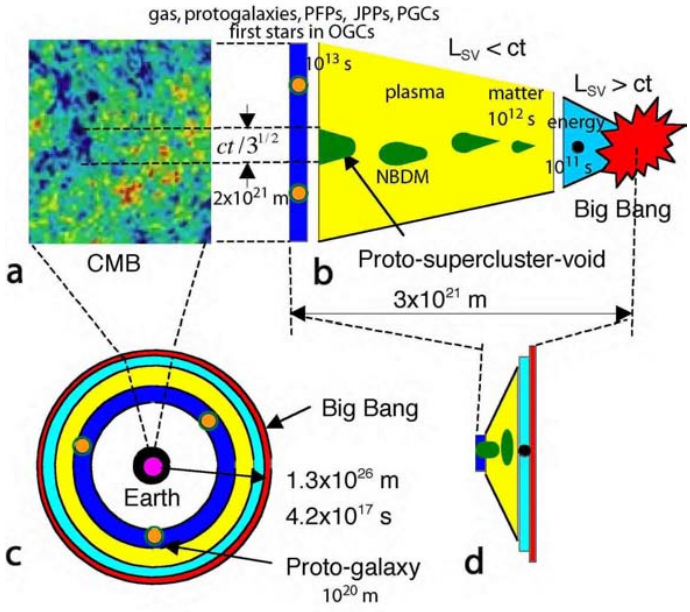

Fig. 9.— Hydro-Gravitational-Dynamics (HGD) description of the formation of structure (Gibson 2005; Gibson 2004). The CMB (a) viewed from the Earth (b) is distant in both space and time and stretched into a thin spherical shell along with the energy-plasma epochs and the big bang (c and d). Fossils of big bang turbulent temperature nucleosynthesize fossil density turbulence patterns in the H-He density (black dots). These trigger gravitational L_{SV} scale structures (Tables 1 and 2) in the plasma epoch as proto-supercluster-voids that fill with NBDM (green, probably neutrinos) by diffusion. The smallest structures emerging from the plasma epoch are linear chains of fragmented L_N scale proto-galaxies. These fragment into L_J scale PGC clumps of L_{SV} scale PFP Jovian planets that freeze to form the baryonic dark matter (Gibson 1996; Schild 1996) and "nonlinear grey dust" sources of SNe Ia dimming presently misinterpreted as "dark energy" (see Fig. 10).

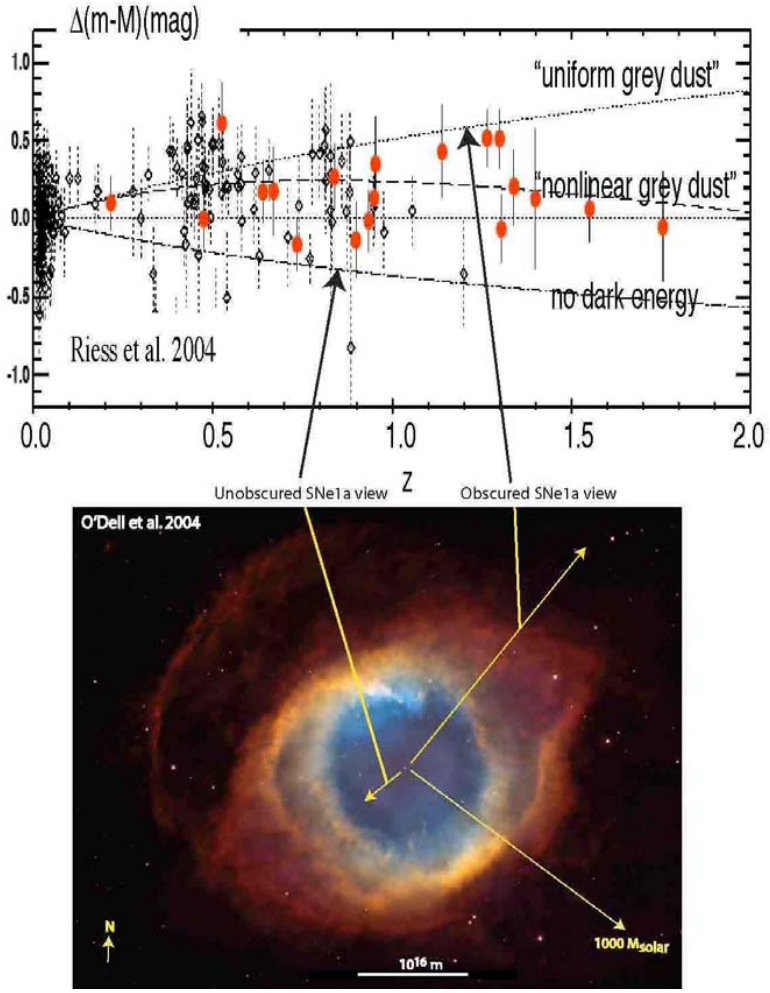

Fig. 10.— Dimming of SNE Ia magnitudes (top) as a function of redshift z (Riess et al. 2004). The "uniform grey dust" systematic error is excluded at large z, but the "nonlinear grey dust" systematic error from baryonic dark matter PFP and JPP evaporated planet atmospheres is not, as shown (bottom) Helix PNe (O'Dell et al. 2004). Frozen primordial planets comprise the ISM beyond the Oort cavity, which is the spherical hole left in a PGC when the central star is formed by accretion of PFPs and JPP planets. Planet atmospheres appear from the dark forming the PNe when the star runs out of fuel and the carbon core of the central star contracts. The rapidly spinning $0.7M_{\odot}$ white dwarf powers axial and equatorial plasma jets and winds that evaporate "nonlinear grey dust" planet atmospheres as the white dwarf is fed to $1.44M_{\odot}$ supernova Ia size by a slow rain of planets.

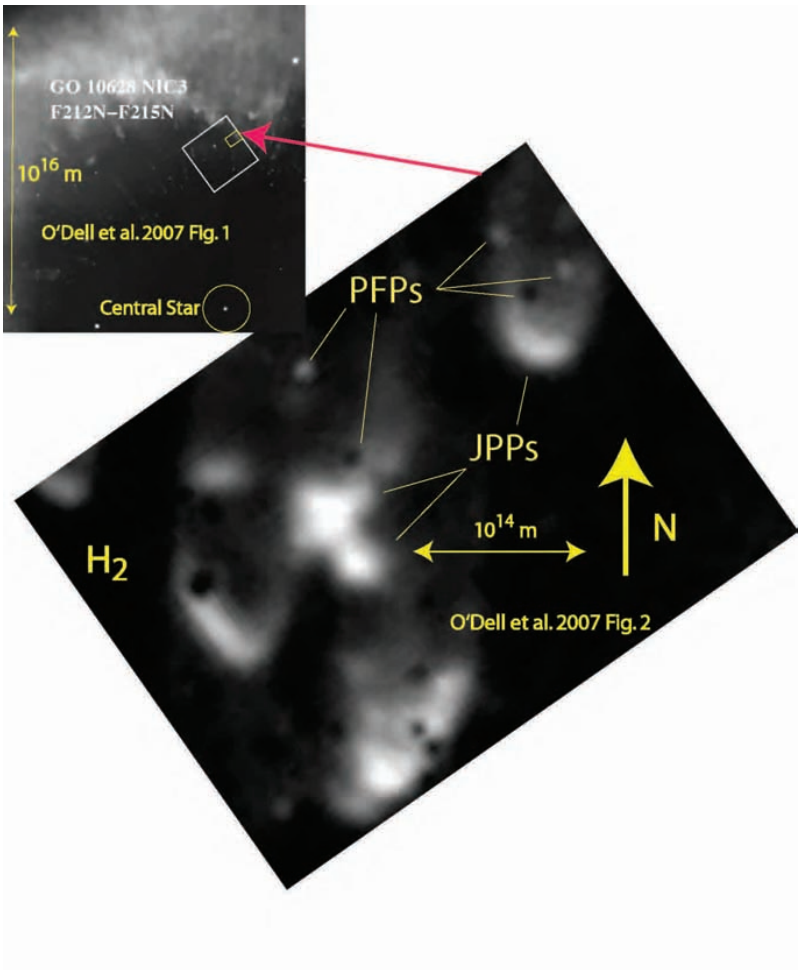

Fig. 11.— Detail of Helix image in H_2 from Figs. 1 and 2 of O'Dell et al. 2007. Distance scales have $\approx$ 10% accuracy (Harris et al. 2007) by trigonometric parallax, giving a Helix distance 219 pc with HST pixel 3.3×10^{12} m, the size of PFPs identified as the smallest light and dark objects. Such PFPs are not detected closer than $\approx 5 \times 10^{15}$ m from the binary central star (Fig. 4) because they have been evaporated by its radiation and plasma beam.

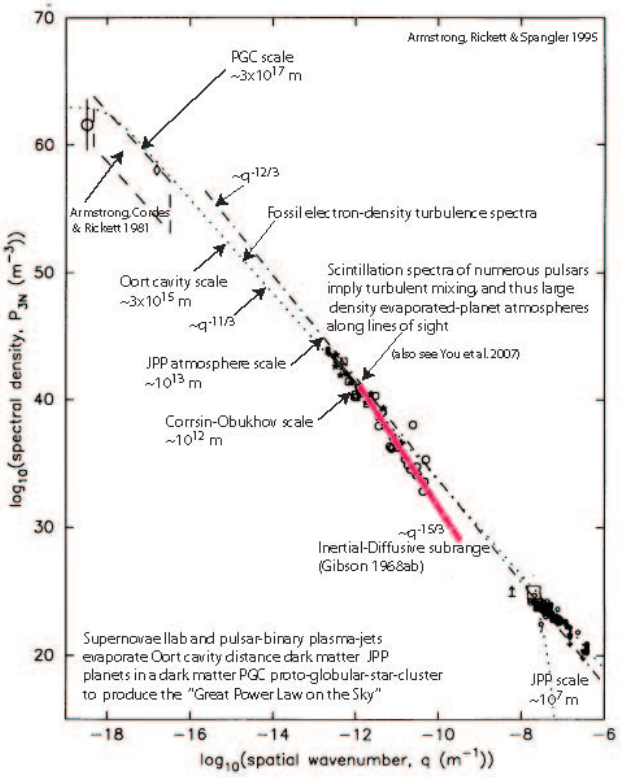

Fig. 12.— Electron density spectral estimates near Earth (within $\approx 10^{19-20}$ m) interpreted using HGD. The remarkable agreement along all lines of sight with the same universal Kolmogorov-Corrsin-Obukov spectral forms reflects the highly uniform behavior of baryonic PCG-PFP dark matter with primordial origin in response to SNe II and their pulsars as radio frequency standard candles. From HGD the large stars, supernovae IIab, and neutron-star pulsars of the Galaxy disk require pulsar scintillations in dense, previously turbulent, JPP planet atmospheres with fossil electron density turbulence. Dissipation rates implied are large, indicating rapid evaporation of the frozen gas planets.

Table 1. Length scales of self-gravitational structure formation

Length scale name	Symbol	Definition[a]	Physical significance[b]
Jeans Acoustic	L_J	$V_S/[\rho G]^{1/2}$	Ideal gas pressure equilibration
Jeans Hydrostatic	L_{JHS}	$[p/\rho^2 G]^{1/2}$	Hydrostatic pressure equilibration
Schwarz Diffusive	L_{SD}	$[D^2/\rho G]^{1/4}$	V_D balances V_G
Schwarz Viscous	L_{SV}	$[\gamma\nu/\rho G]^{1/2}$	Viscous force balances gravitational force
Schwarz Turbulent	L_{ST}	$\varepsilon^{1/2}/[\rho G]^{3/4}$	Turbulence force balances gravitational force
Kolmogorov Viscous	L_K	$[\nu^3/\varepsilon]^{1/4}$	Turbulence force balances viscous force
Nomura Protogalaxy	L_N	$[L_{ST}]_{CMB}$	10^{20} m proto-galaxy fragmentation-shape scale
Ozmidov Buoyancy	L_R	$[\varepsilon/N^3]^{1/2}$	Buoyancy force balances turbulence force
Gibson Flamelet	L_G	$v_f\gamma^{-1}$	Thickness of flames in turbulent combustion
Particle Collision	L_C	$m\sigma^{-1}\rho^{-1}$	Distance between particle collisions
Hubble Horizon	L_H	ct	Maximum scale of causal connection

[a] V_S is sound speed, ρ is density, G is Newton's constant, D is the diffusivity, $V_D \equiv D/L$ is the diffusive velocity at scale L, $V_G \equiv L[\rho G]^{1/2}$ is the gravitational velocity, γ is the strain rate, ν is the kinematic viscosity, ε is the viscous dissipation rate, $N \equiv [g\rho^{-1}\partial\rho/\partial z]^{1/2}$ is the stratification frequency, g is self-gravitational acceleration, z is in the opposite direction (up), v_f is the laminar flame velocity, m is the particle mass, σ is the collision cross section, c is light speed, t is the age of universe.

[b] Magnetic and other forces (besides viscous and turbulence) are negligible for the epoch of primordial self-gravitational structure formation (Gibson 1996).

Table 2. Acronyms

Acronym	Meaning	Physical significance
BDM	Baryonic Dark Matter	PGC clumps of JPPs from HGD
CDM	Cold Dark Matter	Questioned concept
CMB	Cosmic Microwave Background	Plasma transition to gas after big bang
HCC	Hierarchical Clustering Cosmology	Questioned CDM concept
HCG	Hickson Compact Galaxy Cluster	Stephan's Quintet (SQ=HGC 92)
HGD	Hydro-Gravitational-Dynamics	Corrects Jeans 1902 theory
ISM	Inter-Stellar Medium	Mostly PFPs and gas from JPPs
JPP	Jovian PFP Planet	H-He planet formed by PFP accretion
ΛCDMHCC	Dark-Energy CDM HCC	Three questioned concepts
NBDM	Non-Baryonic Dark Matter	Includes (and may be mostly) neutrinos
OGC	Old Globular star Cluster	PGC that formed stars at $t \approx 10^6$ yr
PFP	Primordial Fog Particle	Earth-mass BDM primordial planet
PGC	Proto-Globular star Cluster	Jeans-mass protogalaxy fragment
SSC	Super-Star Cluster	A cluster of YGCs
YGC	Young Globular star Cluster	PGC forms stars at $t \approx$ now

Acknowledgements

As is perhaps obvious from the names of coauthors on the attached preprints it would have been impossible for me to write the present papers without the generous advice, wisdom and experience of Rudy Schild and Theo Nieuwenhuizen. See their pictures from the Practical Problems in Cosmology 2008 conference in St. Petersburg organized by Yuri Baryshev who was kind enough to invite me. I am also most grateful to UCSD for sponsoring several Freshman and Senior seminars on New Cosmology, and for the excellent questions of the students that attended.

Baryshev, Schild, Nieuwenhuizen, Gibson